A Field-Trip Guide to Yellowstone National Park, Wyoming, Montana, and Idaho— Volcanic, Hydrothermal, and Glacial Activity in the Region

By Robert O. Fournier, Robert L. Christiansen, Roderick A. Hutchinson[1], *and* Ken L. Pierce

GENERAL INFORMATION AND BRIEF SUMMARY OF TRIP

This field-trip guide was originally prepared for the 7th International Symposium on Water/Rock Interaction (WRI–7) held in July 1992 in Park City, Utah. A large and diversified group of earth scientists and accompanying family members participated in this 3 1/2-day field trip that focused on water/rock interactions over widely ranging temperatures and pressures in the Yellowstone/Grand Teton region. Emphasis was placed on the geochemical and hydrologic characteristics of the thermal waters in the major "geyser basins" of Yellowstone National Park. Information specific to the WRI–7 trip about logistics, lodging, and meals has been deleted from the present guide. The scientific content remains mostly unchanged, except for the addition of a glossary, two illustrations, all photographs, and some text previously presented to the field-trip participants in supplementary materials (see appendix A).

Most of the geyser basins in Yellowstone National Park are on a high volcanic plateau at elevations of 2,000 to 2,200 m and are surrounded by much higher mountain ranges. In the middle of summer there generally are cool evenings and early mornings and warm afternoons. Visits to the localities described require short walks, mostly on boardwalks, but some are on what may be wet ground. No long, strenuous climbs are required. Expect brief afternoon thunder showers, particularly at Old Faithful. **Please remember that the collecting of any kind of sample in a national park is prohibited except by those who have specific sampling permits issued by the National Park Service. Field-trip participants are asked to leave geologic picks and hammers at home or in their luggage while in Yellowstone National Park.**

Caution

Thermal areas are both delicate and dangerous. Special caution should be exercised when visiting them to avoid damage to yourself and to the fragile environment. Please stay on boardwalks where they are present. Boiling pools of water commonly are covered by thin crusts of sinter that build inward from the sides of hot-spring pools. Assume that all water flowing in streams in and near thermal areas is hot enough to cause pain and blistering if you step into this water.

Day 1—Travel north through the Grand Teton National Park into Yellowstone National Park (fig. 1). Stops are made along the way to view the spectacular scenery and to discuss the glacial and structural history of the Teton Mountains and Jackson Hole, Wyoming. Lunch is at String Lake, a small lake with spectacular mountain scenery. After lunch, proceed to Yellowstone National Park, the scene of some of the largest known Quaternary eruptions of rhyolitic lava flows and caldera-forming ash-flow tuffs. Stop at the West Thumb thermal area on the shore of Yellowstone Lake to look at hydrothermal manifestations and their relation to volcanic, glacial, and postglacial processes. Thick and extensive deposits of sinter have been deposited from hot-spring waters in the West Thumb region since the last glaciation (Pinedale glaciation that ended 10,000–15,000 years ago). (Note that here and in the remainder of this field guide "sinter" refers exclusively to siliceous material deposited at the Earth's surface by flowing hot water.) From West Thumb proceed to Old Faithful, arriving in time to explore the Upper Geyser Basin before dinner. Two nights are spent at Old Faithful.

Day 2—Most of the day is spent walking in the Upper, Midway, and Lower Geyser Basins within the Yellowstone caldera, where many hot springs, geysers, mud pots, and good exposures of silica- and zeolite-cemented sediments will be seen. Specialized bacteria, algae, and diatoms grow in the thermal waters, and various chemical

[1]U.S. National Park Service, Yellowstone National Park, Wyoming 82190.

Manuscript approved for publication May 16, 1994.

precipitates are actively being deposited in different pools, including amorphous silica, calcite plus manganese oxides, smectites, native sulfur, and iron sulfides. Effects of a thick cover of glacial ice on hydrothermal activity are viewed and discussed. Particular attention is focused on Pocket Basin, a large oblong crater about 0.75 km in maximum length that formed as the result of hydrothermal eruptions.

Day 3—Travel from Old Faithful to Mammoth Hot Springs. On the way, stop at Norris Geyser Basin, where both neutral- and acid-chloride thermal waters emerge from ash-flow tuffs and hydrothermally altered glacial deposits. At Norris there are seasonal variations in the degree of boiling during upflow, and there is seasonal underground mixing of chloride-rich and sulfate-rich waters. Native sulfur and amorphous sulfides of arsenic and antimony are common in this basin. Between Norris and Mammoth, make brief stops at Roaring Mountain and Obsidian Cliff. Plan to arrive at Mammoth in time to walk along the extensive

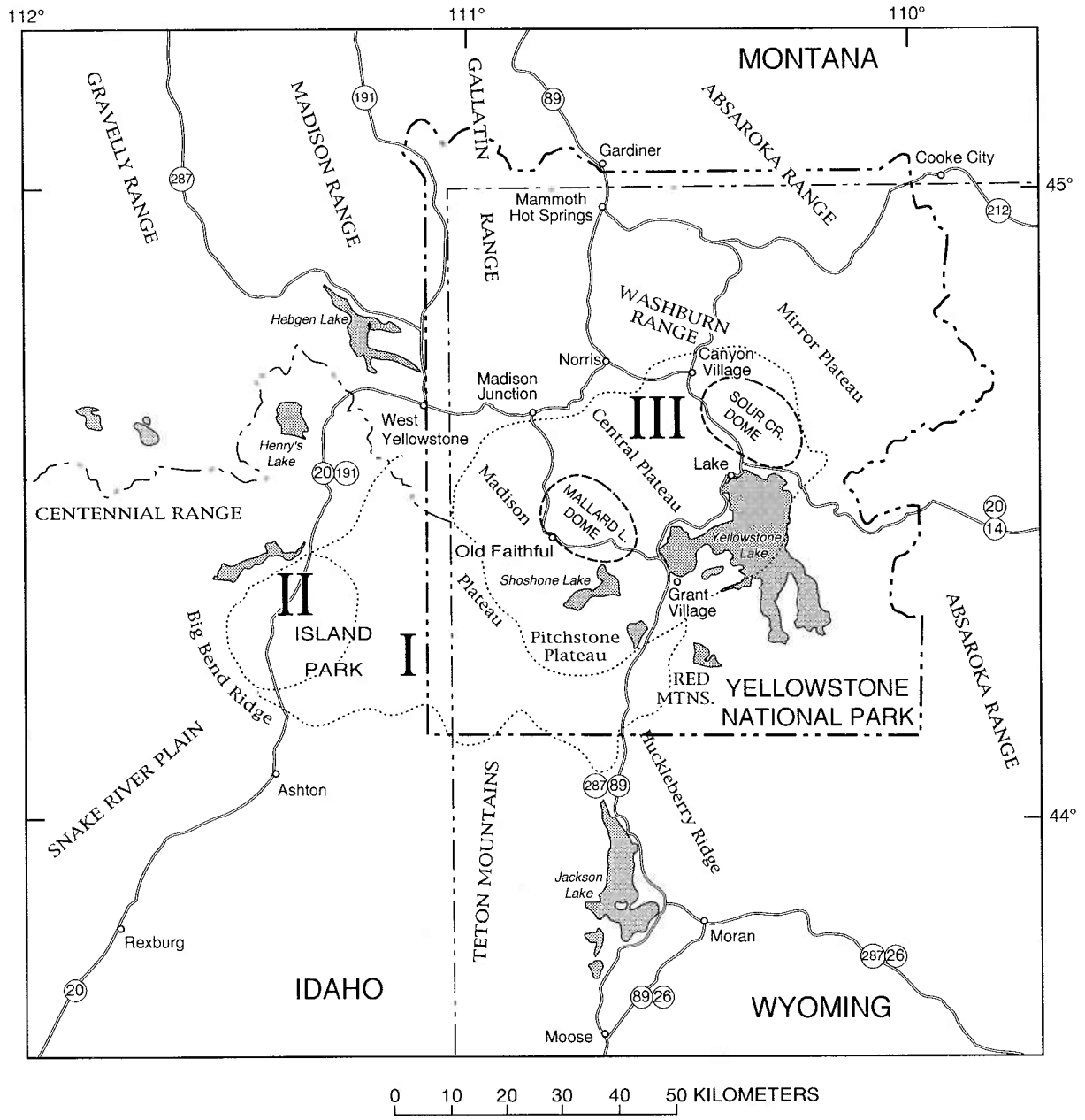

Figure 1. Location and major features of Yellowstone National Park. Dotted lines outline calderas; dashed lines, resurgent domes; I, first-cycle caldera; II, second-cycle caldera; III, third-cycle (Yellowstone) caldera; double lines show major roads in region. Jackson Hole, Wyoming, is just off map, a few kilometers south of Moose. (From Christiansen and Hutchinson, 1987).

system of trails leading to bicarbonate-rich hot springs that emerge from Mesozoic sedimentary rocks and that form ever-changing mounds and thick terraces of travertine.

Day 4—Travel from Mammoth Hot Springs back to the Tetons and Jackson Hole via the eastern route through Yellowstone Park. This provides an opportunity to view from a distance thermal areas where petroleum is being carried to the surface in the hot-spring waters. Stop at the Grand Canyon of the Yellowstone River, where a steep-sided gorge about 30 km long and ranging from about 300 to 500 m in depth has been cut into a thick section of hydrothermally altered volcanic rocks, and at the Mud Volcano area, where violent fumarolic activity and acid-sulfate alteration is the surface expression of a small vapor-dominated hydrothermal system. The route passes through the Yellowstone caldera along a traverse where repeated leveling measurements made over many years showed a rapid rate of caldera uplift (about 2.5 cm/yr) before 1984, followed by a rapid rate of caldera subsidence (also about 2.5 cm/yr) since 1985.

INTRODUCTION TO YELLOWSTONE

Yellowstone Park is situated on a high volcanic plateau that sits astride a region of active crustal extension. The plateau and the adjacent region to the west have been the most seismically active area of the Rocky Mountains in historic time (Smith and Braile, 1984). In 1872 the Yellowstone region became the first national park in the world, largely through the recognition that it displays some of the largest and most spectacular hot-spring and geyser activity on Earth. Early scientists recognized that this hydrothermal activity was related to the same causes as the recent volcanism in the region. Only in the last few decades has it been realized that the compositionally bimodal rhyolite-basalt volcanism of the Yellowstone Plateau volcanic field (Boyd, 1961; Christiansen and Blank, 1972; Christiansen, 1984) is younger than about 2.2 Ma and completely distinct from the predominantly andesitic volcanism of the Eocene Absaroka volcanic field (Smedes and Prostka, 1972). The major hydrothermal activity recognized in Yellowstone National Park (White and others, 1975; Fournier, 1989) is related in time and origin to postcaldera magmatism in the youngest of three calderas. These three calderas resulted from voluminous rhyolitic ash-flow eruptions at 2.0, 1.3, and 0.6 Ma. Each of these caldera-forming ash-flow eruptions was preceded and succeeded by large eruptions of rhyolitic lava. The last eruption of rhyolitic lava was about 70,000 years B.P. (Christiansen, 1984). More than 6,500 km^3 of erupted magma make the Yellowstone Plateau volcanic field one of the major Quaternary volcanic fields on Earth.

Current activity includes not only the high-temperature hydrothermal systems but distinctive seismicity and a spatial and temporal pattern of historic rapid uplift or inflation followed by deflation (Pelton and Smith, 1979, 1982; Jackson and others, 1984; Hamilton, 1985; Dzurisin and others, 1986; Meyer and Lock, 1986; Dzurisin and Yamashita, 1987) that is difficult to explain by processes that do not involve magmatic activity. In addition, a variety of geophysical anomalies coincide with the 0.6-Ma Yellowstone caldera that, taken together, indicate that magma or partially molten rock may be present at depths ranging from about 5 to 10 km, and possibly as shallow as 3 km beneath parts of the eastern half of this caldera (Eaton and others, 1975; Iyer and others, 1981; Lehman and others, 1982; Smith and Braile, 1984; Benz and Smith, 1984; Brokaw, 1985). These anomalies include low densities (Blank and Gettings, 1974), large convective and conductive heat flows (Fournier and others, 1976; Morgan and others, 1977; White, 1978), a magnetic low and shallow calculated Curie-point isotherms (Smith and others, 1974; Bhattacharyya and Leu, 1975; Eaton and others, 1975), low seismic velocities (Iyer and others, 1981; Daniel and Boore, 1982), high seismic attenuation (Benz and Smith, 1984; Brokaw, 1985), a sharp increase in electrical conductivity at a depth of about 5 km, shown by magnetotelluric soundings (Stanley and others, 1977), and a lack of seismic focal depths deeper than about 3 to 4 km beneath much of the caldera (Fournier and Pitt, 1985). Heat-flow considerations indicate that magmatic temperatures could be attained at a depth about 0.5 km deeper than the depth of the transition from seismic to aseismic conditions (Fournier and Pitt, 1985).

Chemical compositions of Yellowstone's thermal waters have been determined by many investigators starting over 100 years ago. Of particular importance are large compilations by Gooch and Whitfield (1888), Allen and Day (1935), Rowe and others (1973), Thompson and others (1975), and Thompson and Yadav (1979).

The exceptional hydrothermal activity at Yellowstone results from a combination of (1) an abundant supply of recharge water that comes primarily from snow that accumulates on the surrounding high mountains, particularly to the north and northwest (based on isotopic data for hot-spring waters from Truesdell and others (1977) and unpublished U.S. Geological Survey (USGS) analyses of meteoric waters in the region by Robert O. Rye and by Tyler B. Coplen), where faulted and folded permeable sedimentary rocks provide permeability for the infiltrating water, (2) a huge magmatic heat source at a relatively shallow depth of 4 to 5 km beneath the 0.6-Ma Yellowstone caldera, and (3) frequent and widespread seismic activity that reopens channels of fluid flow that become clogged by hydrothermal alteration products and mineral precipitates. Upflow of thermal waters is controlled mainly by fracture systems. Important zones of fracturing in the Yellowstone caldera are near the outer edge of the main ring fracture and at the flanks of the two resurgent domes (fig. 2). Outside the caldera, hydrothermal activity is pronounced along a network of faults in a zone extending

northward from Norris Geyser Basin through Mammoth Hot Springs. Most of the surface expression of hydrothermal activity is on the northwest side of the caldera, the side facing the likely direction of maximum water recharge, as determined by isotopic data.

Within the very seismically active Yellowstone region, water likely circulates to the depth at which brittle fracturing is present. Earthquake hypocenters indicate that this depth is about 4 to 5 km beneath the Yellowstone caldera and as deep as 15 to 20 km a few kilometers to the side of the caldera. Furthermore, the transition from brittle to plastic behavior of silicic crystalline rocks in the Earth's crust is likely to occur at about 370 to 400°C for reasonable strain rates in tectonically active regions (Fournier, 1991). Thus, the limit of downward circulation of meteoric water in the Yellowstone hydrothermal system is likely to be the depth where temperatures are about 350 to 400°C. An independent line of evidence, based on brine-gas phase equilibrium considerations, indicates that the maximum likely temperature that can be attained by a fluid of the composition exhibited by the Yellowstone waters is about 425°C (Fournier and Pitt, 1985; Fournier, 1987). At temperatures higher than about 425°C the water would separate into a very saline brine and relatively dilute gas (steam) as it flowed upward toward the surface.

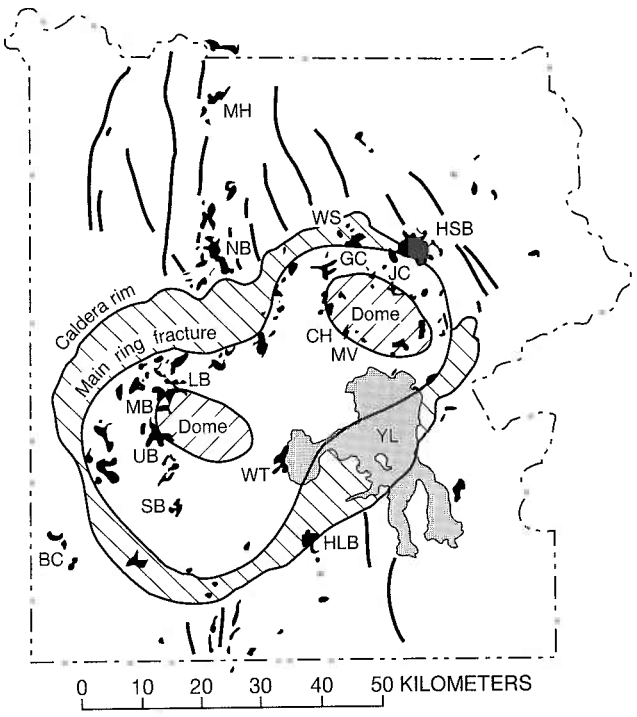

Figure 2. Map of Yellowstone National Park, Wyoming, showing 0.6-Ma Yellowstone caldera, two resurgent domes, active and recently active hydrothermal features (solid black), major faults (solid lines outside caldera region), and locations of selected named thermal areas. Letter codes show approximate locations of major thermal areas mentioned in text: BC, Boundary Creek; CH, Crater Hills; GC, Grand Canyon; HLB, Heart Lake Basin; HSB, Hot Springs Basin; JC, Josephs Coat Hot Springs; LB, Lower Geyser Basin; MB, Midway Basin; MH, Mammoth Hot Springs; MV, Mud Volcano; NB, Norris Geyser Basin; SB, Shoshone Basin; UB, Upper Geyser Basin; WS, Washburn Hot Springs; WT, West Thumb; YL, Yellowstone Lake (stippled area). Outline of Yellowstone National Park shown for reference. (Figure revised and redrawn after Christiansen, 1984.)

A general model of the Yellowstone hydrothermal system has hypersaline brine filling fractures in the deepest parts of the hydrothermal system. The brine is overlain by relatively dilute water that either floats on top of this brine or is separated from the brine by a region of "self-sealed" rock. Although there is no direct evidence for the presence of the hypersaline brine, it is inferred to be present because aqueous magmatic fluid that is evolved from a crystallizing magma at a depth of about 4 to 5 km must dissociate to a hypersaline brine and a coexisting aqueous gas that is rich in CO_2 and sulfur compounds. Above the brine there is a series of successively shallower "local reservoirs" where more permeable rocks are sandwiched within less permeable rocks. Upward convecting waters flow relatively quickly through fractures in otherwise less permeable rocks (such as ash-flow tuff) and reside for relatively long times at a nearly constant temperature in volumes of rock (reservoirs) that have greater inherent porosity and permeability (such as reservoirs in rubble at the bottom and top of rhyolite flows). Chemical and isotopic reequilibrium is attained between water and rock at successively lower temperatures as waters ascend from deeper to shallower reservoirs. On the basis of tritium analyses, Pearson and Truesdell (1978) concluded that Yellowstone hydrothermal systems appear to contain mixtures of two waters—one from an open well-mixed reservoir of relatively short residence time (presumably a cold reservoir at a shallow depth) and the other from a reservoir containing little or no tritium (presumably a hot and deeper reservoir). The estimated rates of discharge of water, chloride, and heat for selected thermal regions and for all of Yellowstone Park are given in table 1.

The Yellowstone Plateau and adjacent upland areas were largely covered by ice during the last two major glaciations—the Bull Lake and Pinedale glaciations—and these had major impacts on the hydrothermal activity. The Bull Lake glaciation (about 160–130 ka) correlates with late Illinoian glaciation in the Midcontinental United States (Pierce and others, 1976). Pinedale glacial deposits (about 10 to more than 30 ka) correlate with the Wisconsin glaciation in the Midcontinental United States. The estimated thickness of glacial ice during the Pinedale glaciation in the Upper and Lower Geyser Basins region is as much as 570 m, at Norris about 740 m, and at Mud Volcano about 1,070 m. When glaciers covered the Yellowstone Plateau, the potentiometric surfaces for ground water in the underlying rocks were raised hundreds of meters above the ground surface, allowing boiling-point curves in regions of upflow to attain higher temperatures at given depths and at

Table 1. Preferred values for average rates of discharge of deep high-temperature component of thermal water (containing 412 mg/kg chloride), chloride in that water, and heat (before boiling during upflow) from selected thermal areas in Yellowstone National Park.

[From Fournier and others, 1976; Fournier, 1989. Mammoth Hot Springs (1), measurements made in 1960's. Mammoth Hot Springs (2), measurements made in 1980's, assumes that deep component of hydrothermal fluid contains 170 mg/kg chloride and flows from a reservoir with maximum temperature of 90°C (calculated using data in Sorey, 1991). Difference in estimated chloride discharges in the 1960's and 1980's at Mammoth Hot Springs is within uncertainty of the measurements, and difference in the calculated discharge of heat is due to different assumptions about chloride concentration and temperature of deep water. —, not calculated]

Region	Deep water (m^3/s)	Chloride (g/s)	Heat (cal/s)	Area (km^2)
Upper Geyser Basin ------	0.417	172	155×10^6	11
Lower Geyser Basin ------	0.985	406	369×10^6	36
Norris and Gibbon Geyser Basins.	0.310	128	116×10^6	—
Mammoth Hot Springs (1)	0.228	94	85×10^6	—
Mammoth Hot Springs (2)	0.590	100	53×10^6	—
Total park ----------	3.300	136	1230×10^6	—

the points of discharge at the Earth's surface beneath the ice (Muffler and others, 1971; Bargar and Fournier, 1988). This situation is analogous to oceanic hot-spring systems that, because of the weight of the overlying ocean water, can have temperatures in the >300°C range at the points where they discharge on the ocean floor. The net result of the raising of potentiometric surfaces and boiling-point curves was that excess thermal energy became stored in rock at shallow depths during glacial periods. When the glaciers receded, this excess energy was available to enhance geothermal circulation and to produce large hydrothermal explosive eruptions of water and rock (Muffler and others, 1971).

Articles by Smith and Christiansen (1980), Christiansen (1984), Smith and Braile (1984), Fournier and Pitt (1985), and Fournier (1989) summarize current thought about the evolution of the Yellowstone Plateau volcanic field and the associated hydrothermal activity.

Figure 1 shows the road system in the Yellowstone National Park/Teton National Park region and major features in Yellowstone. Figure 3 shows the locations of stops within Yellowstone National Park, with numbers corresponding to stop numbers in the "Detailed Itinerary."

Acknowledgments.—Material presented in other field guides and road logs prepared by Christiansen and Hutchinson (1987), Christiansen (1989), and Pierce and Good (1982, 1990) has been of great help in the preparation of this guide. We are also greatly indebted to our colleagues, L.J. Patrick Muffler, Alfred H. Truesdell, and Donald E. White, who have spent many years working with us in Yellowstone Park and who have contributed greatly to our knowledge of the Yellowstone region magmatic-hydrothermal system.

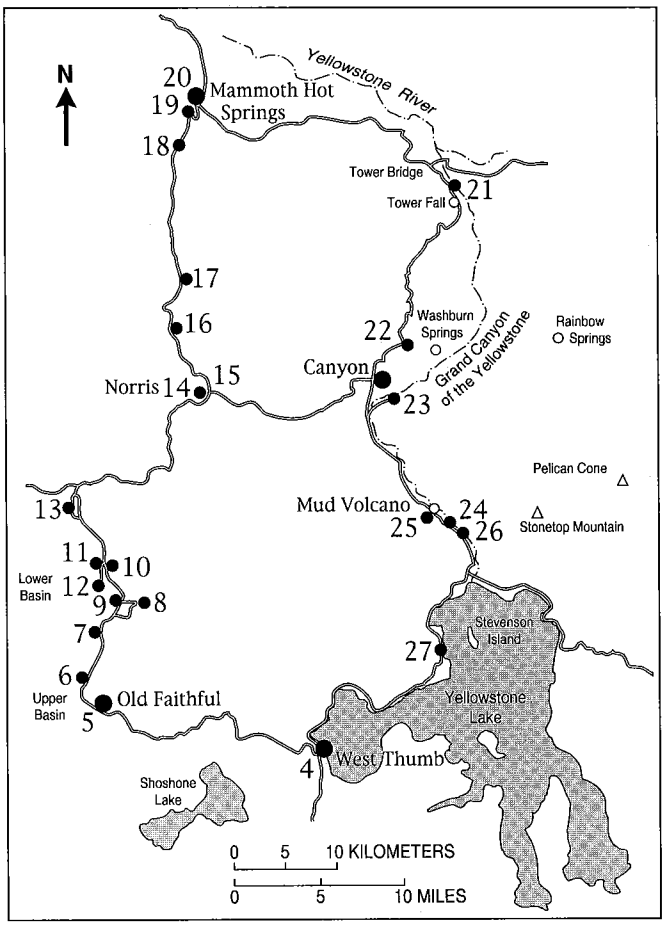

Figure 3. Locations of roads and field-trip stops in Yellowstone National Park. Numbers correspond to stop numbers in detailed itinerary.

DETAILED ITINERARY

DAY 1—JACKSON HOLE, WYOMING, TO OLD FAITHFUL

The original field-trip group started early in the morning at Park City, Utah, and traveled by chartered bus to Wyoming, arriving at Jackson Hole about 11:30 a.m.

STOP 1—WINDY POINT TURNOUT

Windy Point Turnout is on the inner road of Grand Teton National Park about 2.5 km past the national park entrance at Moose, Wyoming.

View Teton Range and Jackson Hole.—Figure 4 shows the view of the Teton Range from Windy Point. To the northwest is the central, highest part of the Teton Range including the Grand Teton (altitude 4,198 m). The glaciated core of the Teton Range exposes Late Archean metamorphic rocks (mostly gneisses) intruded by Proterozoic granitic rocks. The northern and southern thirds of the range are capped by layered rocks, mostly of Paleozoic age. Just south of the stop, the forested hills are loess-mantled deposits of the next-to-last glaciation (Bull Lake?). The sagebrush bench extending more than 10 km north from the stop is outwash gravel of the last glaciation (Pinedale). Further north are the west-tilted blocks of Signal Mountain, Huckleberry Ridge, Wildcat Ridge, and others, some of which are capped with the Huckleberry Ridge Tuff (2 Ma) erupted from the oldest caldera of the Yellowstone Plateau volcanic field. To the west, at the foot of the Teton Range, the recently burned area is underlain by Pinedale moraines from the Tetons.

STOP 2—LUNCH AT STRING LAKE

Quaternary geology along the Teton Range front.—String Lake is at the base of the Teton Range (fig. 5). West across the lake and 100 m above it is the postglacial scarp of the Teton fault. Late Pleistocene debris from local Teton glaciers is offset about 20 m across the fault on a scarp that is 35 m high and as steep as 40°. String Lake is situated between two Pinedale moraines that had different source areas. Just upstream from String Lake are end moraines of a large glacial lobe fed by glaciers from the Yellowstone Plateau and from the Teton Range. Just downstream from String Lake are Pinedale moraines of a local glacier from the Tetons (Cascade Canyon). Moraines deposited by this glacier also are responsible for the formation of Jenny Lake. The lunch stop in the intervening area between the two moraines is on glacial outwash. The outer Pinedale moraines of the Cascade Canyon glacier are buried by this outwash, whereas younger moraines are not. Obsidian-hy-

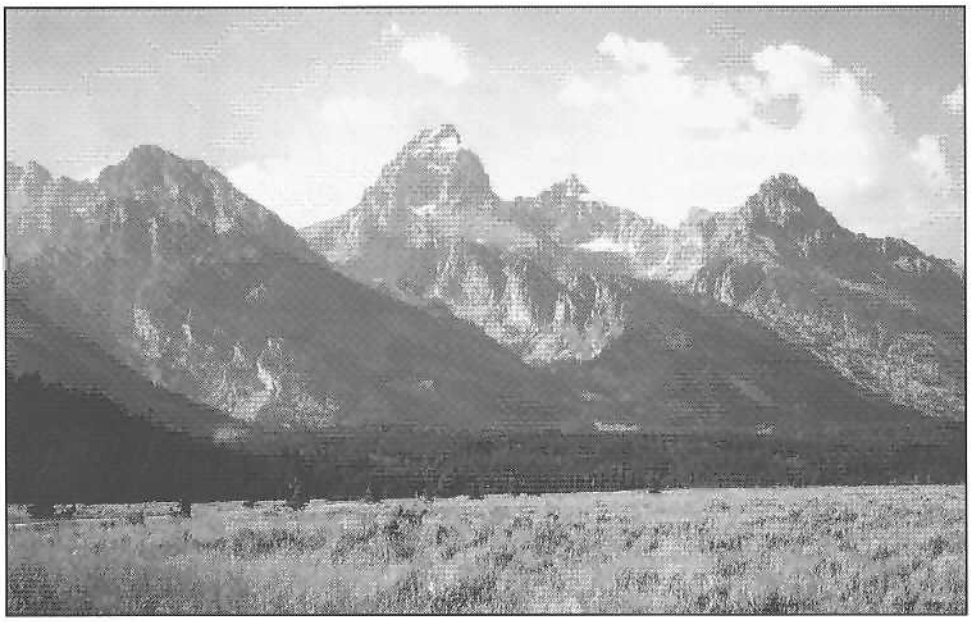

◄ **Figure 4.** View of Teton Range as seen from Stop 1.

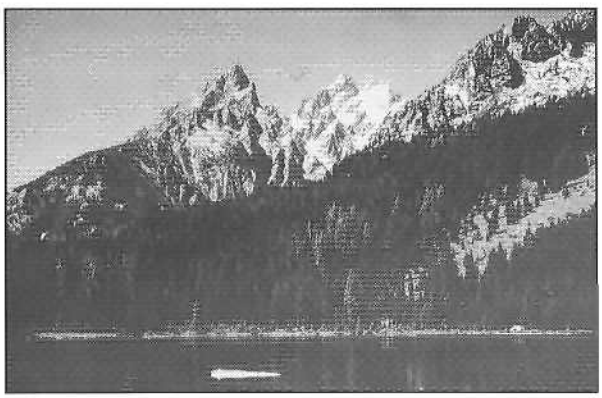

◄ **Figure 5.** String Lake and Teton Range as seen from Stop 2.

dration measurements of obsidian from a well east of the Jenny Lake Lodge suggest that outwash nearly 100 m thick accumulated during the last glaciation (unpub. data, K.L. Pierce, USGS).

STOP 3—WILLOW FLATS OVERLOOK

Late Cenozoic volcanic rocks, structural evolution, and glaciation of northern Jackson Hole.—The west-tilted Teton Range, with its high-standing Precambrian core to the south, becomes lower to the north and exposes north-dipping Paleozoic and Mesozoic sedimentary rocks. This relation and the high structural relief of the Tetons are composite features of the northwest-trending Gros Ventre–Teton uplift of Laramide age and the late Cenozoic north-trending west-tilted normal-fault block of the modern Tetons. Signal Mountain can be seen just south of the overlook. On and around Signal Mountain, ash-flow tuffs and tuffaceous sediments are tilted into the Teton fault with ages and dips as follows: 2 Ma, 11°; 4 to 6 Ma, 22°; about 10 Ma, 20 to 27°. The post-2-Ma rate of tilt is similar to a rate of tilt calculated from offset of glacial deposits viewed at the lunch stop. This progression suggests that the main fault offset started after the 4- to 6-Ma tuff was deposited and has continued at a high rate throughout the Quaternary (1–2 mm/yr).

You are standing inside the moraines of the youngest of three phases of the last or Pinedale glaciation (Pierce and Good, 1990). During the earliest phase, the combined Buffalo Fork and Pacific Creek glacial lobes from the east and northeast flowed westward through this area and scoured a 200-m-deep trough on the north side of Signal Mountain. In the later, Jackson Lake phase, the Snake River and Pacific Creek lobes from the north and northeast joined and flowed south to the type-Jackson Lake moraines that occur around the southern margin of Jackson Lake. As these lobes receded, they separated, and meltwater streams deposited kame gravels between them, such as those between Emma Matilda Lake and Christian Pond off to the east. Willow Flats in the foreground is a postglacial subirrigated alluvial fan that has built southward to Signal Mountain, forming the present outlet of Jackson Lake. The Jackson Lake Dam was built on fine-grained sediment that fills a 200-m-deep glacial trough. The dam was recently redesigned and rebuilt at a cost of $82 million to strengthen sediment beneath the dam that could liquefy during an earthquake on the Teton fault.

STOP 4—WEST THUMB GEYSER BASIN

Hydrothermal activity and its volcanic setting.—Like most geyser basins of the Yellowstone Plateau, West Thumb Geyser Basin (West Thumb) is controlled by the ring-fracture zone of the Yellowstone caldera. It is localized where the zone is intersected by a line of young intracaldera rhyolitic vents that extend north-northwest across the caldera between aligned tectonic fault zones to the north and south to form the Central Plateau. The lake basin of West Thumb is a deep subcircular extension of Yellowstone Lake, the main basin of which is 10 km to the east. West Thumb had its origin as a relatively small caldera within the much larger Yellowstone caldera during a pyroclastic event that was part of the mainly lava-producing postcollapse volcanism of the past 150,000 years. The north, east, and south margins of the West Thumb caldera have been largely buried by younger rhyolite flows. To the east, beyond Yellowstone Lake, are the Absaroka Mountains, which are outside the Yellowstone caldera. To the southeast is Flat Mountain, the truncated north face of which is part of the southern margin of the Yellowstone caldera.

Walk along the boardwalk loop through the basin from the parking lot to the lake shore and back. Hot springs and geysers in the West Thumb Geyser Basin are perhaps more variable in temperature and discharge than in any major thermal area of Yellowstone. Thick sinter deposits (fig. 6) exposed along the shore of the lake to the north of the present hydrothermal activity show that the areal extent and probably also the rate of discharge of thermal water were once much greater than at present. Even at present, there are large variations in the distribution and volume of discharge of thermal waters. Activity in the basin is sometimes quite vigorous, with new springs and increased geyser activity, while at other times the rate and temperature of spring discharge is diminished, allowing abundant bacteria growth to occur closer to vents. The small cones of silica that emerge from lake water close to the shore (fig. 7) probably formed and grew in height at a time when the level of the lake was lower than today.

Many people have speculated that episodic ingress of cold Yellowstone Lake water into the hot-spring system is responsible for the variation in thermal activity. The isotope-chloride relations for West Thumb are poorly understood but may offer support for this idea. In a plot of $\delta^{18}O$ (a measure of the oxygen isotopic composition of a particular substance, such as water or a mineral, compared to the isotopic composition of a standard, expressed in parts per thousand) versus chloride, several West Thumb hot-spring waters plot as much as about 2 parts per thousand (ppt) above the trend line for most Yellowstone thermal waters (Truesdell and Fournier, 1976). This might be the result of mixing with a small amount of partly evaporated lake water. Generally in the Yellowstone hydrothermal system, "self-sealing" (probably mainly by amorphous silica deposition) and relatively high pressures within the hot-spring plumbing system effectively keep local ground waters from entering the discharging hydrothermal system. Research drilling into Yellowstone's hydrothermal systems has shown that the fluid pressures of the thermal waters are

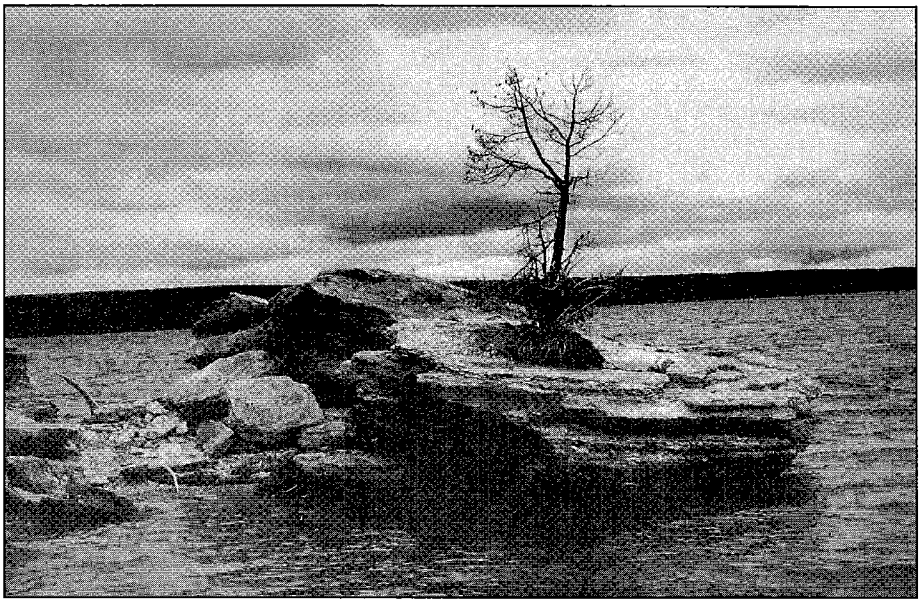

Figure 6. Old sinter at shore of Yellowstone Lake, West Thumb Geyser Basin.

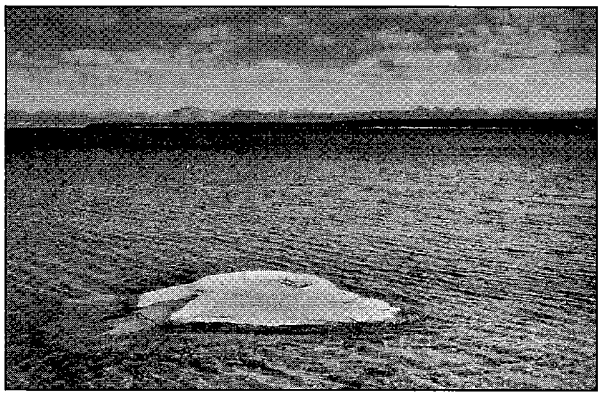

Figure 7. Fishing Cone, West Thumb Geyser Basin.

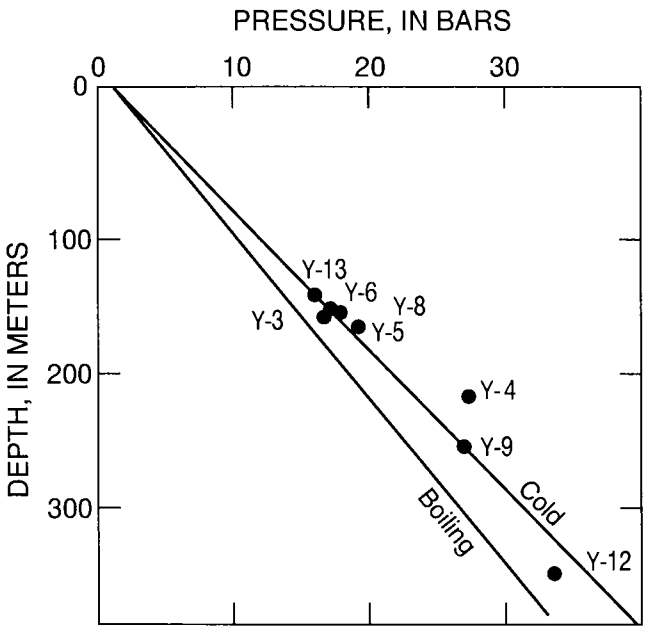

Figure 8. Measured pressure versus depth in U.S. Geological Survey research wells drilled in Yellowstone National Park. Also shown for reference is calculated ideal hydrostatic pressure resulting from weight of a column of cold water extending up to land surface compared to ideal hydrostatic pressure resulting from weight of a column of boiling water. (From Fournier, 1983).

equal to or greater than the hydrostatic pressure that would be exerted by a column of cold water extending downward from the Earth's surface (fig. 8). Pressures in excess of those calculated for hot-water hydrostatic conditions with free discharge at the surface result from throttling of fluid flow at and near the points of spring discharge.

Compositionally the discharging alkaline-chloride waters at West Thumb are virtually identical to the Black Sand-type waters (Fournier, 1989) found in the Upper and Lower Geyser Basins. In table 2, compare the analysis of Lakeshore Geyser water (No. 2) at West Thumb with the analysis of Punch Bowl water (No. 6), a Black Sand-type water, in the Upper Geyser Basin. These waters have nearly identical molar ratios of bicarbonate/chloride and relatively low chloride concentrations. Silica and cation geothermometers indicate a reservoir temperature of about 200 to 210°C.

Waters emerging in different springs and geysers commonly undergo different degrees of boiling and steam loss on the way from the reservoir to the surface. These different amounts of steam loss account for the variations in the

Table 2. Chemical analyses of selected thermal waters from Yellowstone National Park.

[—, no data]

Analysis No.	1	2	3	4	5	6	7	8	9	10
Locality	Mammoth Hot Springs	West Thumb	Shoshone Basin	Heart Lake Basin	Lower Geyser Basin	Upper Geyser Basin	Upper Geyser Basin	Grand Canyon	Norris Geyser Basin	Norris Geyser Basin
Name	Y–10 drill hole	Lakeshore Geyser	Washtub Spring	Unnamed	Ojo Caliente	Punch Bowl	Ear Spring	Unnamed spring at Sevenmile Hole	Porcelain Terrace	Cinder Pool
Sample No.	Y-10	J7484	T7214	T7348	J7560	J7836	J7956	J7615	J7528	J7908
Date	09/13/69	10/09/74	09/72	09/73	—	—	—	09/29/76	—	—
Temp. (°C)	70	90	81	93.5	95	94	94	91	93.5	92
pH	7.48	7.76	9.00	9.48	7.74	8.33	8.49	8.61	—	3.57
SiO_2 (mg kg^{-1})	88	—	328	366	230	312	371	534	654	329
Al	0.01	—	0.14	—	—	—	—	—	0.06	—
Fe	2.4	—	0.05	—	—	—	—	—	—	—
Ca	450	2.0	0.4	0.9	0.75	0.67	0.82	0.5	2.12	6.3
Mg	80	0.51	0.05	0.01	0.01	0.02	0.01	0.02	0.03	0.12
Na	161	408	365	382	330	420	319	366	404	346
K	69	20	16	21	10	17	27	58	81	81
Li	1.8	3.24	1.0	6.6	3.6	3.8	4.9	3.45	5.8	3.9
NH_4	1.0	—	0.1	—	—	—	—	—	—	—
HCO_3	997	531	406	306	246	590	146	223	47	0
SO_4	800	55	48	100	26	19	19	85	31	147
Cl	171	261	328	365	326	289	415	427	669	569
F	4.2	14.5	25.5	36	30	28	24	12.8	5.8	6
B	3.8	3.3	2.8	2.4	3.8	3.8	3.6	16	9.9	8
Reference	1	2	3	3	2	2	4	2	2	4

Analysis No.	11	12	13	14	15	16	17	18	19	20
Locality	Norris Geyser Basin	Crater Hills	Upper Geyser Basin	Hot Springs Basin	Josephs Coat Hot Springs	Josephs Coat Hot Springs	Upper Geyser Basin	Boundary Creek	Washburn Hot Springs	Washburn Hot Springs
Name	Echinus Geyser	Crater Hills Geyser	Iron Spring	Unnamed	Unnamed	Unnamed	Hillside group	Unnamed	Unnamed	Unnamed
Sample No.	J7846	J7804	—	YF448	YF451	YF452	T9-10	J7930	J7304	YF429
Date	—	09/28/78	1920s	06/22/69	06/26/69	06/26/69	—	—	09/22/73	06/22/69
Temp. (°C)	93	88	91	89	86	94	83	92	91	86
pH	3.2	3.18	3.7	2.66	1.82	9.38	8.62	7.94	8.00	—
SiO_2 (mg kg^{-1})	278	676	365	317	333	238	170	210	247	—
Al	0.60	—	—	—	—	—	0.13	—	—	0.2
Fe	—	—	—	—	—	—	—	—	—	—
Ca	4.9	5.64	2	37.1	4.1	3.4	7.9	4.1	2	17.2
Mg	0.52	1.04	Trace	3.75	0.39	0.01	0.27	0.10	4.10	9.3
Na	166	640	77	187	7	109	150	181	9.7	27.1
K	50	133	28	16	17.1	19	7.7	11.2	6.5	13.7
Li	0.7	6.9	—	0.04	0.01	0.18	0.83	1.2	0.1	0.1
NH_4	—	—	4	171	57.3	22.4	0.1	0.51	270	658
HCO_3	0	0	0	0	0	335	251	259	107	8.2
SO_4	337	566	231	1530	1830	24	14.2	10	900	1950
Cl	108	890	1	0.1	0.1	5.4	72	107	7	2
F	5.6	27.5	1.2	0.8	—	3.7	12	19.1	0.1	0.5
B	3.0	20	2.2	5.05	0.07	0.36	1.17	1.0	6.6	7.84
Reference	4	4	5	3	3	3	3	6	3	5

References:
(1) Unpublished data, U.S. Geological Survey (R. Barnes, analyst).
(2) Thompson and Yadav (1979).
(3) Thompson and others (1975).
(4) Unpublished data, U.S. Geological Survey (J. M. Thompson, analyst).
(5) Allen and Day (1935).
(6) Thompson and Hutchinson (1980).

absolute concentrations of the elements found dissolved in the alkaline-chloride thermal waters.

Mud pots and (or) cloudy to muddy nonoverflowing pools of water (acid-sulfate in composition) tend to be present at higher elevations in West Thumb and other geyser basins, and discharging silica-depositing alkaline-chloride waters are present at lower elevations. The acid-sulfate waters occur where H_2S in steam condensate has been converted to sulfuric acid by bacterial activity. Acid attack on the surrounding rock produces clays and muds that diminish vertical permeability and allow perched bodies of ground water to form and persist. Even though these acid-sulfate

bodies appear to be nondischarging, tracer studies show that there is considerable horizontal flow of water into and out of these springs (Brock, 1978). The acidity comes from bacterial oxidation of native sulfur and H_2S to H_2SO_4 in the cool muds surrounding the boiling pools.

The yellow, orange, and green colors seen in some of the pools and bordering the runoff channels are commonly referred to as "algae" mats but are actually bacteria colonies. The higher the temperature of the water, the lighter the color of the bacteria mat. Notice that silica deposits on and in these organic mats yield spongy sinter deposits that are characteristic of this environment of deposition.

STOP 5—OLD FAITHFUL LODGE CABINS, UPPER GEYSER BASIN

Explore Geyser Hill and see an eruption of Old Faithful Geyser before dinner.

Background information on the geology and hydrothermal activity in the Upper to Lower Geyser Basin region.—The western part of the Yellowstone caldera is drained by the Firehole River, which flows northward through a series of large open valleys, including the Upper (fig. 9) and Lower Geyser Basins and narrow constrictions that have been formed by incomplete merging of postcaldera lava flows that have advanced from different directions. The hills surrounding the valleys are part of a general constructional volcanic topography of the Madison and Central plateaus. Generally, the uppermost parts of the hydrothermal plumbing systems of the geyser basins occur in surficial deposits that are composed mostly of sand and gravel deposited during the last (Pinedale) glaciation. However, in some places hot springs and geysers issue directly from rhyolitic bedrock. The road along the river between Old Faithful and Madison Junction provides access to the most outstanding display of hydrothermal features in the world, including more than two-thirds of all known naturally erupting geysers. Measurements of Firehole River flow rates and compositions above and below individual geyser basins, combined with information about hot-spring underground reservoir temperatures and water compositions, has allowed estimates to be made of the total mass and heat flux from individual basins (table 1).

In the Old Faithful area of Upper Geyser Basin, views from Old Faithful Inn and from the walkway between it and the National Park Service Visitor Center show the geologic setting of the basin between rhyolitic lava flows of the Madison Plateau to the west and the Mallard Lake structural dome to the east. A graben that branches from the axis of the Mallard Lake dome is apparent on the skyline east of Old Faithful. This dome, rejuvenating the postcollapse western resurgent dome, rose early in the renewed voluminous rhyolitic volcanism of the past 150,000 years. Plagioclase-rich older postcollapse rhyolites crop out around the west and south base of the structural dome and form the poorly exposed bedrock of Upper Geyser Basin, but the uplifted 150,000-year-old sanidine-rich Mallard Lake flow tops the dome (fig. 10). The Elephant Back flow, also about 150,000 years old, partly buries the east flank of the dome, demonstrating the dome's rapid rise early in the period of renewed rhyolitic activity.

Old Faithful, Yellowstone's best known geyser, is but one of dozens in the Upper Geyser Basin. A list of selected active geysers as of spring 1992 is given at the back of this field guide (see appendix B). Geysers are springs that erupt intermittently. Much of our understanding of geyser activity comes from the classic work of White (1967). It is conceivable that a cold spring could erupt intermittently as a

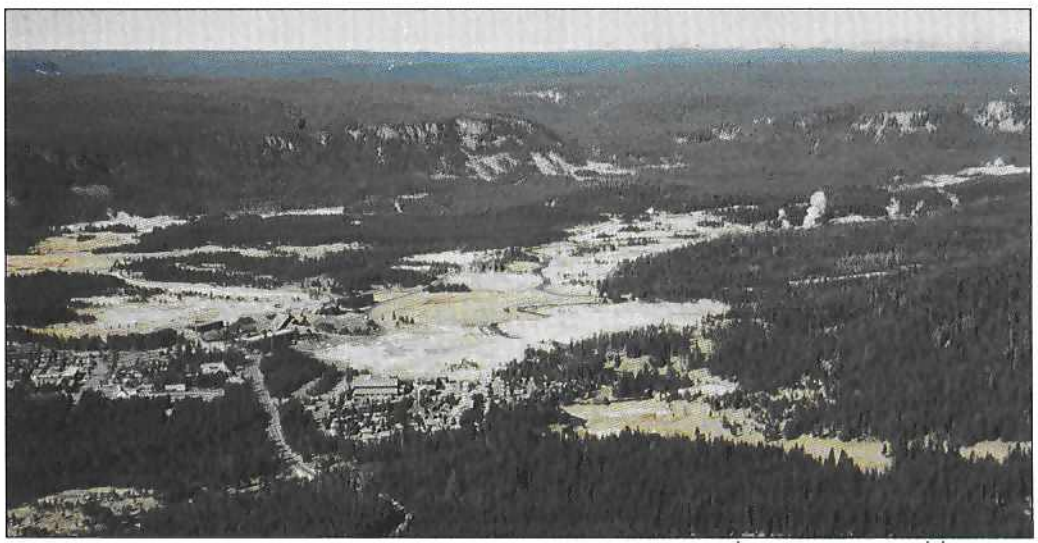

Figure 9. Air view of Upper Geyser Basin.

geyser as a result of the slow and steady accumulation of gas in an underground cavity. At Yellowstone National Park the geysers are fed by boiling waters discharged from high-temperature deeper reservoirs in which substantial amounts of silica are dissolved from the surrounding rocks. Some understanding of subsurface hydrothermal processes, including the mechanism of geyser eruptions, is gained through the resolutions of two seeming anomalies. First,

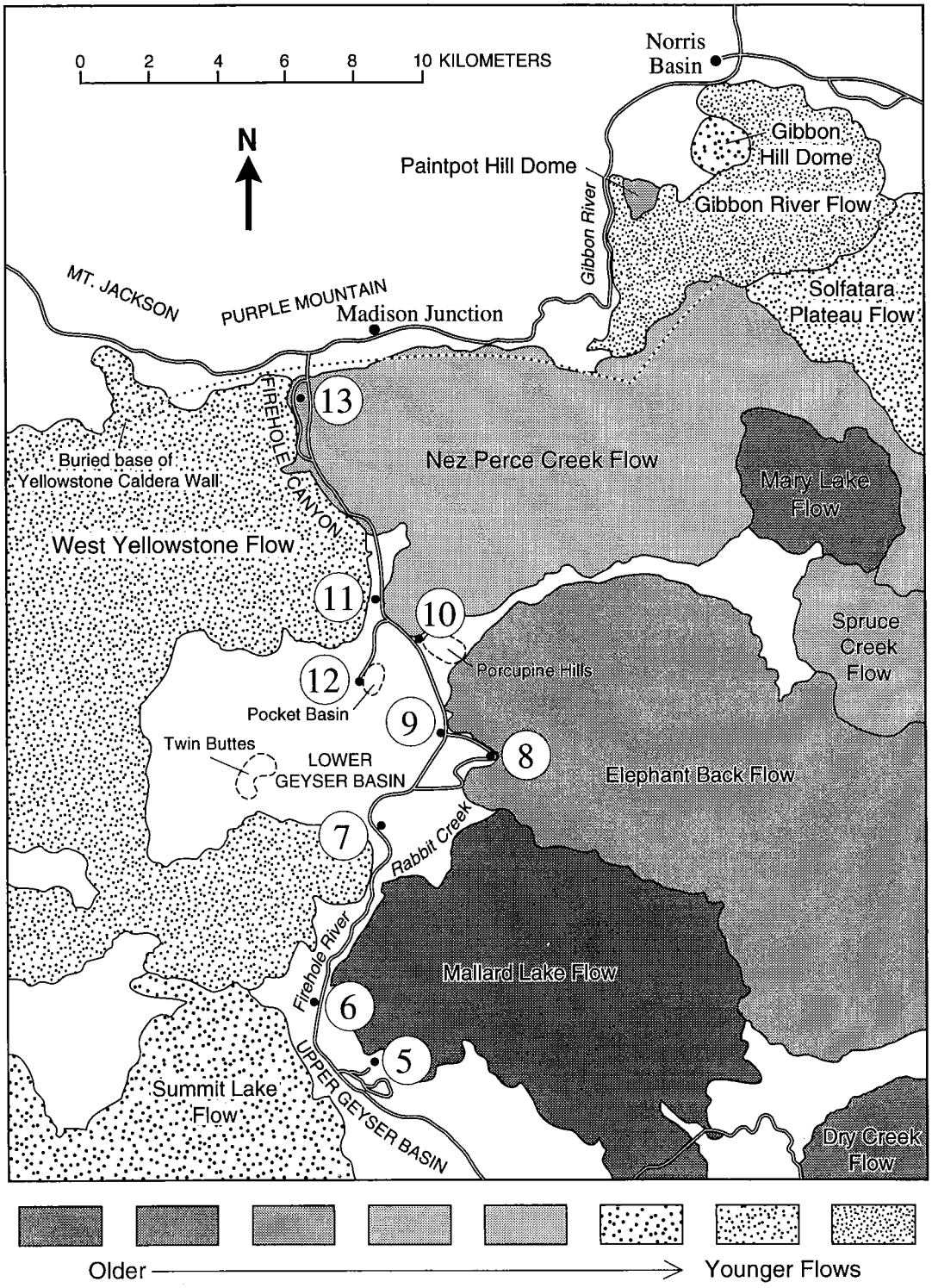

Figure 10. Geologic map showing field-trip route and stops between Upper Geyser Basin and Norris Geyser Basin. Shaded areas show named Quaternary rhyolitic lava flows and domes, with darker shades corresponding to older units. Large numbers show stop locations. (From Christiansen and Hutchinson, 1987).

neighboring springs may have nearly identical temperatures and water compositions but greatly different water levels; for example, Solitary Geyser discharges about 40 m above most springs in Upper Geyser Basin. Second, some hot springs erupt as geysers, but most do not. Research drilling in Yellowstone (White and others, 1975) showed that below about 30 m most reservoirs are "overpressured" relative to calculated ideal hot-water hydrostatic pressure (fig. 8) as a result of partial "self-sealing" of the water-bearing fractures by precipitated silica and zeolites. Water levels are controlled by permeabilities and flow rates in the upflow channels, which are regulated through the competing effects of seismic fracturing and self-sealing and by subsurface outflow (leakage) near ground level. In general, the rate of discharge of water from deep in the system would be faster than the actual rate of discharge if upflow in the shallow part of the system were not restricted by a series of throttles. Pressure discontinuities that occur across these throttles result in the observed overpressures in the shallow parts of the hydrothermal system. The net result is boiling-point temperatures above those expected for local hydrostatic load and very unstable conditions in which massive boiling and rapid discharge of water can be triggered as a result of a slight pressure decline. Such a pressure decline may result from the opening of a new fracture or widening of an old fracture during an earthquake or by the upward surge of a slug of steam that displaces water from a geyser tube.

In the Upper Geyser Basin a typical boiling spring, discharging at 92°C, rises from a subsurface reservoir where the temperature is near 205 to 215°C. The rising water cools by more or less steady-state processes including loss of heat by conduction through the channel walls, adiabatic expansion (boiling) as pressure declines during upflow, and evaporation from the hot-spring pool. In contrast, non-steady-state processes prevail in order for geyser activity to occur (White, 1967). There is likely to be cycling from mainly conductive cooling (a geyser eruption not imminent) to mainly adiabatic expansion (little conductive cooling and initiation of a geyser eruption imminent). The following scenario is typical of many geyser eruptions and draws heavily upon the model of White (1967). At the start of a cycle, shortly after a geyser eruption has occurred, water from deep in the system flows upward and refills a shallow water-holding reservoir immediately below the geyser. Continued convective flow heats the surrounding rock until the entire water-rock system is at the boiling-point curve for the prevailing fluid pressure. There is a progressive change from mainly conductive cooling to mainly adiabatic boiling of the upflowing fluid. With the increase in boiling there is an increase in the amount of steam that is formed. Early in the cycle, bubbles composed of steam and noncondensable gas, such as CO_2, that form in the upward convecting fluid rise through the overlying water column. However, with less conductive cooling the mass fraction of steam steadily increases, and eventually steam starts to move upward through the geyser tube as a slug, lifting and ejecting the overlying water. As a slug of gas bubbles reaches the surface there is a momentary decline in pressure within the geyser tube, and this reduction in hydrostatic head may be sufficient to cause flashing (rapid conversion of liquid water to steam) in the shallow reservoir, resulting in the expulsion of large quantities of water. This expulsion results in further reductions in pressure deeper in the system, and a chain reaction of rapid boiling at ever greater depths is initiated. During an eruption, water and heat are discharged much faster from the shallow holding reservoir than they are recharged, requiring a time of repose between eruptions to "reload" the system.

A variety of behavior in major geysers can be observed in Upper Geyser Basin, including (1) eruptions that average 27 m in height from the large sinter cone at Castle Geyser, (2) eruptions to average heights of 60 m from Grand Geyser, which fountains through a broad pool, and (3) eruptions from Riverside Geyser, which jets a water column about 22 m high at an angle over the Firehole River. Figure 11 shows an eruption of Beehive Geyser, one of the larger geysers on Geyser Hill. Old Faithful has particularly interesting eruptive intervals that are a function of the duration of the preceding eruption. Eruption durations are bimodally distributed between 1.5 and 5.5 minutes; long eruptions are followed by long intervals (70–120 minutes) whereas short eruptions are followed by short intervals (30–65 minutes). The 40-m-tall average height of Old Faithful eruptions is independent of eruptive interval or duration.

DAY 2—UPPER, MIDWAY, AND LOWER GEYSER BASINS

The entire day will be spent in the Upper, Midway, and Lower Geyser Basins. Figure 10 shows the locations of planned stops. The walks will not be strenuous. **Wet and muddy ground may be encountered at Pocket Basin.**

Typical compositions of thermal waters in the Upper and Lower Geyser Basins are shown in tables 2 and 3. Figure 12 shows schematically the likely hydrologic conditions within the hydrothermal system(s) beneath Upper, Midway, and Lower Geyser Basins. Knowledge of the changing behavior of CO_2 dissolved in thermal water with decreasing temperature is vital to understanding variations in composition of hot-spring waters in the Yellowstone region. At temperatures of 270°C and higher, most CO_2 dissolved in water is nonreactive. As temperature decreases, CO_2 reacts with water to form H_2CO_3, and with further cooling, the H_2CO_3 dissociates to H^+ and HCO_3^-. At about 200 to 220°C, hydrolysis reactions involving the hydrothermal fluid and minerals in the wall rock consume much of the H^+ and liberate an equal number of moles of Na^+, yield-

ing dissolved sodium bicarbonate. Now consider the flow paths and reservoir temperatures shown in figure 12. There is good evidence from enthalpy-chloride relations that an intermediate reservoir (or multiple reservoirs) at about 270°C is present beneath the Upper and Lower Geyser Basins and that in some places water boils as it moves from that reservoir to shallower and lower-temperature reservoirs. All or most of the steam and noncondensable gas, such as CO_2, that separate from boiling water flowing upward toward the 215°C reservoir beneath Geyser Hill takes a separate path to the surface so that the portion of the boiling water that reaches the Geyser Hill reservoir is depleted in CO_2 and gas, in general. Thus, there is little CO_2 available to form carbonic acid that would otherwise react to form sodium bicarbonate. Some waters that flow to the surface from the Geyser Hill reservoir undergo maximum boiling (adiabatic expansion), other waters cool entirely by conductive loss of thermal energy to the surrounding rock, and still others cool partly by boiling and partly by condensation. The range in concentrations of dissolved constituents that results from no boiling at one extreme to maximum boiling at the other provides a powerful method of estimating temperatures of subsurface reservoirs that feed the springs. This method relates temperature to the specific heat, or enthalpy, of the reservoir fluid and to the amount of steam that can separate from a superheated fluid as it decompresses during upflow. See Fournier (1989, p. 25–28) for a discussion of the use of enthalpy-chloride and enthalpy-silica diagrams to estimate reservoir temperatures beneath the Upper Geyser Basin. In contrast to the hydrothermal fluids that emerge at Geyser Hill, waters flowing from the 270°C reservoir toward Black Sand-type reservoirs (about 205°C and $Cl \approx HCO_3^-$ in equivalents) either do not boil as they flow upward, or most of the steam that forms stays with the liquid until reaching the shallower Black Sand-type reservoir. This fluid does have significant quantities of CO_2 available for subsequent reaction with rock to form sodium bicarbonate. Thus, the Geyser Hill-type waters and the Black Sand-type waters flow to the surface from reservoirs that are not greatly different in temperature (about 215°C versus about 205°C), but they are greatly different in Cl/HCO_3. Partial loss of steam or partial conductive cooling in migration from a deeper reservoir to a shallower Black Sand-type reservoir will result in waters with intermediate Cl/HCO_3 ratios. Indeed, regions of intermediate Cl/HCO_3 are found between Geyser Hill-type and Black Sand-type waters. $^3He/^4He$ isotopic data are compatible with the above model in that ^3He is relatively depleted in waters that have high Cl/HCO_3 ratios, a condition which is indicative of underground loss of CO_2 and other gases (Kennedy and others, 1987). Most of the steam that takes a separate path toward the surface condenses in ground water at high elevations, yielding $NaHCO_3$-rich waters, such as those discharging at Hillside Springs. Some of this steam discharges directly to the atmosphere through acid-sulfate pools that become acid as a result of oxidation of H_2S carried in the steam.

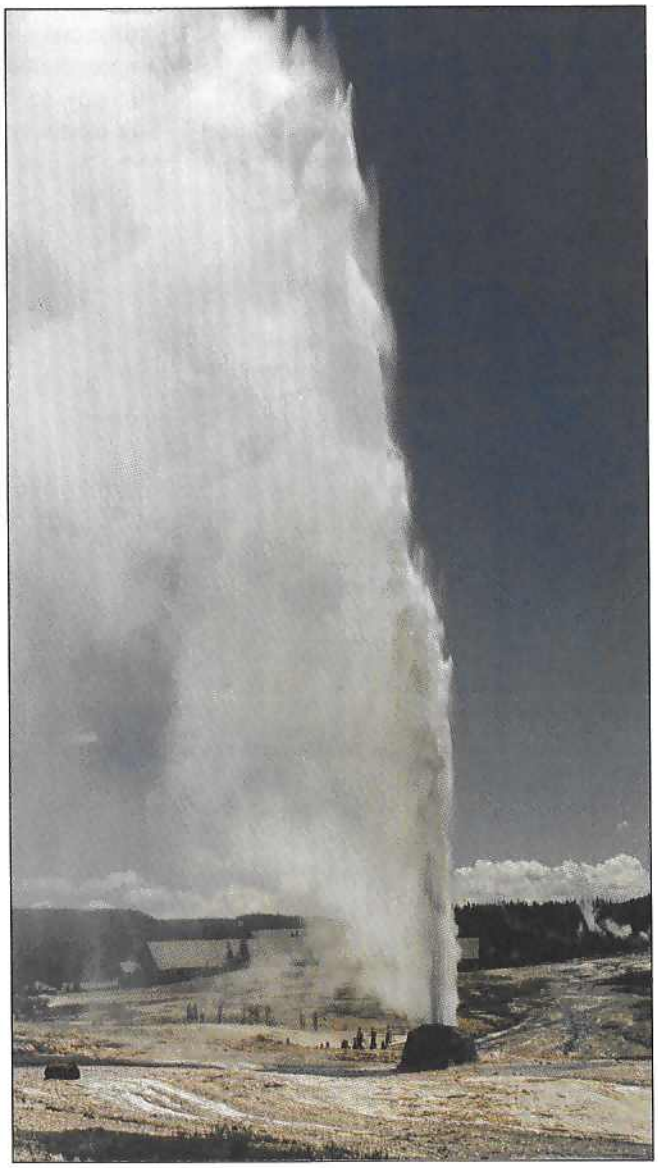

Figure 11. Beehive Geyser in eruption, Geyser Hill, Upper Geyser Basin.

Variations in rock type conceivably also may affect Cl/HCO_3 ratios in the Upper and Lower Geyser Basins. In the Upper Geyser Basin, the thermal waters at Geyser Hill emerge directly from lithic rhyolite, whereas those at the Black Sand Basin emerge from obsidian-rich sands, and it is possible that glassy volcanic sediments may play a role in "fixing" CO_2 as HCO_3^-. However, in the Upper Geyser Basin it is likely that the reservoirs supplying water to the Black Sand-type waters ($Cl/HCO_3 \approx 1$) and to the Geyser Hill-type waters ($Cl/HCO_3 \geq 3$) are well within the underlying rhyolite flow or flows. In these reservoirs, water/rock reactions occur that fix Cl/HCO_3 ratios, dissolved silica,

and cation ratios at temperatures of 200 to 215°C. The geologic map of the Old Faithful quadrangle (Christiansen and Blank, 1974) shows that the Biscuit Basin flow underlies much of the Upper Geyser Basin, including Geyser Hill. This flow is a perlitic vitrophyre of flow-brecciated rhyolite. It appears to underlie all or most of the other flows that surround Upper Geyser Basin. Thus, it is likely that all or most of the waters in the Upper Geyser Basin come in contact with this rhyolite that initially contained abundant glass. Although it is true that many of the Geyser Hill-type waters emerge directly from this rhyolite (and from the Mallard Lake flow) with no overlying obsidian sediments, other Geyser Hill-type waters do not, such as a group of springs to the west of the Old Faithful Inn. Also, in some places Black Sand-type waters emerge from rhyolite with no apparent overlying obsidian-rich sediments. For the above reasons, variations in rock type probably play a minor, if any, role in fixing Cl/HCO_3 ratios. The most plausible explanation for the differences in Cl/HCO_3 ratios exhibited by the Upper and Lower Geyser Basins' waters appears to be different degrees of subsurface boiling and escape of CO_2-rich steam prior to the thermal water entering the shallowest reservoir directly supplying fluid to the springs and geysers.

STOP 6—BISCUIT BASIN

Sites of the Y–7 and Y–8 drill holes and small modern hydrothermal explosions.—The Biscuit Basin parking lot is situated at the northern downstream margin of the Upper Geyser Basin hydrothermal system. Here about 50 to 55 m of hydrothermally altered obsidian-rich bedded sands and gravels overlie altered rhyolite flow breccia and associated pumiceous tuff of the Biscuit Basin flow (Keith and others, 1978). The sediments probably are outwash stream deposits from receding glaciers of Pinedale age; Black Sand-type water (fig. 12) discharges here. Figures 13 and 14 show subsurface temperatures and hydrothermal alteration products (mostly zeolites and clays) encountered in the USGS research drill holes Y–7 (a relatively cool well at the north end of parking lot) and Y–8 (a relatively

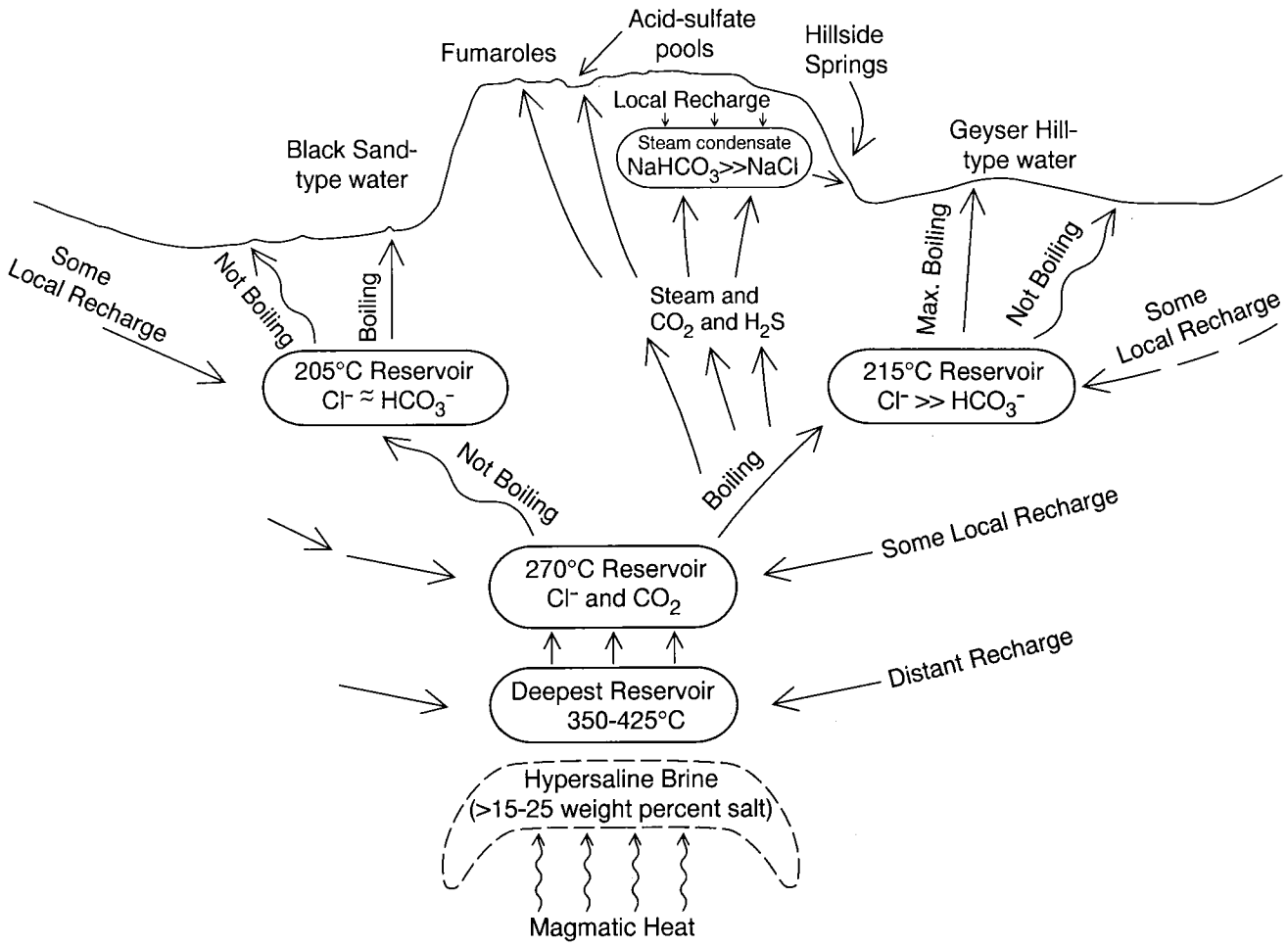

Figure 12. Schematic diagram showing approximate reservoir temperatures beneath Upper and Lower Geyser Basins and effects of subsurface boiling with steam loss on bicarbonate relative to chloride in the shallowest reservoirs.

hot well only 125 m away at the southeast margin of parking lot, near a cluster of hot springs and small geysers). The zeolites are dominantly clinoptilolite and mordenite, and the clays are dominantly montmorillonite and celadonite. Positive wellhead pressures were encountered in the Y–8 drill hole (the well erupts like a geyser when the wellhead valve is opened), whereas water does not flow from the Y–7 drill hole when the wellhead valve is opened. The

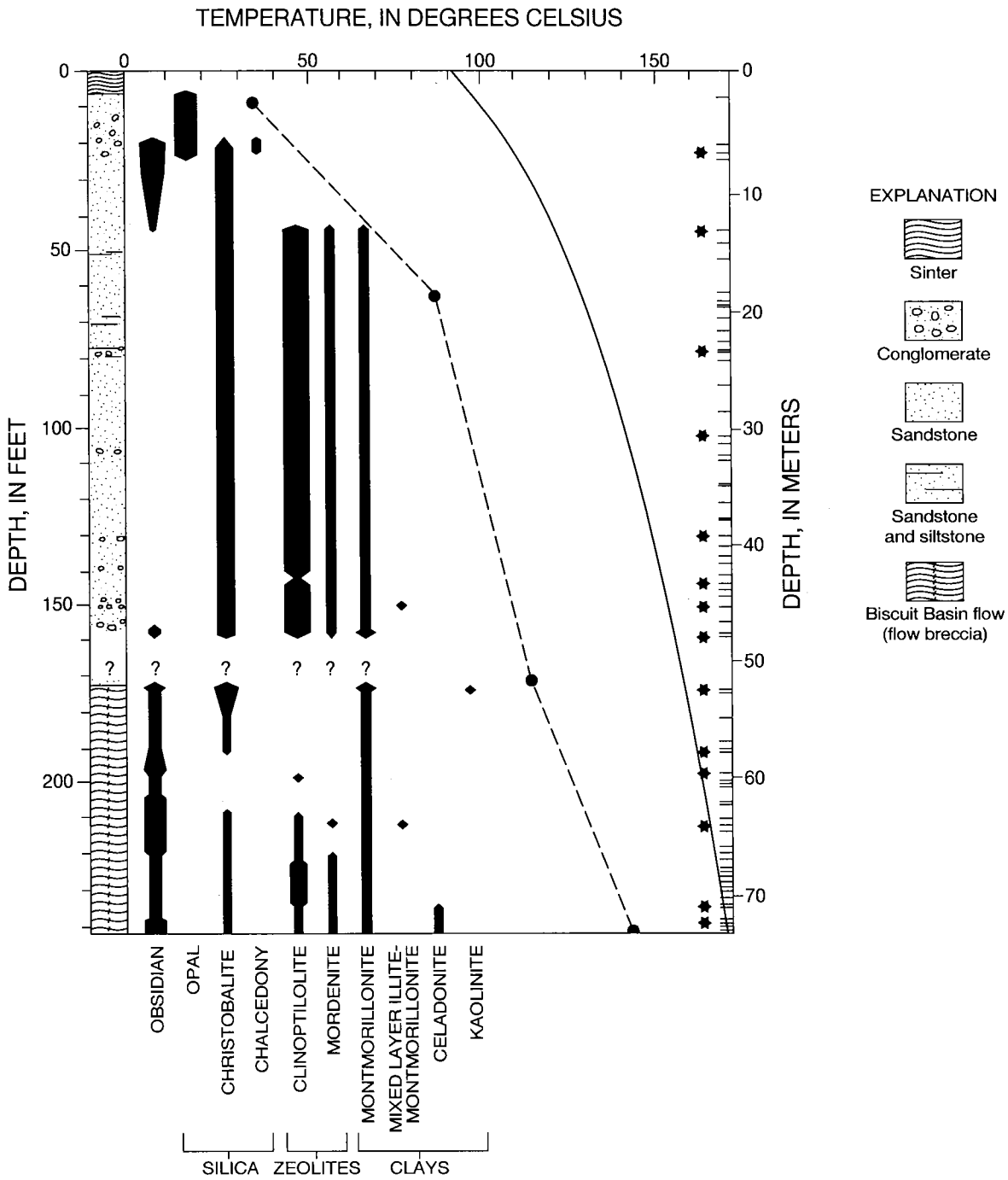

Figure 13. Distribution of fresh obsidian and hydrothermal minerals in groundmass of core from U.S. Geological Survey Y–7 drill hole. Column on left shows generalized stratigraphic section. Horizontal lines at right indicate samples studied in detail, and starred samples were chemically analyzed for major elements. Width of mineral columns shows relative abundance based mainly on X-ray diffraction data and petrographic study. Interpolation between data points assumes linear variation. Dashed line connects data points of bottom-hole temperatures, and solid line is reference boiling curve for pure water. (From Keith and others, 1978, p. A7).

water level in the Y–7 drill hole rises and falls as the water level in the Firehole River seasonally rises and falls. Subsurface temperature relations between the two drill holes are shown in figure 15. Whole-rock samples of rhyolite from the Y–7 and Y–8 drill holes have been studied for Th–U isotope disequilibrium by Sturchio and others (1987) and for Ra–Th isotope disequilibrium by Sturchio and others (1989). These authors conclude that U was added to the rock about 19,000 years ago, but thereafter the system became "closed" to U transport when pore-water chemistry changed from oxidizing (surface water) to reducing (thermal water). The $^{226}Ra/^{230}Th$ ratios correlated with Th-normalized Ba concentrations (Sturchio and others, 1989). These data indicated that zeolite-water ion exchange has been operating for at least 8,000 years in the Y–7 and Y–8 region and that a water flux ranging from about 2.5 to 23

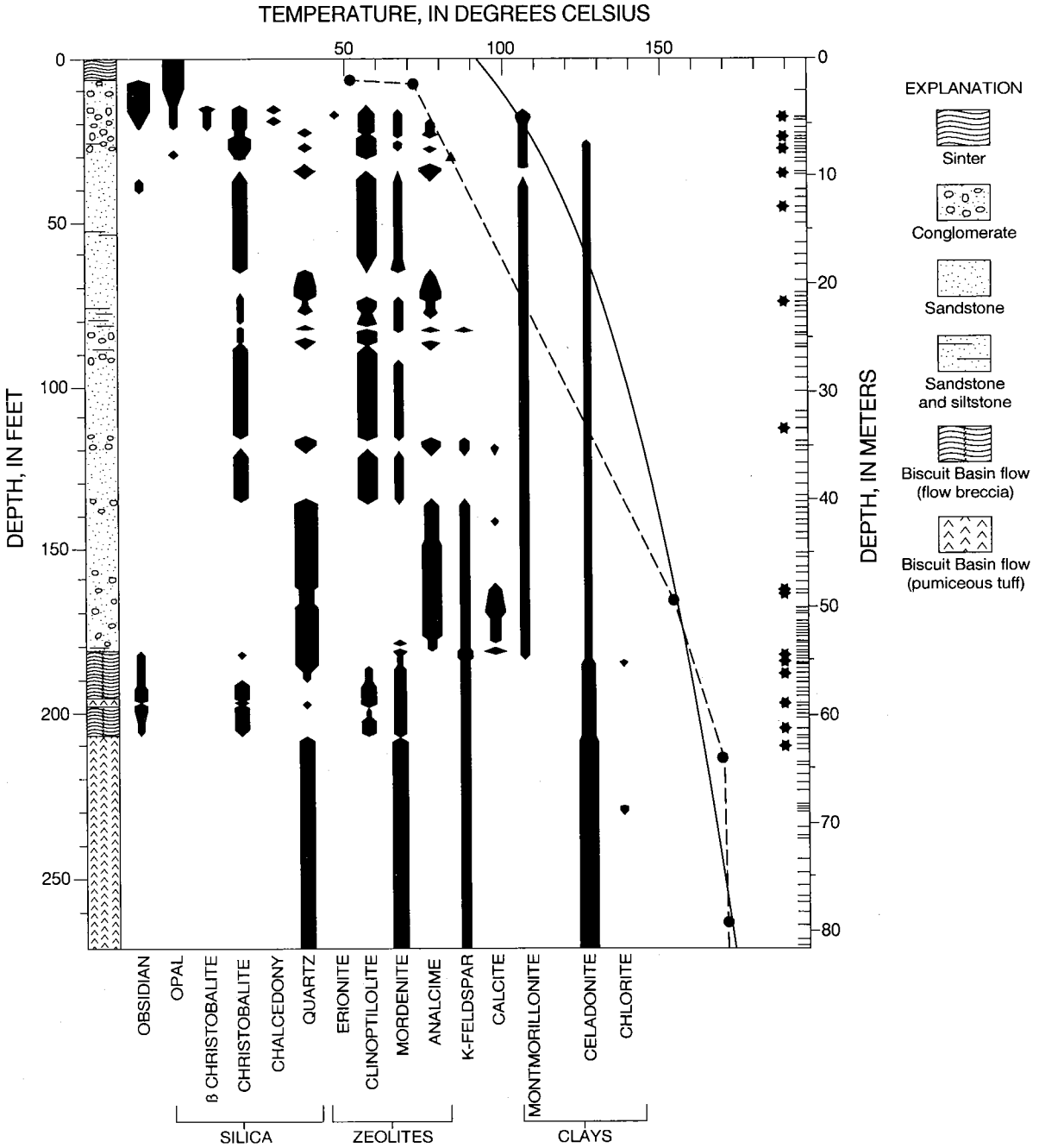

Figure 14. Distribution of fresh obsidian and hydrothermal minerals in groundmass of core from U.S. Geological Survey Y–8 drill hole; data shown in same manner as in figure 13. Depths below 82.3 m not shown because of general uniform alteration mineralogy from 63.0 to 153.4 m depth. (From Keith and others, 1978, p. A8).

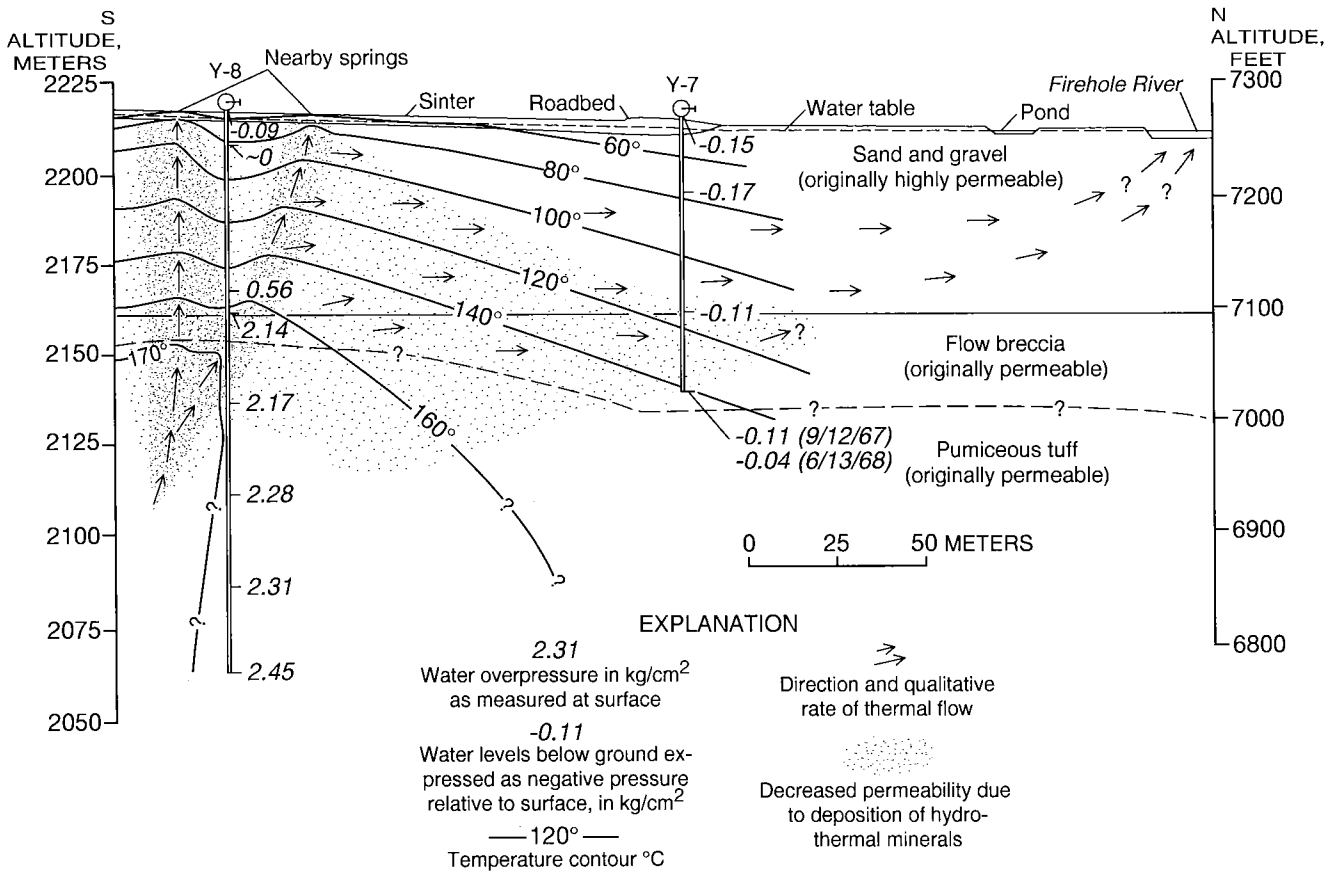

Figure 15. Section through U.S. Geological Survey Y–7 and Y–8 drill holes, showing pressures, temperature contours, and inferred self-sealing by deposition of hydrothermal minerals in originally permeable ground (from White and others, 1975, p. 21).

$(cm^3_{water}/cm^3_{rock})yr^{-1}$ is required over that period of time to account for the isotopic compositions (Sturchio and others, 1989). It appears that during the climactic stage of the Pinedale glaciation (20,000–40,000 years ago; Pierce, 1979) cold-water recharge into the hydrothermal system took place in the Biscuit Basin region (the margin of the hydrothermal system). Later, as the ice melted, the direction of fluid flow reversed and the region became one of discharge.

Proceed across the bridge over the Firehole River and go only as far as Sapphire Geyser. On the west side of the Firehole River, to the north side of the boardwalk, a few large blocks of zeolite-cemented sands and gravels can be seen lying on the ground near Black Opal Pool, a large pool of warm water (fig. 16). This pool and adjacent Wall Pool are hydrothermal explosion craters that emerged in the spring of 1925 and that may have been deepened by additional eruptions during the winter of 1931 to 1932. Sapphire Pool/Geyser Crater is located farther uphill on the north side of the boardwalk. Prior to the 1959 magnitude-7.5 Hebgen Lake earthquake that was centered a few kilometers outside the western boundary of Yellowstone Park (fig. 1), Sapphire was a relatively small boiling spring. A

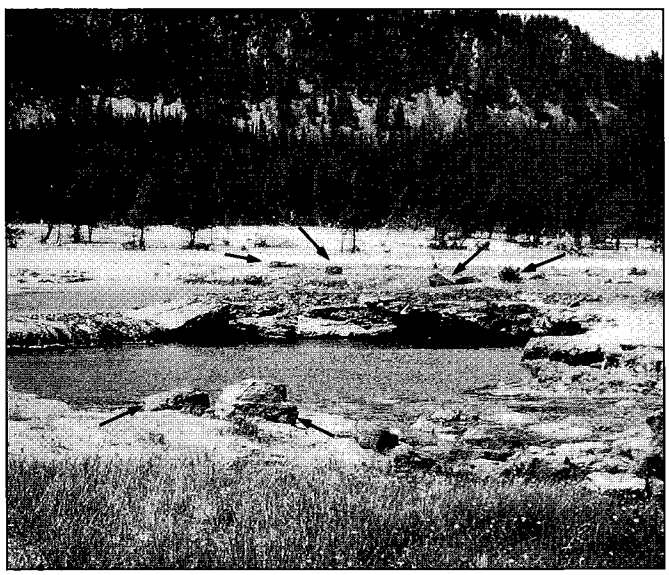

Figure 16. Blocks of zeolite-cemented sediments (arrows) blown from Black Opal Pool, Biscuit Basin.

Table 3. Chemical compositions (mg/kg) of selected thermal waters in Lower Geyser Basin.

[Compositions of waters from the drill holes probably have been affected by reactions at uncertain temperatures between water and "fresh" rock in uncased parts of wells. —, no data]

Name	SiO_2	Na	K	Ca	Mg	Li	Cl	SO_4	HCO_3	F	B
Steady Geyser	213	85	16	15.10	0.05	0.4	44	27	165	10	0.5
Surprise Pool	280	333	15	0.47	0.14	3.2	313	25	365	24	3.1
Clepsydra Geyser	414	380	13	0.50	0.01	2.8	325	22	380	22	3.5
Spring by Y–13	222	341	19	0.77	0.01	4.6	312	23	274	31	4.3
Y–13 drill hole	—	299	28	1.50	0.22	3.7	256	31	291	28	3.2
Ojo Caliente	230	317	9	1.10	0.02	4.5	331	27	249	33	4.0
Y–3 drill hole	—	270	11	1.26	0.02	3.5	278	19	177	30	3.6

short time after the earthquake it erupted explosively, enlarging its pool size to that which you see today and sending a sheet of boiling water about 0.3 m deep surging downhill to the south. Many large blocks of sinter were left scattered about the terrace after the explosion, but as these blocks have dried out, they have disintegrated and are quickly disappearing.

STOP 7—MIDWAY BASIN

Excelsior Geyser Crater and Grand Prismatic Spring.—Rhyolitic flow-front scarps of the 117±8-ka West Yellowstone flow emplaced between the last two glaciations (Bull Lake and Pinedale glaciations) form the valley walls to the west. Just across the river is the Midway Geyser Basin, where Excelsior Geyser Crater discharges boiling waters to the Firehole River. The crater was enlarged to its present size by eruptions of water and debris, some of which was ejected as far as 150 m from the crater, during 1878 and the 1880's. **Cross the river and follow the boardwalk past Excelsior Geyser Crater and Grand Prismatic Spring.** The first eruptions of Excelsior since the 1880's were in the summer of 1985. Grand Prismatic Spring, just beyond, is nearly 90 m across and reveals graded colors from the clear blue boiling waters of its center to lower-temperature bands around its margins that are brightly colored by cyanobacteria. In the distant southwest is Twin Buttes, formed of hydrothermally cemented Pleistocene glacial sediments deposited by localized hydrothermal melting of the ice. The buttes enclose a complex hydrothermal explosion crater. The crater eruptions were not hydromagmatic but were strictly hydrothermal, probably occurring as the hydrostatic head in a glacial thermal lake was catastrophically lowered during one or more glacial-outburst floods (Muffler and others, 1971). The large obsidian-sand plain filling the West Yellowstone basin probably was built by the same, or similar, glacial-outburst floods (Pierce, 1979). Beyond Lower Geyser Basin, the skyline ridge along Mount Jackson and Purple Mountain is the northwest rim of the Yellowstone caldera (fig. 10).

Across the road from the parking area, a conspicuous bluff exposes perlitic glassy rhyolite with well-developed flow layering. This plagioclase-rich early postcollapse rhyolite probably was emplaced into a caldera lake. Most of the glassy intracaldera rhyolites of Yellowstone are virtually nonhydrated and obsidianlike, though commonly fractured. The hydrated perlitic glass of this outcrop is suggestive of high-temperature hydration, which probably occurred during emplacement of this rhyolite flow. This observation supports the interpretation that the flow was emplaced into a caldera lake. (Similar perlites can be seen farther east in Yellowstone Park, where the younger Hayden Valley flow plowed into and was diked by the plastic sediments of a glacial lake.)

STOP 8—FIREHOLE LAKE AND STEADY GEYSER

Steam-heated waters depositing travertine and manganese-oxides.—You have come slightly uphill from where sinter-depositing hot springs and geysers prevail. Large parts of the Midway and Lower Geyser Basins are floored by sinter or silica-rich silts composed mainly of diatom tests. At the head of the small valley where Firehole Lake is located there is a large discharge of relatively dilute thermal water that now precipitates travertine and manganese oxides. At an earlier time, however, silica-depositing hot-spring activity occurred here. No stream of cold meteoric water flows from the narrow valley that extends to the east. Apparently, meteoric water in this local drainage basin mostly infiltrates into the ground, where it becomes heated to about 170°C by interaction with and condensation of CO_2-rich superheated steam that flows upward from the deeper boiling chloride-rich water (fig. 12). The CO_2-rich mixture of heated ground water and steam condensate reacts with the surrounding rock, extracting Ca as it flows laterally to discharge points at elevations above the discharge points of the alkaline-chloride springs. Compare the composition of water from Steady Geyser with Surprise Pool (table 3). The tritium content of Steady Geyser was studied by Pearson and Truesdell (1978). In 1970

its water contained about 7 tritium units (Tu), and in 1974 about 9 Tu. They concluded that this change in tritium with time cannot be explained by a simple model of mixing of waters from a well-mixed tritium-bearing reservoir and zero-tritium water. **Walk along the boardwalk to get a close view of Steady Geyser.**

STOP 9—FOUNTAIN PAINT POT WALK

Hot springs, geysers, fumaroles, and mud pots.—The Fountain Paint Pot area is the most convenient place in Yellowstone Park where one short walk displays good examples of the four principal types of hydrothermal discharge features—hot springs, geysers, fumaroles, and mud pots. Distributions of these discharge features allow relations between the ground surface and local static water levels in the boiling system to be readily inferred. The large, clear hot springs are chloride-rich and nearly neutral, representing unrestricted discharge of hot waters from a reservoir. Geysers result from the effects of variations in plumbing geometry, discharge rate, and heat loss in the hot-spring system. Fumaroles (steam vents) discharge through fractures where only vapor finds access to the surface. New fumaroles were opened here during the magnitude-7.5 Hebgen Lake earthquake of 1959. During dry seasons, the fumaroles vent only vapors. In wet seasons, shallow condensation of steam mixed with locally derived meteoric water can drown the fumaroles, and the oxidation of H_2S forms small acid-sulfate hot springs. The acid waters attack their enclosing rocks and, with enough decomposition of the rocks, form mud pots or (with ferric-oxide coloration) paint pots (fig. 17).

Take the loop trail to view the hydrothermal activity. The boardwalk trail around the Fountain Paint Pot area leads to a group of geysers that share episodic exchanges of discharge function. These include Fountain, Morning, Clepsydra (fig. 18), Jet, Spasm, and Jelly geysers. For most of the time since the 1959 Hebgen Lake earthquake, Clepsydra has been a perpetual spouter rather than a true (episodically erupting) geyser. Also visible from this walk are other features of Lower Geyser Basin and its surroundings (fig. 10). Note the broad expanse of siliceous sinter. Much of the basin floor that is not sinter is diatomaceous alluvial sediment (see the geologic map of Lower Geyser Basin by Muffler, White, Truesdell, and Fournier, 1982). The wide meadows of the basin are bounded by flow-front scarps of young rhyolitic lava flows of the Madison Plateau on the west and the Central Plateau on the east. In the western part of the basin is Twin Buttes. The Pocket Basin hydrothermal-explosion crater (Muffler and others, 1971) is visible to the north as a low tree-covered rim near the center of the basin, rising as much as 21 m above the basin floor. To the northeast are the ragged Porcupine Hills, another group of hydrothermally cemented glacial hot-spring deposits. Visible 13 km to the north are the northwestern wall and rim of the Yellowstone caldera.

STOP 10—PORCUPINE HILLS AND Y–13 DRILL HOLE

Interactions of hot springs with glacial ice.—**Walk to the Y–13 drill site collared in siliceous sinter near the largest hot spring between the two Porcupine Hills.**

Figure 17. Mud pots seen at high point on Fountain Paint Pot nature walk, Lower Geyser Basin.

The Porcupine Hills are composed of sands, gravels, and cobbles that are believed to have been deposited as a result of local melting of glacial ice where hot water discharged at the base of a glacier that slowly moved across this area during the Pinedale glaciation. These sediments have been altered by hydrothermal activity and are now cemented with zeolites and clay minerals. At the time of the Pinedale glaciation, the potentiometric surface for ground water was elevated to far above the present ground surface, allowing temperatures in upflowing parts of the hot-spring system to become much hotter than at present (in otherwords, the temperature of the boiling-point curve increased at given depths). The raised potentiometric surface also allowed hot water to flow upward through the pile of glacial sediments (Porcupine Hills) that now stand well above the floor of Lower Geyser Basin. Contouring of the glacial surface indicates that ice was about 500 m thick above the Y–13 drill site during the Pinedale glaciation. Fluid-inclusion studies (Bargar and Fournier, 1988) suggest that the temperature of the fluid at the point of discharge from the earth beneath the glacier could have been as high as 240 to 250°C. Micrometer-sized particles resembling microorganisms have been found in liquid-rich fluid inclusions in hydrothermal quartz crystals in core samples from the Y–13 drill hole (Bargar and others, 1985). The fluid inclusions containing these strange particles were obtained from depths of 59.5 m, 102.1 m, and 102.5 m. The present temperature at 102.1 m is 190°C, whereas the filling temperatures of the inclusions from that depth range from 190 to 280°C. It is believed that the microorganism-like particles became trapped in pseudosecondary fluid inclusions during the last glaciation when there was vigorous upflow at this locality and when temperatures may have been below boiling because of the effect of the ice on pore-fluid pressures. Compositions of waters from the Y–13 drill hole and the boiling spring near Y–13 are given in table 3.

STOP 11—LUNCH IN LOWER GEYSER BASIN

A convenient place to eat lunch is at the Fountain Flat Drive picnic area. Restroom facilities are available.

STOP 12—THE Y–3 DRILL SITE AND POCKET BASIN EXPLOSION CRATER

Walk toward the river to Ojo Caliente spring. Caution: A thin silica crust extends over part of Ojo Caliente. The site of the Y–3 drill hole is 76 m north and 2 m higher than Ojo Caliente Hot Spring. The temperature-depth profile, stratigraphy, and hydrothermal alteration encountered in Y–3 are given in Bargar and Beeson (1985). Compositions of waters from Ojo Caliente and the Y–3 drill hole (88 m depth) are given in table 3. The reservoir supplying water to Ojo Caliente has a temperature of about 175°C. Fluid inclusions in quartz obtained from Y–3 core samples show that subsurface temperatures at this location were higher during the time of the last glaciation (Pinedale glaciation that ended 10,000 to 15,000 years ago) (Bargar and Fournier, 1988; Bargar and Beeson, 1985), and contouring of the glacial surface indicates that there was about 475 m of ice above the Y–3 drill site. The hydrothermal alteration assemblage differs from that en-

Figure 18. Clepsydra Geyser, Fountain Paint Pot nature walk, Lower Geyser Basin.

countered in the Y–7 and Y–8 drill holes in that the Y–3 assemblage includes a greater variety of alteration products, including mixed-layer clays and illite, which generally forms at >200°C. The illite probably formed during the last glaciation, when subsurface temperatures were higher than at present. Recall that the Y–8 area probably was a zone of cold-water recharge rather than hot-water discharge during the main stage of the Pinedale glaciation, as indicated by the oxidizing nature of fluids in the area prior to about 19,000 years ago.

Ojo Caliente spring is located on the west flank of the Pocket Basin (fig. 19) hydrothermal explosion crater described by Muffler and others (1971). Refer to their publication for a geologic map (their fig. 4) and a discussion of the mode of formation. In brief, Pocket Basin is one of several large hydrothermal explosion features in Yellowstone Park that are thought to have formed during the waning stage of the last glaciation. These explosions generally occurred where there was vigorous upflow of thermal water during glaciations and discharge of hot springs beneath the ice; these conditions are indicated by thick accumulations of water-worked sediments that were derived from the melting ice. Horizontally bedded siltstones (probably lake deposits) were encountered in the Y–3 drill hole and are present in the explosion debris on the flanks of Pocket Basin. It is likely that a rapid draining of a local lake in the region lowered the hydrostatic head to such an extent that pore water flashed to steam, producing the explosion. **Cross the road near Ojo Caliente spring and follow the fishermen's trail along the river into Pocket Basin (fig. 20). Climb to the top of the crater rim to get a good view of the basin.** Examine the

Figure 19. Air view of Pocket Basin hydrothermal explosion crater (elongated meadow in center of photograph, ringed by trees and high ground). Large vapor plume (arrow) in right foreground rises from Ojo Caliente pool located outside of Pocket Basin near the Firehole River. U.S. Geological Survey Y–3 drill site is near the tree line to left of Ojo Caliente pool. Mud pots are located on high ground at distant side of Pocket Basin.

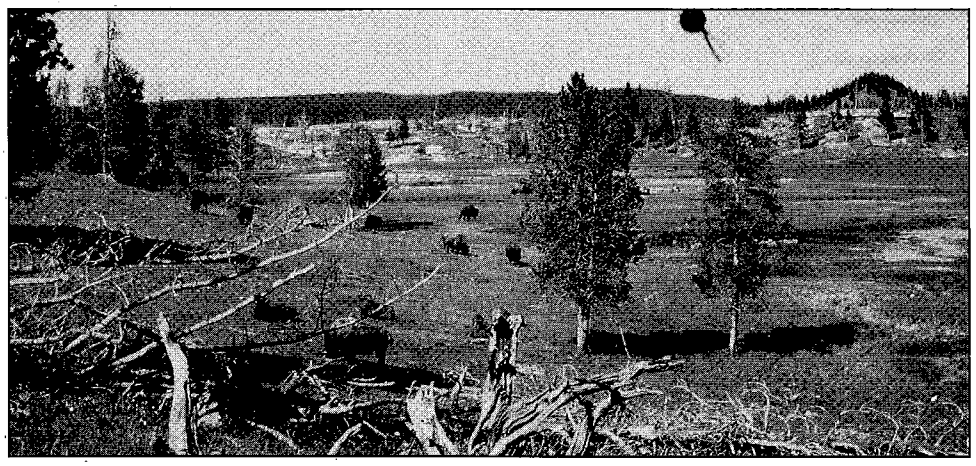

Figure 20. Floor and rim of Pocket Basin hydrothermal explosion crater, looking east from where main trail enters the crater.

blocks of silicified and hydrothermally altered sediments that form the rim of the crater, looking for evidence of repeated explosive hydrothermal activity at this locality.

Exercise extreme caution in approaching hot springs, as many in this region have thin silica crusts around their edges that are underlain by boiling water. Follow the fishermen's trail to the far side of Pocket Basin and then turn left to climb onto the eastern flank of the crater. There, a series of interesting mud pots and mud cones can be observed (fig. 21). Note that the "mud" is dominantly white, which is in contrast to the mud in other mud-pot areas in Yellowstone Park where brown, red, and cream colors generally prevail. The reason for the white color is that the mud pots at Pocket Basin are in a region that was once a silica terrace. The "mud" is dominantly finely divided silica, with little clay present. The black material that can be seen "floating" on some of the muddy water is very fine grained iron sulfide. **Return the way you came along the river trail. Do not take the more direct route across the crater floor, as it is likely to take you over dangerous and (or) very muddy ground.**

STOP 13—FIREHOLE CANYON

Flow structures in rhyolite lavas.—North of Lower Geyser Basin the Firehole River flows into the Firehole Canyon. A one-way 3.2-km-long scenic-loop road provides good views of flow structures in the rhyolitic lavas. The course of the river through the canyon is topographically controlled along the contact between two rhyolitic lava flows—the 150,000-year-old Nez Perce Creek flow that vented on the Central Plateau and flowed westward across the area and the 117,000±8,000-year-old West Yellowstone flow (J.D. Obradovich, *in* Pierce, 1979) that forms the marginal scarp of the Madison Plateau, across the river to the west. The glacial sequence relates to these flows as follows: (1) emplacement of the older flow (~150 ka), (2) glacial streamlining of the older flow during the Bull Lake glaciation, (3) emplacement of the young (117 ka) flow, and (4) glacial deposition during Pinedale time on the younger flow.

Outcrops along the road demonstrate especially clearly some internal features typical of viscous rhyolitic lavas. Shortly after turning onto the one-way loop, the road approaches the little-modified flow-front scarp of the West Yellowstone flow, which is across the Firehole River. The gray glassy carapace and steeply dipping contorted flow layering are conspicuous, even from across the river. A short distance beyond, in the roadcut on the left of the road where the road turns southward and climbs above the river, is a noteworthy outcrop of the upper flow breccia of the Nez Perce Creek flow. Viscous lavas generally flow by marginal shear and pluglike movement of a more or less fluid core. Their chilled surfaces break up into rafts of blocky rubble, some of which is dumped at the front and partly overridden by the still-moving flow in tractor-tread fashion. The result

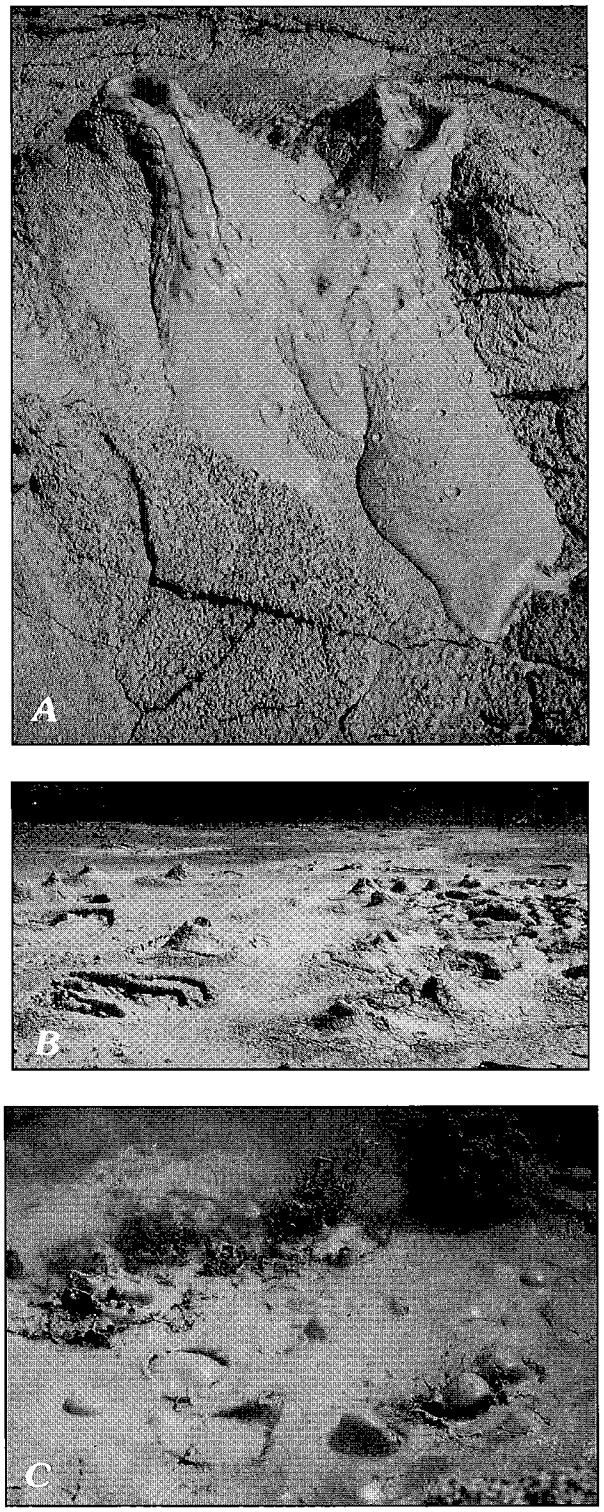

Figure 21. Mud pots located on the southern flank of Pocket Basin. *A*, Flows of viscous mud; *B*, small mud volcanoes; and *C*, pools of violently boiling muddy water, which are more common in the spring and early summer at Pocket Basin.

is an enveloping flow breccia (fig. 22). This outcrop along the south side of the roadcut demonstrates fluidal layers locally arrested in the process of brecciation. The fluidal layers themselves are seen to intrude the glassy upper flow breccia formed in earlier stages of brecciation. The blocks have various textures, some hydrated, others more obsidian-like, and some partly devitrified. These porphyritic rhyolite glasses are generally fractured on a centimeter scale, resulting in their rapid reduction to obsidian-rich sand and gravel, the material that makes up the glacial deposits in the area. Following the loop road southward, further examples of fluidal layering and varied degrees of brecciation in the upper part of the Nez Perce Creek flow can be followed through a series of roadcuts. Firehole Falls, below a large parking area, is held up by nearly vertical, erosionally resistant flow layers in the Nez Perce Creek flow (fig. 23). The marginal scarp of the younger West Yellowstone flow continues to form the western rim of the canyon across the river.

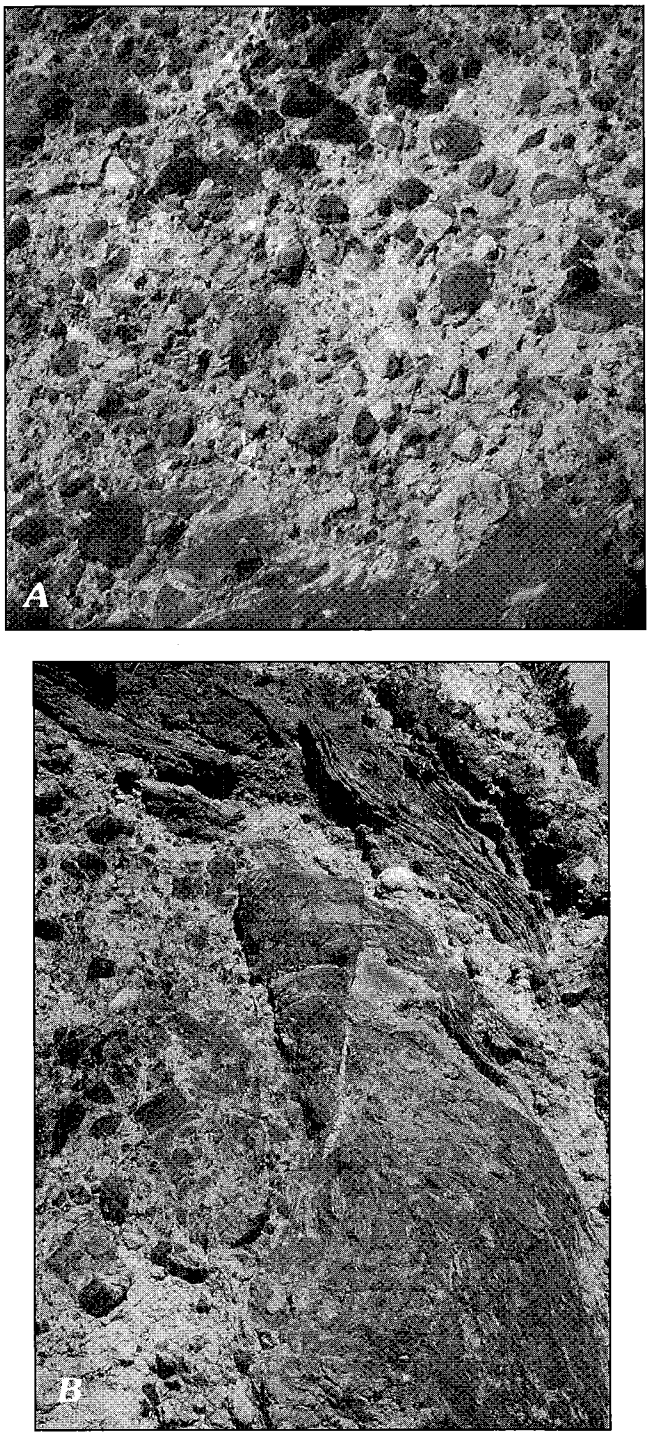

Figure 22. Flow-front breccia exposed in Firehole Canyon. *A*, Rounded blocks of chilled lava in matrix of smaller rock and glass fragments and *B*, detail of flow-banded magma within breccia showing fluidal layers locally arrested in process of brecciation.

DAY 3—TRAVEL OLD FAITHFUL TO MAMMOTH HOT SPRINGS

Take a bag lunch, as there are no restaurant facilities along the way. Most of the morning will be spent walking through Norris Geyser Basin. Try to arrive at Mammoth Hot Springs early in the afternoon to allow plenty of time to explore the huge travertine terrace. Locations of today's stops are shown in figure 24.

STOP 14—NORRIS GEYSER BASIN

Long-term and seasonal changes in hydrothermal activity.—The geology and thermal activity of Norris Geyser Basin is described in detail and beautifully illustrated in U.S. Geological Survey Professional Paper 1456 by

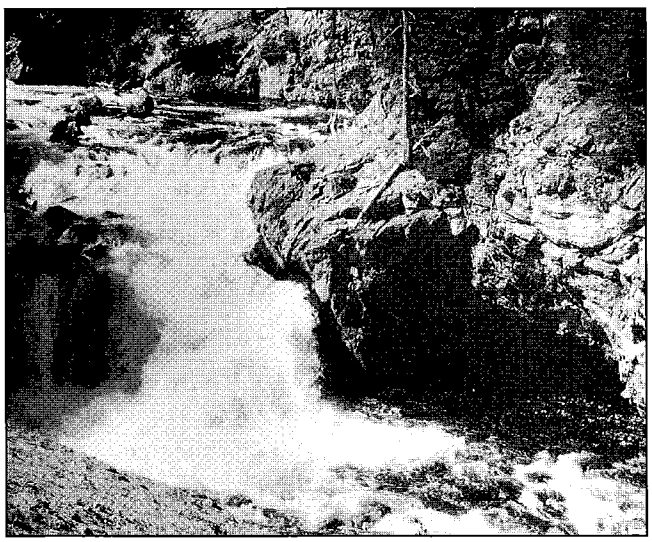

Figure 23. Firehole Falls in Firehole Canyon, held up by nearly vertical, erosionally resistant flow layers in the Nez Perce Creek flow.

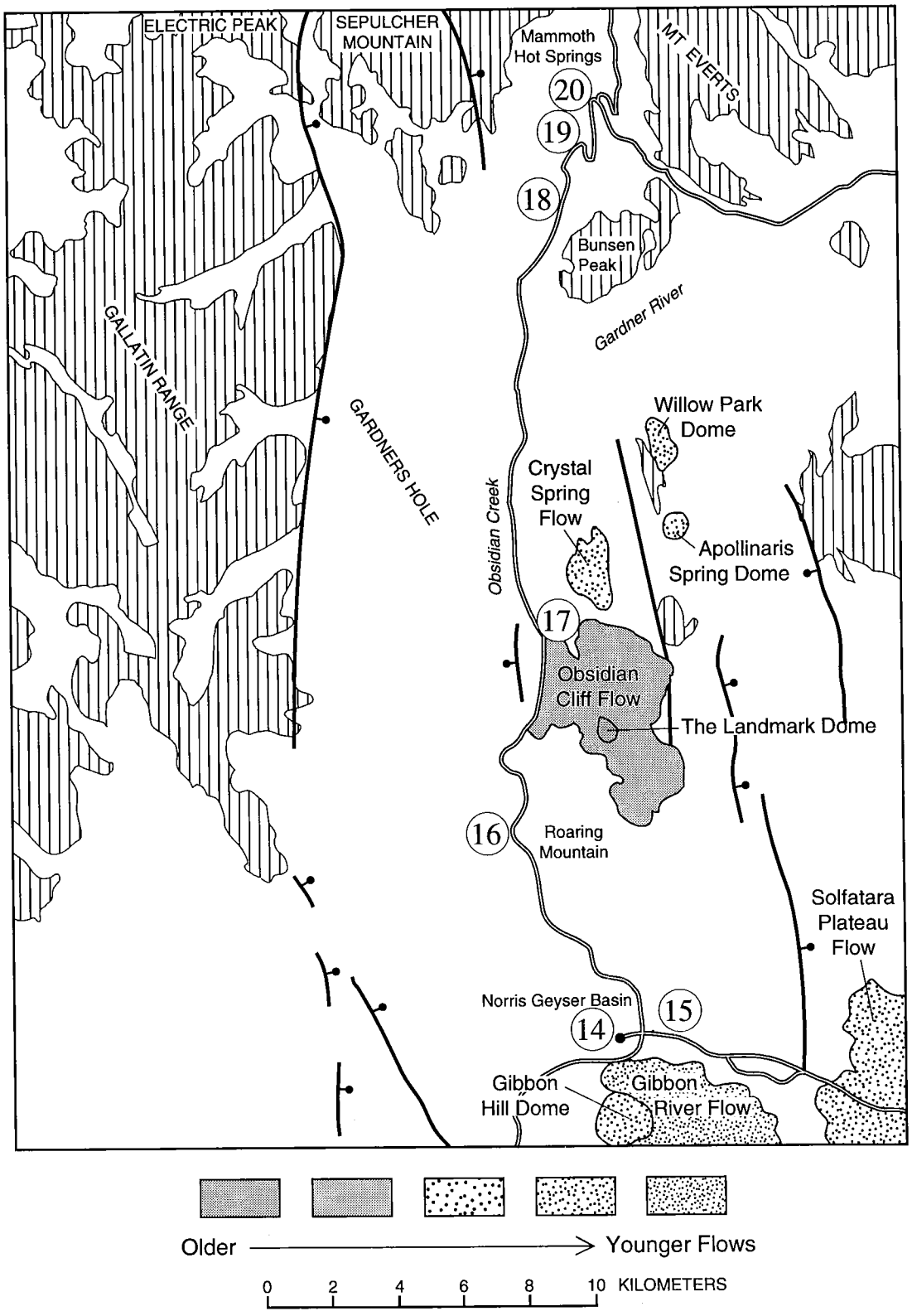

Figure 24. Generalized geologic map showing field-trip route and stops between Norris Geyser Basin and Mammoth Hot Springs. Stippled areas show Quaternary rhyolitic flows and domes; hashed areas show pre-Tertiary and Tertiary rocks (older than Yellowstone Plateau volcanic field); white areas are mostly surficial deposits with some exposures of Huckleberry Ridge Tuff, Lava Creek Tuff, and Swan Lake Flat Basalt. Heavy lines indicate faults—ball and bar on downthrown side. Large circled numbers show stop locations. (Modified from Christiansen and Hutchinson, 1987).

White and others (1988). Unfortunately this publication is presently out of print but can be found in USGS and many university libraries. Norris Geyser Basin is a large area of varied hydrothermal activity that is easily examined on two loop trails from the visitor center. One loop goes to Porcelain Terrace and Porcelain Basin and the other to the Back Basin. **Before starting your walk through Norris, note that the National Park Service trail guide is inexplicably oriented with west toward the top of the map. Figure 25 shows locations of selected springs and geysers mentioned in the text.**

The Norris Geyser Basin (Norris) is noted for (1) the highest-erupting geyser (Steamboat) presently active anywhere in the world, (2) "acid-chloride" geyser activity in Porcelain Basin, and (3) the highest reservoir temperatures in Yellowstone Park. In contrast to other parts of the park, at Norris there is a yearly basinwide hydrothermal disturbance or event (generally in the fall) that is characterized by (1) increased turbidity of many hot springs, (2) increased discharge of thermal water and steam, (3) extreme fluctuations in temperatures of pools, and (4) in some years, small hydrothermal explosions (White and others, 1988). This "disturbance" has some characteristics of a basinwide subterranean geyser eruption.

At Norris, over 360 samples of thermal waters have been collected and analyzed for major dissolved constituents from about 70 hot springs and geysers over a period of 108 years (for example, Gooch and Whitfield, 1888; Allen and Day, 1935; Rowe and others, 1973; Thompson and others, 1975; Thompson and Yadav, 1979; Kharaka and others, 1990). The results provide a remarkable and unique picture of areal and temporal variations in water compositions, mostly resulting from underground mixing of neutral-chloride and acid-sulfate waters that have reacted with rock at high temperatures after mixing. Representative chemical analyses of thermal waters at Norris are shown in table 4.

Bedrock of the Norris area is the Lava Creek Tuff, much of which has little primary permeability, whereas in the Upper and Lower Geyser Basins bedrock generally is rhyolitic lava that appears to have good primary permeability in brecciated material at tops and bottoms of flow units and at flow fronts.

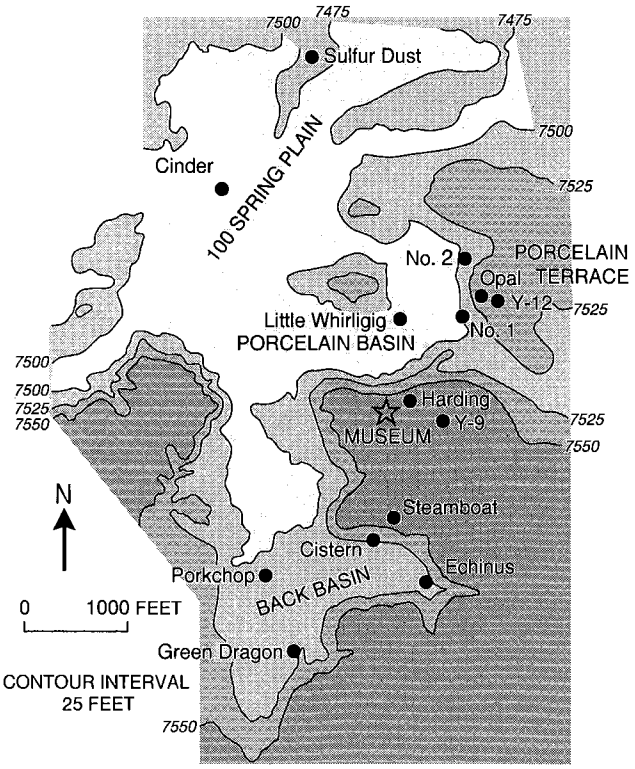

Figure 25. Sketch map of Norris Geyser Basin showing topographic features, U.S. Geological Survey drill holes Y–9 and Y–12, and locations of selected hot springs and geysers. Contours show equal altitude. No. 1 and No. 2 show locations of springs represented by analyses 1 and 2, table 4. Stippling has been added to accentuate the topographic relief in Norris Geyser Basin region. Darker shading indicates higher elevations.

THE PORCELAIN TERRACE AND PORCELAIN BASIN LOOP TRAIL

Walk through the visitor center to Porcelain Basin and Porcelain Terrace. From the visitor center, looking out to the north over Porcelain Basin (fig. 26), much of what at first appears to be white hot-spring deposits is actually the acid-leached Lava Creek Tuff. Although the waters that discharge in Porcelain Basin and in the 100 Spring Plain (beyond the low hills on the far side of the basin) are supersaturated in respect to amorphous silica, very little sinter is deposited there because the water has a low pH (3–4). In contrast, at Porcelain Terrace at the east side of Porcelain Basin (fig. 27), silica is depositing from pH-neutral waters at the fastest rate of any place in Yellowstone Park. At this locality, Cl-rich and SO_4-poor water flows directly to the surface from the deepest and hottest reservoir at Norris (275–325°C, based on silica and Na-K-Ca geothermometry, $\Delta^{18}O(SO_4–H_2O)$, $\Delta^{13}C(CO_2–CH_4)$, and on mixing models).

The Y–12 drill hole is situated at the south end of Porcelain Terrace near the tree line. It attains a temperature of 238°C at a depth of 332 m. Very little permeability or hydrothermal alteration was encountered in the Lava Creek Tuff, the only rock unit encountered in the Y–12 drill hole (White and others, 1988). The δD (a measure of the hydrogen isotopic composition of a particular sample compared to the hydrogen isotopic composition of a standard, expressed in parts per thousand) value of −149.5 for water obtained from this well was critical for the determination of the likely isotopic composition of the deep water in the hydrothermal system (Truesdell and others, 1977). It also sparked the search for isotopically light recharge

Table 4. Chemical compositions (mg/kg) of selected thermal waters, Norris Geyser Basin.

Analysis No.	Name	Date	Ref.	°C	pH	SiO_2	Na	K	Ca	Mg	Li	Cl	SO4	HCO_3
1	South base Porcelain Terrace	07/03/75	1	92	7.00	589	400	93	2.60	0.01	7.18	675	24	60
2	South base Porcelain Terrace	09/02/90	2	88	2.82	520	334	100	1.82	0.21	4.07	527	133	0
3	South base Porcelain Terrace	09/06/90	2	89	5.36	665	400	112	2.82	0.08	5.36	634	99	32
4	Little Whirligig	09/27/71	3	91	3.20	420	349	83	2.50	0.50	5.30	607	113	0
5	Sulfur Dust	09/12/61	4	50	2.75	280	250	57	4.50	0.15	3.50	427	197	0
6	Porkchop	09/18/60	4	72	7.45	435	526	66	6.40	0.50	7.40	860	33	18
7	Porkchop	06/??/89	5	92	8.50	741	388	91	3.60	0.06	6.60	687	23	62
8	Echinus Geyser	11/15/81	2	90	3.14	257	151	45	3.70	0.52	1.00	125	170	0
9	Echinus Geyser	09/15/86	2		3.06	296	148	52	4.30	0.52	0.75	117	360	0
10	Opal Spring	09/19/60	4	90	1.90	168	5	2	0.70		0.05	5	760	0
11	Harding	06/07/71	3	93	3.53	325	26	18	0.90	0.25	0.09	2	123	0
12	Y–12 drill hole	09/13/69	2	238	7.86	352	377	21	1.90	0.20	1.43	528	34	79
13	Y–9 drill hole	09/16/69	2	195	8.58	412	268	16	0.80	0.04	0.98	80	43	488

References:
(1) Thompson and Yadav (1979).
(2) Unpublished U.S. Geological Survey data.
(3) Thompson and others (1975).
(4) Rowe and others (1973).
(5) Kharaka and others (1990).

Figure 26. Porcelain Basin, viewed from near the Norris museum, Norris Geyser Basin.

water for the Yellowstone hydrothermal system. An analysis of a water sample collected from the Y–12 drill hole is shown in table 4 (No. 12). The most significant chemical information provided by this sample is the chloride concentration of 528 mg/kg. This value is probably close to the concentration of chloride in the deep reservoir beneath Norris prior to any separation of steam during upflow. The relative concentrations of cations in the sample reflect the reaction of hot water with glass-rich ash-flow tuff at an unknown temperature in the range 190 to 238°C. There are uncertainties about the depth(s) and temperature(s) where fluid(s) enters the drill hole.

Along the top of Porcelain Terrace, and elsewhere in topographically high regions surrounding the geyser basins at Norris, nondischarging, boiling pools of low-chloride, acid-sulfate waters are found (for example, Opal Spring, No. 10, table 4). At Porcelain Terrace these acid-sulfate pools all formed after the 1959 Hebgen Lake earthquake,

when newly formed fractures allowed the hot-spring waters to leak sideways and flow onto the ground at slightly lower elevations at the side of the terrace. Prior to this earthquake only silica-depositing neutral-chloride waters discharged from the top of the terrace. Cavities in the sinter that were once filled with water are now partly drained, and the rock beneath the sinter is now being attacked and leached by boiling sulfuric acid-rich water. The sinter is decaying and crumbles relatively easily. **Because of these factors, Porcelain Terrace is one of the more dangerous places in Yellowstone Park.**

At the side of Porcelain Terrace relatively high-chloride (550–800 mg/kg) low-sulfate (10–50 mg/kg) pH-neutral waters generally issue from a deep reservoir with an estimated temperature of 270 to 325°C. Analysis No. 1, table 4 (south base Porcelain Terrace), is typical of thermal waters issuing along a north-trending zone at the west side of Porcelain Terrace. However, for short periods of time after basinwide hydrothermal disturbances, pH-neutral springs at Porcelain Terrace may become acid by mixing with a sulfate-rich water that appears to have equilibrated with rock at a high temperature (>200°C) before mixing. One usually neutral-chloride spring was sampled on the first day of a seasonal hydrothermal disturbance (No. 2, table 4); its pH was 2.82 and its sulfate concentration was 133 mg/kg. Four days later its pH had increased to 5.36 and its sulfate concentration had dropped to 99 mg/kg (see No. 3, table 4). Chemically, waters from this and other nearby springs generally have been found to be very similar in composition to analysis 1 in table 4. Perhaps the most significant information provided by this spring is that the more-acid water contained helium with a higher $^3He/^4He$ ratio than the less-acid water (B.M. Kennedy, written commun., 1991), and it also had a δD isotopic composition almost as heavy as the water in boiling acid-sulfate pools in the region (fig. 28) that have undergone considerable evaporation. One might be tempted to conclude that the acid-sulfate-rich composition of analysis 2 in table 4 is the result of simple mixing of the neutral chloride-rich water

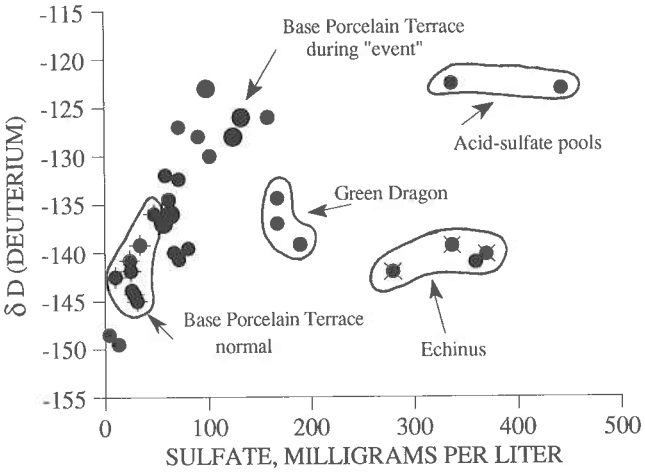

Figure 28. Sulfate (SO_4) versus δD (deuterium) for Norris Geyser Basin thermal waters. See text for discussion.

Figure 27. Hot spring activity at Porcelain Terrace, Norris Geyser Basin.

from deep in the system with acid-sulfate water that percolates downward from boiling pools at the top of Porcelain Terrace. However, note that in figure 28 the mixing trend from the "normal" sulfate-poor water issuing at the base of Porcelain Terrace to the acidic sulfate-rich water collected during the yearly Norris "event" does not project to compositions normally found in acid-sulfate pools. Also, the $^3He/^4He$ data of B.M. Kennedy (written commun., 1991) strongly suggested that the acidity of the "event" water issuing at the base of Porcelain Terrace is not the result of simple downward infiltration of acid-sulfate water from pools at the top of Porcelain Terrace.

Moving west from Porcelain Terrace through Porcelain Basin and moving to the northwest through 100 Spring Plain (fig. 25) there is a decrease in chloride, an increase in sulfate, a decrease in pH (for example, Little Whirligig and Sulfur Dust, Nos. 4 and 5, respectively, table 4), and the estimated reservoir temperature decreases to about 200 to 230°C. All of the acid-chloride waters in the Porcelain Basin and 100 Spring Plain regions plot along the trend shown by the "normal" and "event" waters at the base of Porcelain Terrace in figure 28. These waters also are relatively rich in $^3He/^4He$ compared to other Norris waters.

As you walk through Porcelain Basin note the bright green color of a few of the hot-water discharge channels. This color is produced by cyanobacteria (*Cyanidium* sp.) that require low-pH environments, in contrast to the yellow, red, and brown organisms and precipitates of the near-neutral discharge channels.

THE BACK BASIN LOOP TRAIL

As you approach the Norris visitor center from the parking lot, the trail that branches to the left leads past Steamboat Geyser into the Back Basin. In the Back Basin a series of reservoirs with different temperatures are present so that waters with similar chloride concentrations attain chemical equilibrium with rock at a variety of temperatures ranging from about 210 to 300°C before rising to the Earth's surface. Reservoirs of sulfate-rich waters with moderate chloride also exist in the Back Basin region, and as at Porcelain Terrace, annual mixing of sulfate-rich and sulfate-poor waters occurs in the Back Basin (well documented for Cistern Spring, Fournier and others, 1986). Some waters in the Back Basin, such as those from Green Dragon Spring, are always acidic and appear to be the result of mixing of chloride-rich water from deep in the hydrothermal system with acid-sulfate water that infiltrates downward from surface pools (fig. 28).

As you walk through the Back Basin note the large amount of old silica that is now decaying and collapsing into what were once water-filled cavities within the sinter. To the northwest the Back Basin is bordered by the Ragged Hills, low hills of hydrothermally cemented kame deposits that likely formed beneath a glacier by melting of the ice due to hot-spring activity. Features of particular interest in the Back Basin are Steamboat Geyser, Cistern Spring, Echinus Geyser (erupts about once an hour), and Porkchop Geyser Crater and its hydrothermal explosion debris (fig. 25 and "Trail Guide to Norris Geyser Basin," see appendix A).

STEAMBOAT GEYSER

Steamboat Geyser exhibits two modes of eruption. Generally, it erupts every few minutes to a height of a few meters (fig. 29). On rare occasions, it erupts massive amounts of water 70 to 120 m high. All of the conspicuous erosion around this geyser has occurred since 1960 and is the result of water discharged during the big eruptions (fig. 30).

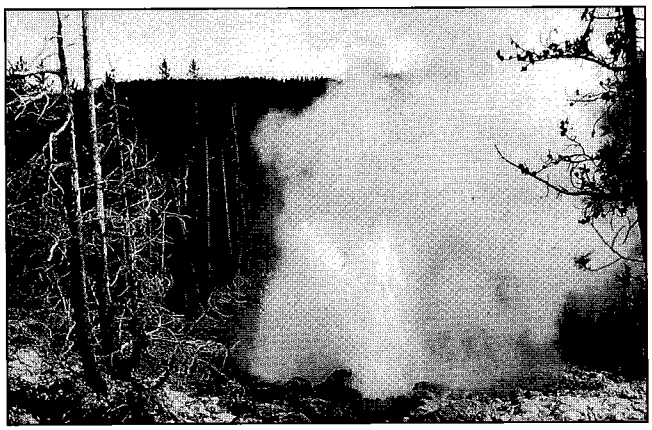

Figure 29. A typical small eruption of Steamboat Geyser, Norris Geyser Basin.

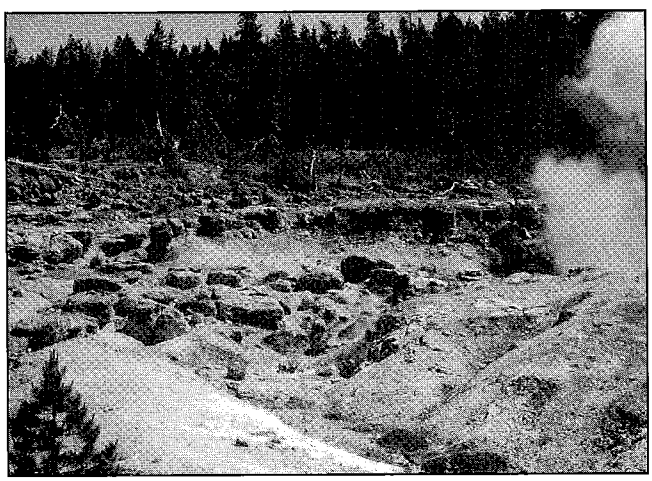

Figure 30. Eroded ground resulting from infrequent big eruptions of Steamboat Geyser, Norris Geyser Basin.

CISTERN SPRING

Cistern Spring has been active since about 1966, and the silica terrace that now surrounds the pool has formed since then (fig. 31). Note how fallen trees have played a major role in the formation of the sinter terrace. Cistern Spring was sampled more than 100 times during a 25-year period. Monthly collections of water from 1976 to 1985 showed that increased boiling preceded yearly hydrothermal disturbances and that chloride content decreased and sulfate content increased immediately following the onset of these disturbances (Fournier and others, 1986). The mixed waters of Cistern Spring lie along the trend shown in figure 28 for the base of Porcelain Terrace waters. Figure 32 shows Cl–SO_4 relations for Cistern Spring waters. The variations shown in figure 32 result partly from different amounts of mixing of different waters and partly from different degrees of steam loss (adiabatic expansion) during upflow (Fournier and others, 1986).

PORKCHOP GEYSER CRATER

Between 1960 and 1989 Porkchop Geyser Crater evolved from an intermittently flowing spring, to a geyser, to a perpetually spouting geyser, and finally to its present condition after a hydrothermal explosion in September 1989 (fig. 33). Porkchop now discharges water mainly from a hotter (presumably deeper) neutral-chloride reservoir where dissolved silica concentrations and K/Na ratios are relatively high (No. 7, table 4) and the reservoir temperature is likely to be in the range 275 to 300°C. In 1960 it discharged from an apparently different (presumably shallower) reservoir where pH-neutral water had reacted with rock at lower temperatures (215–230°C), yielding lower concentrations of dissolved silica and lower K/Na values (No. 6, table 4). A gradual change in the composition of water discharged by Porkchop Geyser over the period 1960 to 1990 was documented by Fournier and others (1991), who showed that the calculated temperature at which the discharged water last equilibrated with rock (the presumed reservoir temperature) increased by about 60 to 70°C during that same period of time, accompanied by the

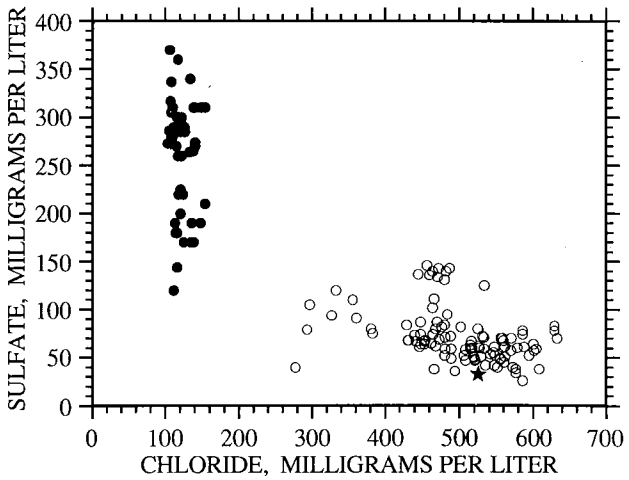

Figure 32. Chloride (Cl) versus sulfate (SO_4) for waters collected at different times from Cistern Spring (circles), Echinus Geyser (dots), and U.S. Geological Survey Y–12 drill hole (star).

Figure 31. Silica terrace formed by waters discharged from Cistern Spring. Morphology is controlled mostly by distribution of fallen trunks of trees killed by hot water, Norris Geyser Basin.

increase in eruptive activity that culminated in a hydrothermal explosion that destroyed the geyser.

ECHINUS GEYSER

Echinus Geyser is named for spiny dark-red iron- and arsenic-rich coatings of silica that once coated the sides of its pool and the cobbles in its runoff channel. For about the last 20 years these silica spines have been slowly overgrown by white to gray relatively smooth silica encrustations. Echinus discharges large amounts of acid-sulfate water (Nos. 8 and 9, table 4) during its fairly predictable eruptions, which occur about every 50 to 60 minutes. However, it also has long periods of inactivity. If it is in its usual predictive mode of behavior, it is worth waiting to witness an eruption of this geyser. The waters discharged by Echinus are chemically and isotopically different from other thermal waters found in Yellowstone Park; sulfate is relatively high, whereas the isotopic composition of its water is relatively light (fig. 28). The concentration of sulfate in Echinus water ranges widely, whereas there is relatively little change in chloride concentration. Figure 32 shows Cl-SO_4 relations for 53 samples from Echinus collected from 1884 to 1986, mostly during 1980 to 1983. The pH of the Echinus waters (3.0–3.5) appears to be buffered by the assemblage kaolinite-muscovite at about 195 to 215°C (the silica geothermometer temperature range). The Na/K values found in the Echinus waters are inconsistent with equilibration involving dissolved constituents and alkali feldspars at about 190 to 215°C, whereas K/H values are consistent with the assemblage kaolinite-muscovite. Fragments of banded marcasite and pyrite are sometimes ejected from Echinus during its larger geyser eruptions. Two samples of iron sulfide from Echinus were recently analyzed for trace elements and were found to be anomalously rich in As, Tl, and Sb (T.E. Keith, written commun., 1992).

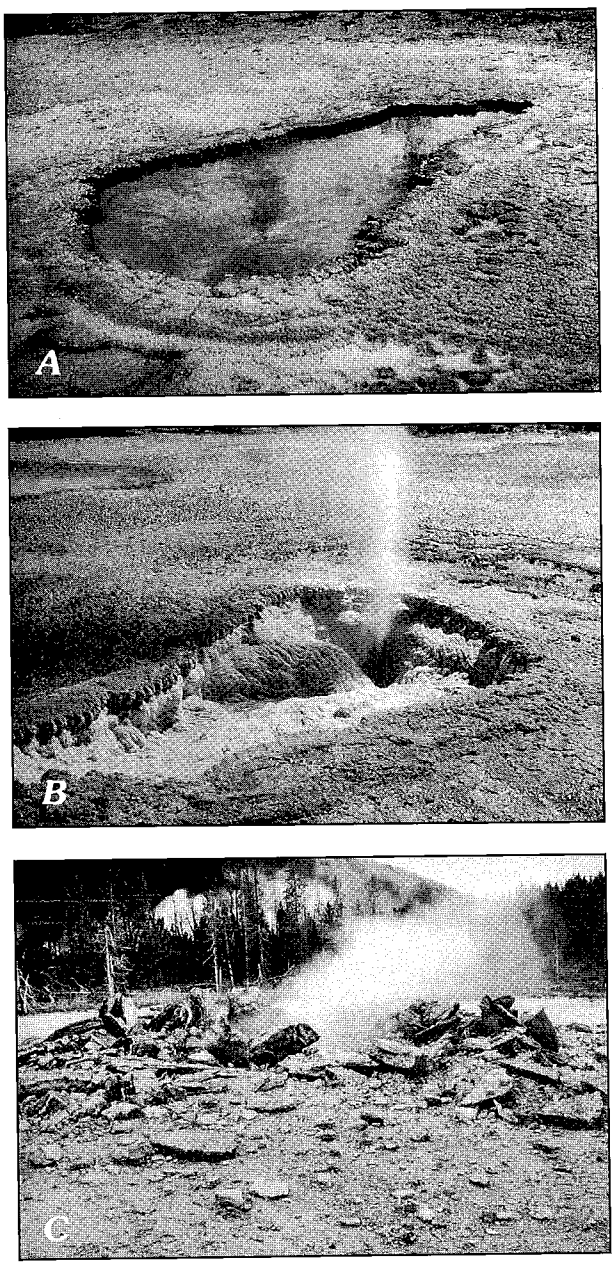

Figure 33. Porkchop Geyser, Norris Geyser Basin. *A*, Quiescent pool in 1984; *B*, in eruption in 1986; and *C*, after hydrothermal explosion in 1989.

CHARACTERISTICS AND ORIGIN OF ACID-SULFATE WATERS

The acid-sulfate waters at Norris that originate by oxidation of H_2S where steam and other gases bubble through surficial pools of perched ground water and condensed steam have relatively heavy δD and $\delta^{18}O$ values (Truesdell and others, 1977) and are strongly depleted in Na relative to K as a result of nonequilibrium acid dissolution of silicic volcanic rocks (for example, Opal Spring, No. 10, table 4). Many steam-heated acid-sulfate pools also are strongly depleted in Li relative to K (for example, Harding, No. 11, table 4). Conversely, discharging acid-sulfate waters that equilibrated underground with rock at >190 to 200°C have significantly higher Na/K ratios than waters from steam-heated acid-sulfate pools and K/Li weight ratios less than 80 (generally in the range 40–60).

The $\delta^{34}S$ (a measure of the sulfur isotopic composition of a sample compared to the sulfur isotopic composition of a standard, expressed in parts per thousand) values for sulfate dissolved in several Yellowstone Park thermal waters, including some from Norris, were determined by Truesdell and others (1978). The waters from deep in the Norris hydrothermal system, issuing at the base of Porcelain Terrace, have $\delta^{34}S$ values of about +18, whereas all of the sulfate-rich waters have $\delta^{34}S$ values of about 0 to +6. According to Truesdell and others (1978) the +18 value reflects high-temperature (270–300°C) equilibrium fractionation of sulfur isotopes between H_2S (initial $\delta^{34}S \approx 0$)

and sulfate derived by oxidation of H_2S; this high-temperature oxidation must occur deep in the hydrothermal system. In contrast, the sulfate derived by nonequilibrium oxidation of H_2S at and near the ground surface has $\delta^{34}S$ close to 0. Native sulfur at Norris has $\delta^{34}S$ values ranging from about +1 to +3 (Schoen and Rye, 1970).

Oxidation of H_2S at depth using oxygen initially dissolved in meteoric recharge water can account for only about 13 mg/kg of the dissolved sulfate in waters deep in the hydrothermal system. Oxidation at and near the water table of H_2S initially carried in steam, followed by downward percolation, may account for some of the sulfate and acidity found in the underground acid-sulfate-chloride waters at Norris (particularly waters such as Green Dragon, fig. 28), but mass and thermal balance considerations, and light δD and $\delta^{18}O$ values, make it difficult to account for all of the sulfate in Echinus waters by the present-day oxidation of H_2S in and around nearby surface pools. The mass and thermal balance problems may be explained if old deposits of native sulfur occur locally at relatively shallow depths in the Norris area. Sulfur-consuming bacteria (*Sulfolobus* sp.) are very effective at generating sulfuric acid using native-sulfur deposits and oxygen in the cool margins of hydrothermal systems (Brock, 1978). Such native-sulfur deposits could be related to early volcanic activity that produced silicic domes south of Norris and underwent subsequent burial either by later volcanic flows or by glacial material deposited on hot ground. Cold ground water, after picking up sulfate where it comes in contact with old native sulfur, could then flow toward the (Norris) hydrothermal system where it mixes with and becomes heated by a small amount of chloride-rich water and steam from deep in the system. The $\delta^{34}S$ of the dissolved sulfate and δD of the water from Norris observed by Truesdell and others (1977, 1978) are compatible with this interpretation.

The origin of the sulfate-rich water that is characteristic of Porcelain Basin and 100 Spring Plain is uncertain. This water appears to be relatively uniform in composition and is widespread. The highest $^3He/^4He$ ratios (>8–9 relative to atmospheric concentrations) in Norris waters are found in Porcelain Basin and 100 Spring Plain waters (B.M. Kennedy, written commun., 1991), and the δD in these waters is also relatively heavy. The possibility cannot be ruled out that there is a component of magmatic gas containing SO_2 that is entering parts of the Norris hydrothermal system.

THE Y–9 DRILL HOLE

The Y–9 drill hole is located at the northeast edge of the main Norris parking lot. This hole attained a depth of 248 m and a maximum temperature of 195°C. Water collected from it is shown by sample 13, table 4. In contrast to other Norris waters, the Y–9 water is relatively rich in bicarbonate and relatively poor in chloride. Superheated steam enters this drill hole through a nearly vertical kaolinite-coated fracture at a depth of 64 m (White and others, 1975). It is likely that some of this CO_2-rich steam condenses in the drill hole and that this condensate becomes ponded in the relatively impermeable bottom of the drill hole, where it reacts with wall rock at 170 to 190°C. Apparently a small component of "normal" thermal water in the region is mixed with the condensate.

STOP 15—PICNIC LUNCH IN THE NORRIS REGION

The closest official picnic spot with toilet facilities is located about a mile east of Norris Geyser Basin. From Norris Junction take the road to Canyon Village, the road leading into the picnic area will be on the left-hand (north) side of the main road.

STOP 16—ROARING MOUNTAIN

Acid-sulfate alteration of tuff.—Much acid-sulfate alteration and fumarolic activity occurs along the north-trending corridor from Norris to Mammoth Hot Springs. Bedrock is mostly the Lava Creek Tuff, but vents for local rhyolitic and basaltic eruptions are found in this corridor of volcanic and hydrothermal activity. Roaring Mountain was named in 1885 by Arnold Hague and Walter Weed, both of the USGS, for the loud noise produced by its steam vents. It is a bluff composed of the hydrothermally altered Lava Creek Tuff with numerous fumaroles and small acid-sulfate seeps (fig. 34). The fumaroles are now generally inconspicuous on warm sunny days but can be impressive in cool cloudy weather. Schoen (1969) measured the rate of sulfate discharge from Roaring Mountain into the small stream that drains the area. He recorded an average discharge of about 1,180,000 grams of sulfate per day. Averaged over the area of acid-altered ground, about 9.2 g/m^2/day of sulfate is produced by bacterial oxidation of H_2S.

Although not visible from the road, the top of Roaring Mountain is a flat mesa-like bench. In the central part of this bench are several large craters in the Lava Creek Tuff. Around these craters is an apron of angular rock fragments in a muddy matrix. The craters were formed by hydrothermal explosions, which threw bedrock fragments and mud out for distances of as much as 0.8 km. These hydrothermal explosions probably occurred when a lake surrounded by stagnant glacial ice drained rapidly, as discussed previously for the origin of Pocket Basin (Stop 12).

STOP 17—OBSIDIAN CLIFF

From the parking area, Obsidian Cliff can be seen to lie along the margin of a rhyolitic lava flow that abuts the

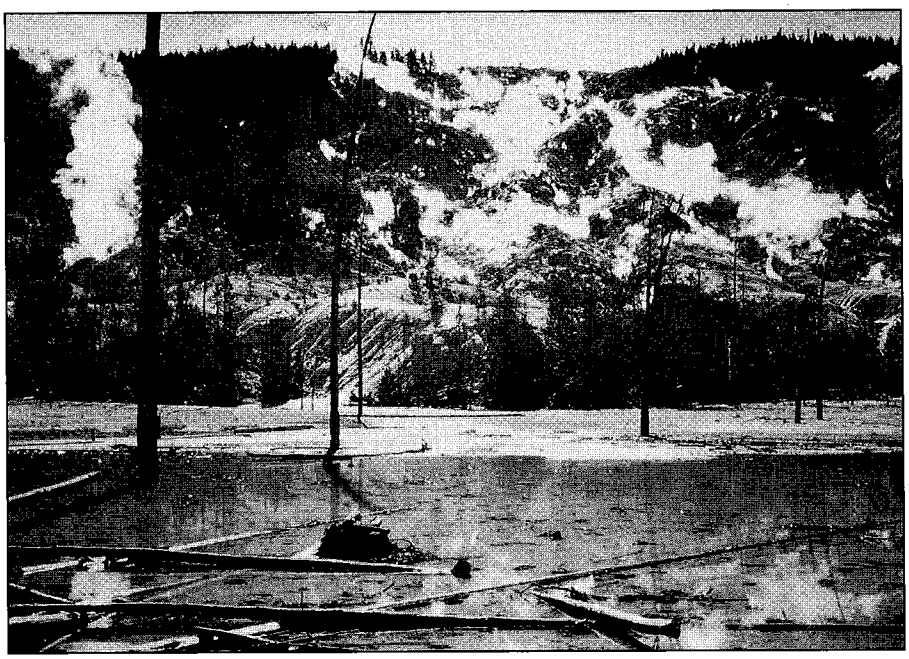

Figure 34. Roaring Mountain.

wall of a paleovalley near here. Large columnar joints mark the base of the flow near the road, and steep contorted flow layering is visible near the top of the flow (fig. 35). Obsidian Cliff is an excellent locality to examine rhyolitic obsidian and its crystallization textures. **(Specimen collecting is not allowed.)** Some visitors to this locality are somewhat disappointed to find that clear undevitrified blocks of obsidian are uncommon; sites once used by Native Americans to quarry crystal-free obsidian for implements are located away from the road along other margins of the same flow.

Characteristic textural features are readily seen in talus boulders at the base of the cliff near the road. The rhyolite here is entirely free of phenocrysts, indicating that the magma erupted above its liquidus temperature. The obsidian occurs in basal and marginal chilled zones of the flow, which has a pumiceous top and a crystallized interior that is seen in a single gully exposure. Fluidal laminations are distinct in the talus boulders and are generally marked by bands of small gray spherulites that formed by partial high-temperature devitrification of the rhyolitic glass. Further devitrification is represented by larger pinkish spherulites and lithophysae, generally 1 to 5 cm. Lithophysae are hollow spherulites lined by concentric shells of small crystals—generally tridymite, alkali feldspar, and minor accessory minerals such as fayalite—separated by open interspaces. The lithophysae represent high-temperature vapor exsolution and crystallization of minerals from the vapor phase.

The Obsidian Cliff flow was dated by John Obradovich (1992) as 183,000±3,000 years old. Three thicknesses of hydration rims occur on different cracks in the

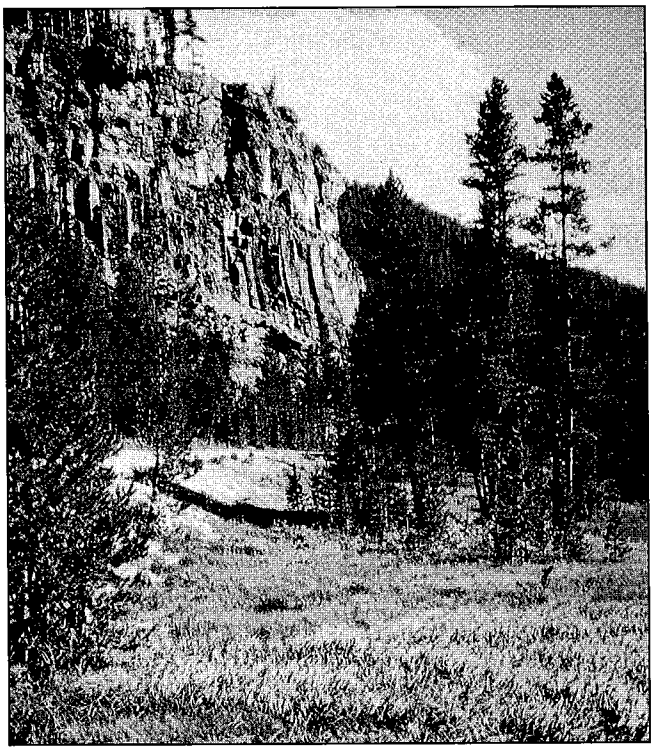

Figure 35. Obsidian Cliff.

Obsidian Cliff flow and averaged 16.2, 14.5, and 7.9 μm thick (Friedman and others, 1973). The 16.2-μm-thick rim corresponds to the original cooling of the flow. The 14.5- and 7.9-μm thick rims are very similar in thickness to the

hydration rims on glacial abrasion cracks in obsidian from the Bull Lake and Pinedale end moraines near West Yellowstone (Pierce and others, 1976). The hydrated cracks are thought to result from glacial loading, which first occurred in Bull Lake and then in Pinedale time. During the Pinedale glacial recession, about 15,000 years ago, the icecap on the Yellowstone Plateau had melted, and glaciers from the Gallatin Range (west of here) deposited glacial erratics on top of Obsidian Cliff (Pierce, 1979).

STOP 18—HOODOOS

Travertine landslide deposit.—The Hoodoos are a blocky landslide deposit of bedded Pleistocene travertine from Terrace Mountain, which rises above the road to the west (fig. 36). The morphology of the Terrace Mountain travertine deposit is unusual compared to other travertine deposits in the Mammoth Hot Springs region of Yellowstone Park in that no fissure ridges or cascading terraced mounds are evident. Layering is monotonously horizontal, and no trees or other woody materials have been found imbedded in this travertine. This travertine may have formed as a result of the emergence of CO_2-rich springs at the bottom of a lake throughout a long period of time, suggesting that much erosion has occurred in the Mammoth Hot Springs region since deposition of the travertine. U–Th age determinations on the travertine by N.C. Sturchio (Pierce and others, 1991) yield an age of 406±30 ka. This relatively old age is consistent with the observation that Pinedale glacial deposits occur on top of the Terrace Mountain travertine.

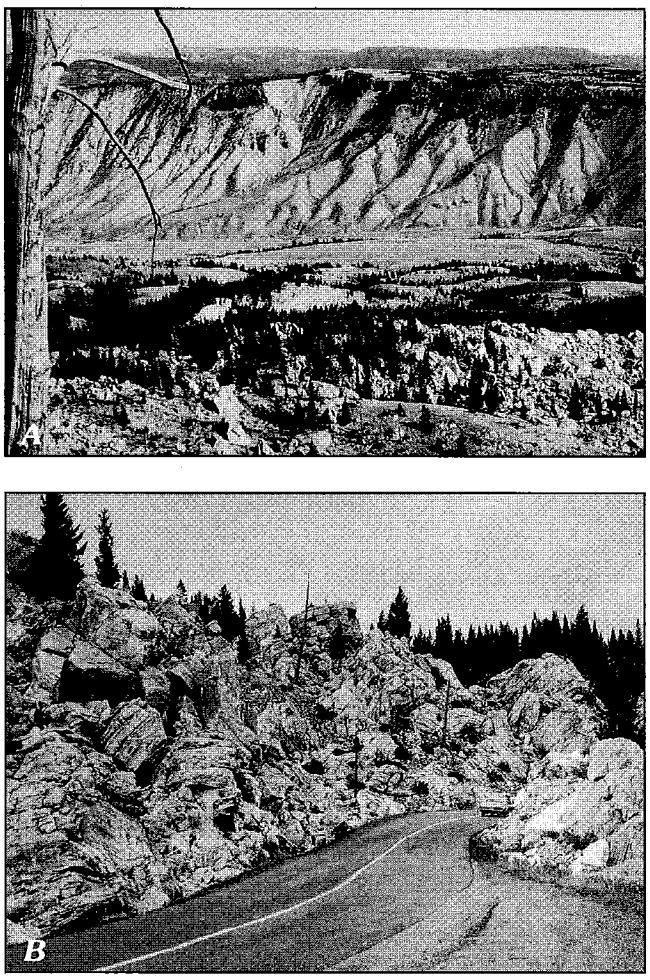

Figure 36. *A*, Large landslide with blocks of white travertine in foreground. In distance is Mt. Everts, consisting of Cretaceous sandstones and shales capped by Huckleberry Ridge Tuff. Photograph taken from top of Terrace Mountain. *B*, The Hoodoos, composed of blocks of travertine in a landslide deposit.

STOP 19—OVERLOOK ABOVE MAMMOTH HOT SPRINGS

Geologic and topographic setting of Mammoth.—Geologic, geochemical, and hydrologic relations in the Mammoth Hot Springs (Mammoth) region are described in a series of chapters in Sorey (1991). Mammoth is situated on the steep western side of the Gardner River valley. The bedrock consists of Mesozoic sandstones and shales, which are prone to landsliding. A thick limestone (not exposed) that is a regional aquifer underlies the Mesozoic rocks. To the south is the Bunsen Peak dacitic stock of Eocene age. Pleistocene travertine caps Terrace Mountain to the west. To the east, Mount Everts consists of Cretaceous shales and sandstones, capped by the Huckleberry Ridge Tuff. Northward the valley opens toward the glaciated Yellowstone River Valley. In the Yellowstone River Valley are other Pleistocene travertine terraces above the town of Gardiner, Montana, which have ages of about 15,000, 20,000, and 50,000 years old by U–Th dating (Pierce and others, 1991). Farther north are Precambrian to Eocene rocks of the glaciated Snowy Range.

The hydrothermal activity at Mammoth is described in detail by Bargar (1978). Mammoth is different from any of the other thermal areas of this guide. In contrast to the silica-depositing hot waters described previously, Mammoth is presently the world's largest carbonate-depositing spring system (fig. 37). The characteristic form of the deposits is a large travertine terrace. Older travertine underlies Mammoth Hot Springs village and much of the slope all the way down to the Gardner River. The oldest travertine deposits at Mammoth have been dated at about 10,000 years B.P. (Pierce and others, 1991). The waters of Mammoth Hot Springs, with a subsurface reservoir temperature of 73°C, are cooler than those of the geyser basins. These waters (1) rise through Paleozoic and Mesozoic sedimentary rocks, including limestones, (2) are high in dissolved carbonate and sulfate, and (3) release excess CO_2 as they discharge because of lower pressure at the surface. The deposited travertine initially forms ridgelike mounds above

the water-bearing fractures. The water pools and evaporates behind these mounds, losing CO_2 to the atmosphere and depositing carbonate as it flows across the rims of the pools to enlarge the terraces.

The reservoir rock for the thermal waters discharging at Mammoth is probably limestone. Various explanations have been proposed to account for the heat that is discharged. One possible explanation is that heat extracted

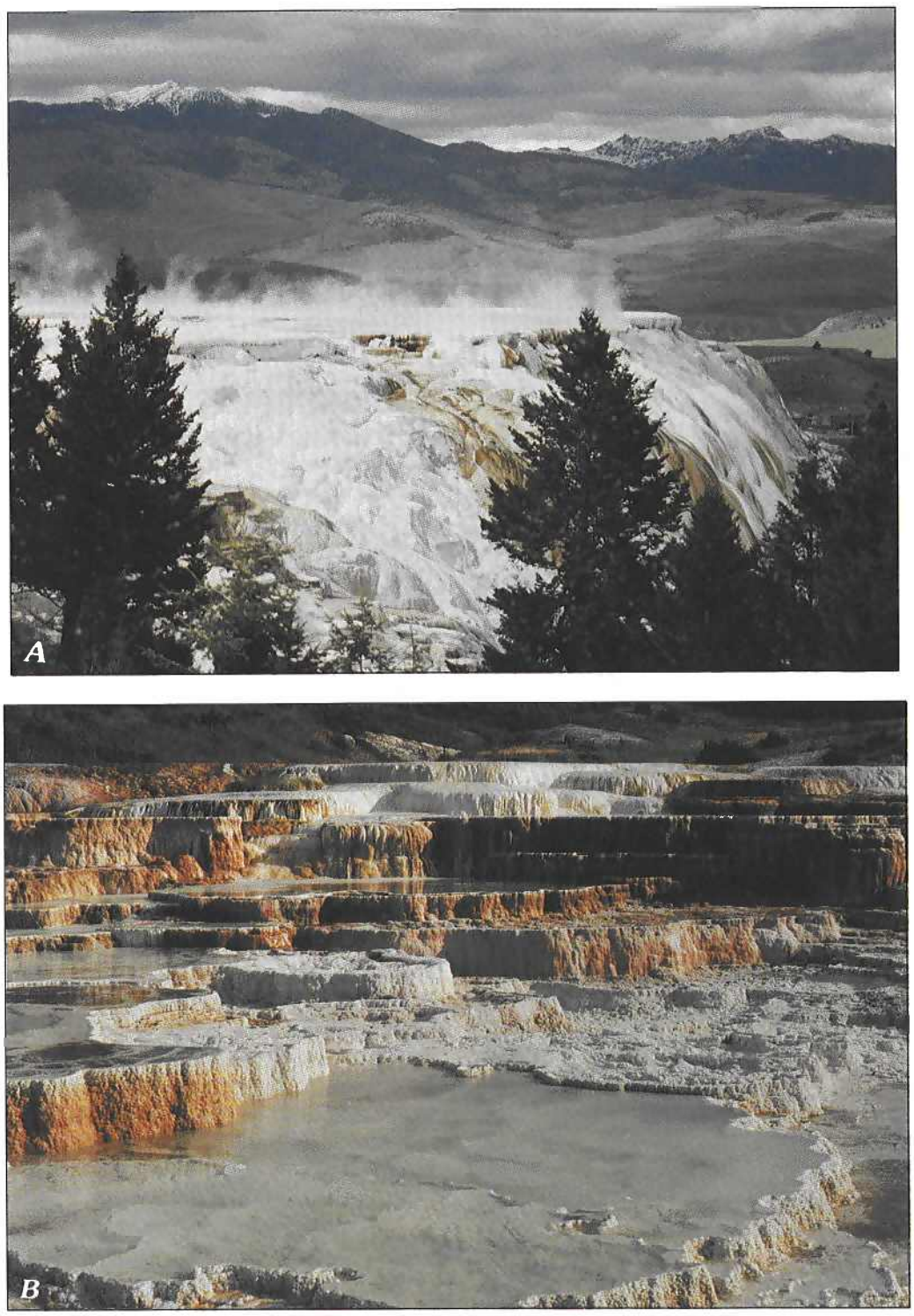

Figure 37. *A*, Main travertine terrace seen from overlook above Mammoth Hot Springs; *B*, travertine terrace at Mammoth Hot Springs.

from the Yellowstone caldera magmatic system is carried northward by deeply circulating chloride-rich hydrothermal fluids that move through extensional faults in the Norris–Mammoth corridor. In this explanation these chloride-rich fluids mix with cooler ground water in the Mammoth region and then pick up bicarbonate and sulfate by reaction with calcite and gypsum in the local sedimentary rocks. Another possible explanation is that a local magmatic heat source exists beneath Roaring Mountain or Obsidian Cliff and that hydrothermal fluids flow from this heat source to the south, toward Norris, and to the north, toward Mammoth. A third possible explanation is that a local heat source exists beneath the Mammoth region, perhaps a crystallized but still relatively hot body of basalt. A high value of $^{3}He/^{4}He$ relative to air of 8.4 in water from the Y–10 drill hole indicates that a relatively undiluted mantle component of helium is being discharged with waters from Mammoth Hot Springs (Kharaka and others, 1991).

STOP 20—MAMMOTH HOT SPRINGS

Explore the travertine terrace using the U.S. National Park Service map of the trails at Mammoth and, if available, the USGS Bulletin on Mammoth by Bargar (1978) as your guides (see appendix A). The upper terrace loop drive will take you past the Y–10 drill site. A good view of a tension fissure that has opened along the top of a fissure ridge mound can be seen at White Elephant Back Springs (Bargar, 1978, southwest corner of plate 1).

DAY 4—MAMMOTH HOT SPRINGS TO JACKSON HOLE

This is a long drive leaving time for a minimum number of stops. If time is available, an overnight stay at Canyon Village or Lake is advised, leaving additional time to visit the Grand Canyon of the Yellowstone area.

STOP 21—OVERLOOK OF LOWER GRAND CANYON AT THE NARROWS

Early Pleistocene and volcanic stratigraphy and petroleum-bearing Calcite Springs.—**Proceed up the stairs and along the walkway.** Here the Yellowstone River has cut a deep gorge in well-stratified andesitic breccias of the Absaroka Volcanic Supergroup and latest Cenozoic basalt flows (fig. 38). The full depth of this gorge and Calcite Springs can be seen from the overlook (fig. 39).

Several late Cenozoic canyons have been filled and recut in this area. The geologic sequence is (1) Eocene Absaroka Volcanic Supergroup; (2) quartzite-rich stream gravel capped by the 2-Ma Junction Butte Basalt; (3) a younger canyon cut into the Junction Butte Basalt then filled with 1.30±0.01-Ma ash (Obradovich and Izett, 1991), gravels, lake sediments, and till containing striated boulders

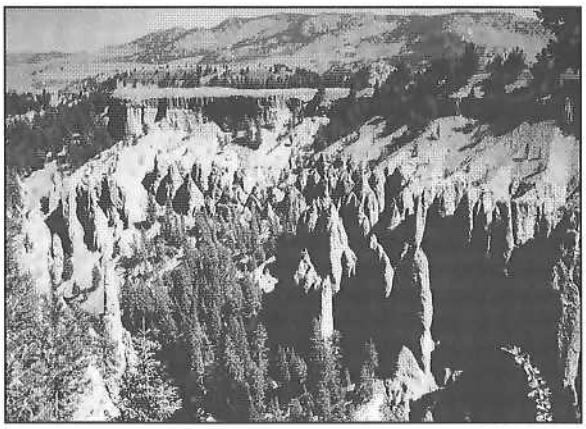

Figure 38. Stratified andesitic breccias of Absaroka Volcanic Supergroup capped by columnar-jointed basalt flows.

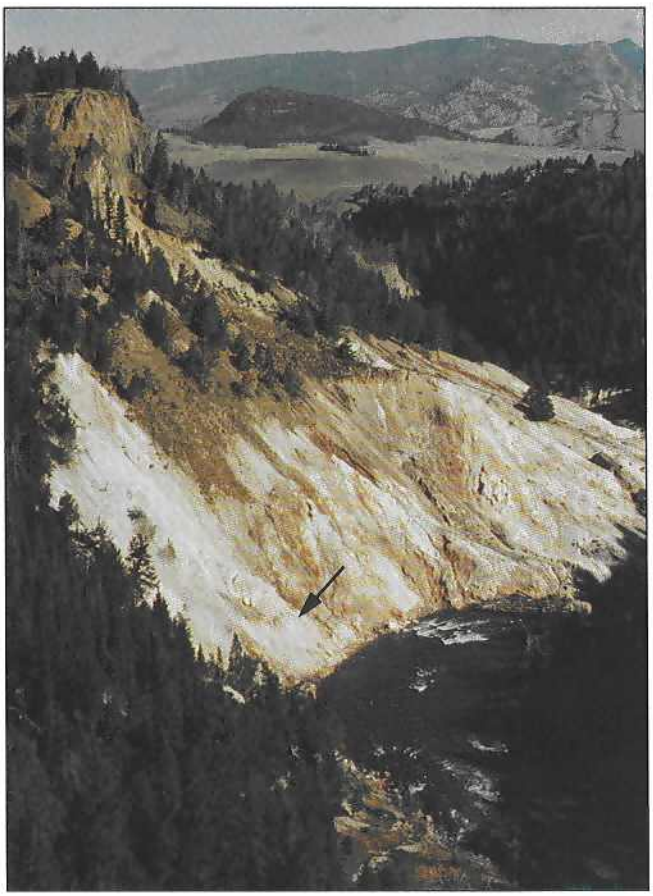

Figure 39. View from Calcite Springs overlook showing lower Grand Canyon of the Yellowstone at The Narrows. Steaming ground near river (arrow) shows location of Calcite Springs, which emerge from hydrothermally altered rock.

and Precambrian granitic rocks—this sequence is overlain by ~1.0–1.5-Ma basalt and the Lava Creek Tuff (0.6 Ma); and (4) beyond the far canyon wall, Alden Paleovalley, filled with Pinedale glacial deposits. The canyon beneath the overlook is called "The Narrows" and was cut by the Yellowstone River following the last glaciation. Less than 1.6 km upstream is Tower Falls, where Tower Creek plunges into this postglacial canyon alongside the postglacial Hoodoos, which are almost as tall as the canyon is deep.

Calcite Springs is a geothermal area that takes its name from masses of milky white calcite crystals nearby. Barite crystals are also common. Oil seeps and tarry residues issue from fissures and conduits lined with euhedral sulfur crystals. Seeps extend as much as 60 m up from river level and occur in altered Absaroka andesitic breccias.

Hydrocarbons in Yellowstone thermal waters have been described by Love and Good (1970) and Clifton and others (1990). The hydrocarbon-bearing springs occur in an arcuate southeastward- to eastward-trending area 115 km long in northwestern Wyoming. The main points at which these springs discharge in Yellowstone are at Tower Bridge, Calcite Springs, and Rainbow Springs (about 18 km southeast of Calcite Springs). The following quotes Clifton and others (1990, p. 169).

> Petroleum from Calcite Springs occurs as vapor condensates in steam vents. Detailed geochemical analyses show a complex origin for the petroleum fluid. Deeply buried, hydrothermally altered sedimentary rocks are believed to have contributed a high temperature pyrolysate consisting largely of polynuclear aromatic hydrocarbons and heterocyclic compounds. Shallow sedimentary rocks, which are also hydrothermally altered, have contributed large amounts of aromatic and polar compounds, as well as minor amounts of hydrocarbons. The Permian Phosphoria Formation is suggested as a likely source rock for the bulk of the oils. Autochthonous pyrolysates and lipids from thermally altered surface and near-surface bacterial and land plant debris have also been introduced to the vents. The latter may have been introduced by downward percolating meteoric water.
>
> The oil from Rainbow Springs is a highly paraffinic, low-S crude oil, depleted in light hydrocarbons. Unlike the Calcite Springs samples, the oil from Rainbow Springs is believed to have originated from a single sedimentary source rock with little or no hydrocarbon contributions from subsurface biota. The oil contains a unique molecular marker assemblage that suggests both gymnosperm and angiosperm input and places the age of the source unit in the Tertiary. Consideration of the local stratigraphy and water temperatures limits the probable source zone to the Eocene Aycross Formation, a syn-volcanic lacustrine mudstone. Calculation of deep water temperatures indicates that this unit is exposed to thermal waters in an extensive near-surface aquifer. Such conditions are consistent with the widespread surface manifestations and biomarker kinetic models.
>
> Consideration of the petroleum chemistry and regional hydrodynamics indicates that the Yellowstone Park oils did not migrate into the park from distant sources. The chemical data are also inconsistent with the oils being generated and trapped prior to Tertiary volcanism. At both Calcite Springs and Rainbow Springs, oil generation appears to be contemporaneous and is attributed to thermal alteration of relatively shallow sedimentary rocks by hydrothermal fluids.

Chemical geothermometers indicate that at Calcite Springs the temperature of the reservoir from which the fluids discharge is about 150 to 170°C.

STOP 22—WASHBURN OVERLOOK

Overview of Yellowstone caldera from its north wall, the Washburn Range.—On the far (north) side of Dunraven Pass, which we have just crossed, the road traverses the north half of Washburn volcano, a major center of the Absaroka volcanic field of Eocene age. The south half of the Washburn volcano is downdropped within the Yellowstone caldera. We are now essentially on the northern wall of the caldera. In the foreground is the tree-covered surface of the Canyon flow, which abuts the caldera wall from within (fig. 40). The Grand Canyon of the Yellowstone cuts the flow in middle distance. Beyond is the low rise of Sour Creek dome, broken by a northwest-trending graben. To the east are the Mirror Plateau and Absaroka Mountains. Far to the southeast are the Red Mountains and, visible on a clear day, the Teton Range. The caldera rim can be followed from the Washburn Range, across the Grand Canyon, to the ridge with a prominent crescentic grassy area and beyond to the ridge on the far side of Broad Creek. The Canyon flow and Sour Creek dome block the view of the wall beyond, but it continues along the far shore of Yellowstone Lake and in front of the Red Mountains, which are 55 km away. The southwest skyline is the Central Plateau, and farther to the west is Madison

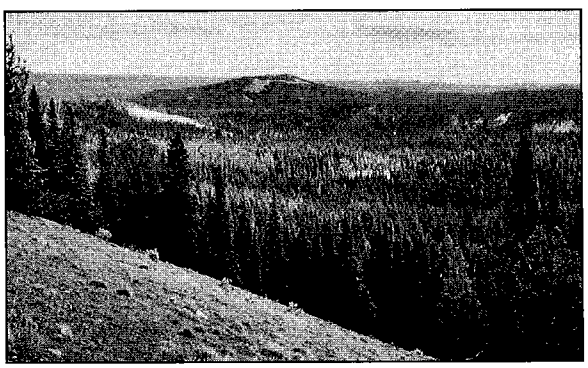

Figure 40. View looking east from Washburn overlook on north side of Dunraven Pass. Hydrothermally altered patches of white ground in middle distance mark location of Washburn Springs. Grand Canyon of the Yellowstone is between Washburn Springs and Sour Creek Dome, seen in background.

Plateau, which is 55 km away but still within the western margin of the Yellowstone caldera.

Andesitic debris-flow breccia or conglomerate in the adjacent roadcut is cut by a 4-m-thick silicic andesite dike of the Eocene Washburn volcanic center. Till-mantled outcrops of andesitic breccia and a few lava flows continue up the road toward Dunraven Pass. The top of Mt. Washburn (alt 3,123 m) was striated by north-flowing ice from an icecap occupying the Yellowstone Lake basin (Pierce, 1979).

The hydrothermally altered patches of ground that can be seen below us in the distance mark the location of Washburn Springs. The waters at that locality are noted for their relatively high NH_4, high SO_4, and low Cl concentrations; amounts of dissolved NH_4 and sulfate are highly variable, as is the pH, which ranges from slightly acid to alkaline. Allen and Day (1935) noted that the gases there contain appreciable methane (13.2 percent) and ethane (1.15 percent). Representative chemical analyses are listed in table 2, Nos. 19 and 20. It is likely that organic material in sediments is being distilled at high temperatures and high pressures at the base of a vapor-dominated system, producing steam that is rich in organic gases and NH_3>H_2S in the vapor. The steam rises and then condenses near the Earth's surface, where the accompanying H_2S is oxidized to sulfuric acid, which is immediately converted to ammonium sulfate by excess NH_3.

STOP 23—ARTIST POINT

Grand Canyon of Yellowstone.—**Walk down short trail (about 100 m) to the constructed overlook.** The deeper part of the Grand Canyon is carved into the intensely altered Canyon flow. Upstream, the flow is relatively unaltered, and Lower Falls drops 94 m across a resistant ridge of steeply dipping flow layers (fig. 41). Downstream about 2 km the flow is again relatively unaltered. In the highly altered and colorful part of the canyon (fig. 42), hydrothermal activity remains vigorous near river level, although it is hard to see from the canyon rim unless the day is cold and humid. Alteration along the deep, narrow part of the Grand Canyon is controlled by the buried ring-fracture zone of Yellowstone caldera and by crossing fractures. Precanyon sedimentary rocks at the rim of the canyon on both sides are bleached white by surficial acid-sulfate alteration; rhyolite deeper in the canyon was pervasively pyritized and then oxidized to the yellowish colors that give the Yellowstone region its name. Across the canyon is an abandoned channel segment at about half the present depth of the canyon. That channel was filled by sediments behind an ice dam of Bull Lake(?) age downstream and was probably kept free of ice, at least during stagnation of the ice sheet, by local thermal activity. On the skyline to the west, above Lower Falls, is the Solfatara Plateau flow at the north end of the Central Plateau.

The compositions of the thermal waters discharged from springs deep in the canyon are similar to alkaline-chloride waters found in the Upper and Lower Geyser Basins.

STOP 24—LUNCH AT BUFFALO FORD PICNIC AREA

The suggested picnic spot is about a mile south of the Mud Volcano area. It offers nice facilities near the Yellowstone River.

STOP 25—MUD VOLCANO AREA

A small vapor-dominated system.—The Mud Volcano area is an excellent example of a small vapor-dominated hydrothermal system. The thermal discharge is gas-rich, and the enclosing rocks and surficial deposits are intensely altered. The acidic thermal waters probably reflect shallow

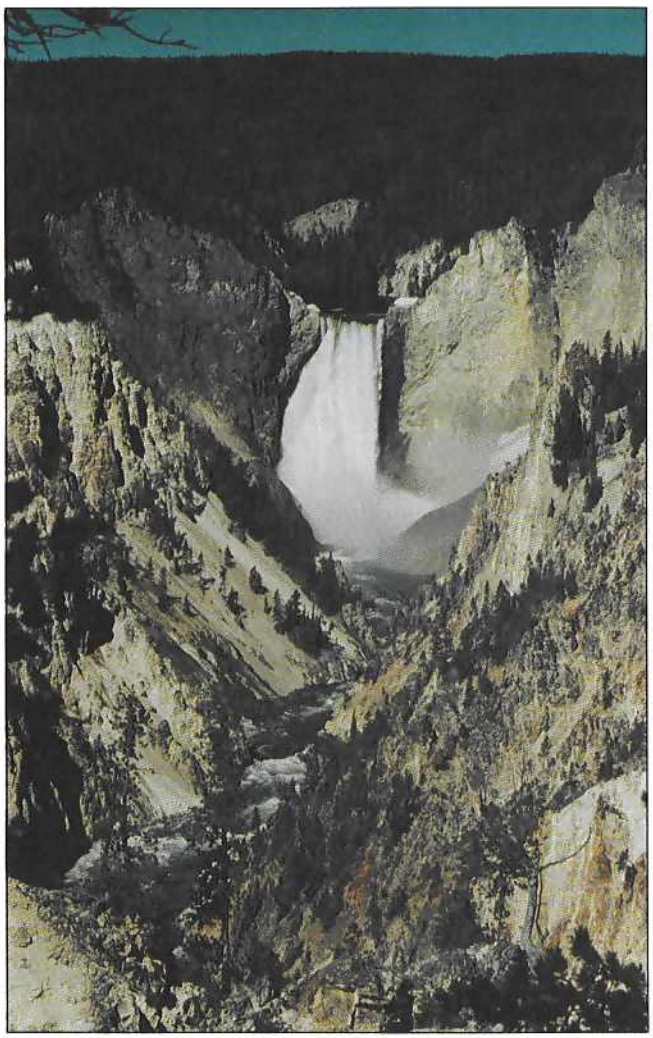

Figure 41. Lower Falls seen from Artist Point.

condensation above a reservoir in which liquid water is subordinate to steam in fractures and pore spaces; steam is the pressure-controlling phase (White and others, 1971). Gases including H_2S rise with the steam and dissolve in the condensate to produce the acid waters.

A USGS research drill hole (Y–11), north of the main parking area and between the road and the river, provided some of the data on which the concept of vapor-dominated hydrothermal systems is based (White and others, 1971). The thermal waters at Mud Volcano are typical of acid-sulfate waters in which there is little chloride and compositions are controlled by nonequilibrium water/rock reactions in a near-surface oxidizing environment. Brock (1978) studied the rate and mode of generation of sulfuric acid in the pools at Mud Volcano and concluded that most of the acidity comes from bacterial oxidation of elemental sulfur at the cool margins of the pools by *Sulfolobus* sp. Even though these boiling pools show little to no surface discharge, there is seepage in and out through their permeable sides. Brock (1978) measured rates of seepage by adding known amounts of chloride and measuring the rate of dilution. For Moose Pool and Sulfur Caldron his measurements give 818 and 452 L/hr, respectively. The amount of sulfate discharged by these pools was estimated to be 44,352 and 24,504 g/day, respectively.

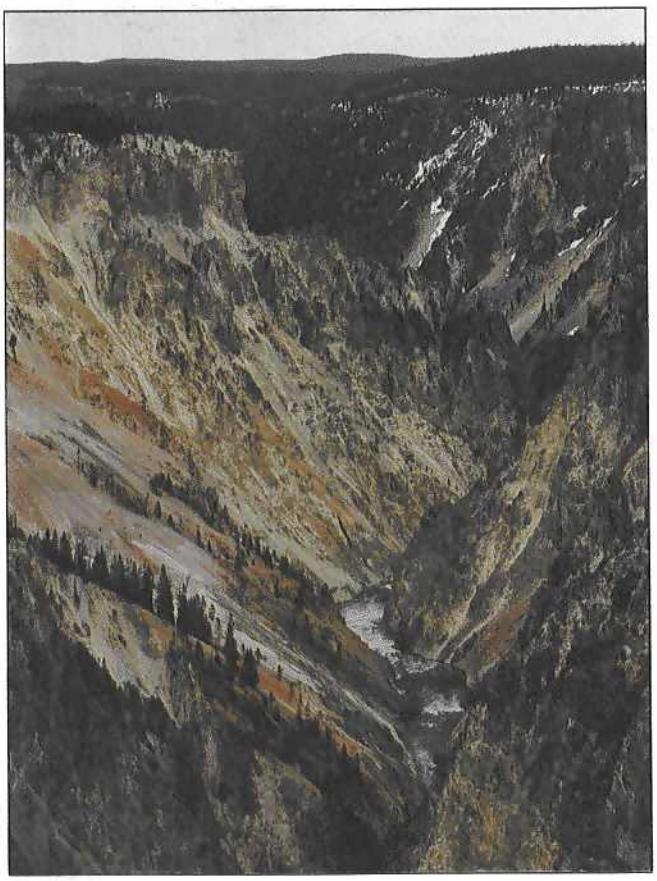

Figure 42. Hydrothermally altered rhyolite exposed in walls of Grand Canyon of the Yellowstone. View from Artist Point looking downstream.

Very high $^3He/^4He$ ratios, up to 16 times the atmospheric ratio, are found at Mud Volcano. These are the most ^3He-enriched gases in Yellowstone Park (Craig and others, 1978; Kennedy and others, 1985). Fournier and others (1989) attributed the variations of $^3He/^4He$ ratios throughout the park mainly to variations in permeability and hydrologic conditions. Recall that most ^3He is derived from a mantle source, whereas ^4He is a product of radioactive decay reactions that occur in the crust. Deep waters tend to have high $^3He/^4He$ ratios, and shallow waters tend to have low $^3He/^4He$ ratios. The $^3He/^4He$ ratios tend to be relatively low in the thermal waters that discharge in the Upper and Lower Geyser Basins because considerable deep subsurface boiling occurs there, and helium preferentially partitions into the steam, which takes a separate path to the Earth's surface from the water. The residual helium-depleted water then picks up radiogenic ^4He from the wall rock in intermediate-depth reservoirs, and there also is a decrease in the $^3He/^4He$ ratio where there is subsurface mixing with meteoric water. The net result is waters that have relatively low absolute concentrations of dissolved helium and relatively low $^3He/^4He$ ratios. In contrast, at Mud Volcano the ^3He-rich steam that separates from boiling water at great depth moves upward through relatively impermeable rock, and there is little opportunity for contamination by ^4He-rich local ground waters. Because the total helium concentration in the steam is relatively high and because that helium is relatively rich in ^3He, the $^3He/^4He$ ratio is not changed significantly by the leaching of radiogenic ^4He from the wall rock as the steam moves upward.

Temporal changes in activity in the Mud Volcano area appear to correlate with local seismicity. Only Pinedale glacial deposits are exposed in the Mud Volcano area, except for a single outcrop of the Lava Creek Tuff at Dragon's Mouth Spring and outcrops near Sulfur Caldron. **Walk the well-maintained loop trail starting from either the north or south end of the parking lot.** Black Dragon's Cauldron (fig. 43) is at the topographic high point on the trail. From above Mud Geyser at the south end of the loop trail, a good view to the east shows the west flank of the Sour Creek Dome broken by a graben of the Elephant Back Fault Zone.

STOP 26—LE HARDYS RAPIDS

Inflation and deflation of Yellowstone caldera.—Following the 1959 magnitude-7.5 Hebgen Lake earthquake, a level line was run across the Yellowstone caldera that indicated a significant uplift had occurred since the previous level line was run in 1923. Subsequently, several additional level lines have been run to monitor this uplift (Pelton and Smith, 1979, 1982; Dzurisin and others, 1986; Dzurisin and Yamashita, 1987; Dzurisin and others, 1990).

It is not known when the uplift started, but it continued until 1984 with an average rate of uplift of about 19.5±1 mm/yr between 1976 and 1984. The caldera stopped rising during the 1984 to 1985 period and since then has been subsiding at rates as high as 35±7 mm/yr. However, the rate of subsidence has recently decreased. Le Hardys Rapids is near the center of this inflation and deflation (fig. 44). Although most of the level lines were run in the eastern part of Yellowstone Park, on the southwest flank of the Sour Creek resurgent dome (fig. 1), level lines along the southwest flank of the Mallard Lake resurgent dome also have shown a similar pattern of uplift followed by subsidence. It appears that the entire Yellowstone caldera has been subjected to these movements. Studies of raised and submerged shoreline terraces show that there has been episodic uplift interspersed with local deflation of the caldera throughout the Holocene (Hamilton, 1985; Meyer and Lock, 1986). Late Holocene uplift at Le Hardys Rapids has backflooded the Yellowstone River so that it has become an extension of Yellowstone Lake. The timing of cycles of uplift/subsidence using cores that contain materials suitable for carbon-14 dating is currently being studied by K.L. Pierce, USGS. Preliminary results indicate that uplift/subsidence events in the past generally have been of longer duration and higher in amplitude than those that have occurred this century. The cause of the uplift/subsidence is still under investigation. This deformation may be related to various mechanisms, including (1) episodic accumulation of magmatic fluids at the top of a crystallizing magma with pressure buildup, followed by leakage of fluids and pressure decline, (2) episodic intrusions of new pulses of magma, (3) regional stresses, or (4) a combination of these processes.

Walk down the boardwalk to the river. The roadcut across the road exposes only Pinedale alluvial deposits, but the Yellowstone River cuts down into an upthrown fault block of the Lava Creek Tuff. The erosionally resistant near-basal spherulitic zone forms the rapids. The Lava Creek Tuff here is uplifted within the Yellowstone caldera on the flank of the Sour Creek resurgent dome. Outcrops across the river are the Lava Creek Tuff overlain by Pinedale glacial deposits. The fault that brings the spherulitic zone up to the level of exposure here can be seen across the canyon; it and other northeast-trending faults that cut the Sour Creek Dome are parts of the Elephant Back Fault Zone, a complex graben coaxial with the axis of historical uplift and subsidence within the Yellowstone caldera.

Below Le Hardys Rapids, in the direction from which we have come, the road follows a straight segment of the Yellowstone River controlled by a northwest-trending fault that locally breaks the Sour Creek Dome.

STOP 27—YELLOWSTONE LAKE

View across the main Yellowstone Lake Basin.—To the northeast is Stonetop Mountain (in the southern part of the Sour Creek resurgent dome in the eastern part of the Yellowstone caldera), which has a prominent area of hydrothermal

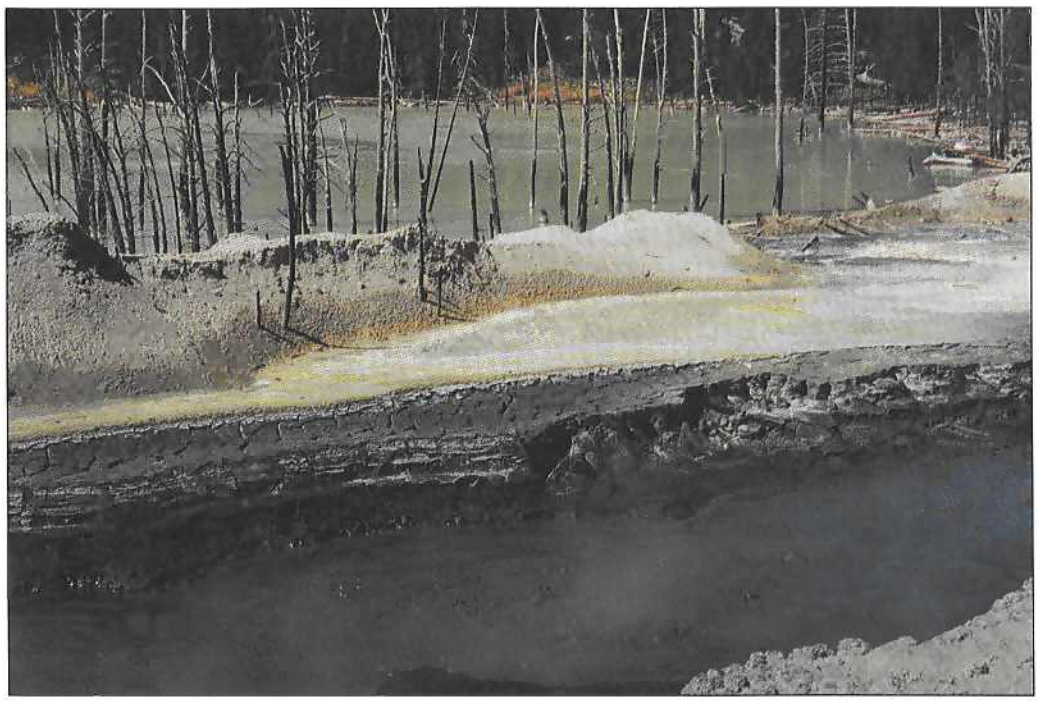

Figure 43. Black Dragon's Cauldron, Mud Volcano area.

alteration (Sulphur Hills) on its south side. Beyond the south (right) flank of Stonetop Mountain is Pelican Cone, which is a peak of Eocene andesites of the Absaroka Volcanic Supergroup outside the eastern margin of the caldera. The margin continues south along the west front of the Absaroka Mountains to Lake Butte, seen over Stevenson Island, then follows the east shore of Yellowstone Lake as far to the right as the area of view. The high plateau rising toward the Absaroka Mountains is underlain mainly by the Lava Creek Tuff. Beyond the southern part of the lake, the Two Ocean Plateau is a gently west-tilted fault block—the easternmost basin-range fault block south of the Yellowstone Plateau.

STOP 28—SNAKE RIVER OVERLOOK

Overview of geologic and glacial relations.—The Snake River overlook is an excellent place to view the distant Teton Mountains (fig. 45). It is also a good place to observe Pinedale moraines and outwash deposits. The southern part of the Yellowstone-Absaroka ice mass formed three glacial lobes that flowed into Jackson Hole. These lobes are named for the drainages they occupied (from east to west): Buffalo Fork, Pacific Creek, and Snake River (Pierce and Good, 1990). The succession of glacial lobes and associated moraines reflects westward migration of the center of gravity of the Yellowstone-Absaroka glacial source area, probably in response to orographic build-up on the western downwind side of the icecap. Great volumes of quartzite-rich outwash accumulated and buried much of these moraines. Here at the overlook we can see moraines of the Burned Ridge phases of the Buffalo Fork-Pacific Creek lobes. Stones in the moraine across the road to the east and in moraines to the south are dominated by roundstones that are typical of quartzite of the Pinyon Con-

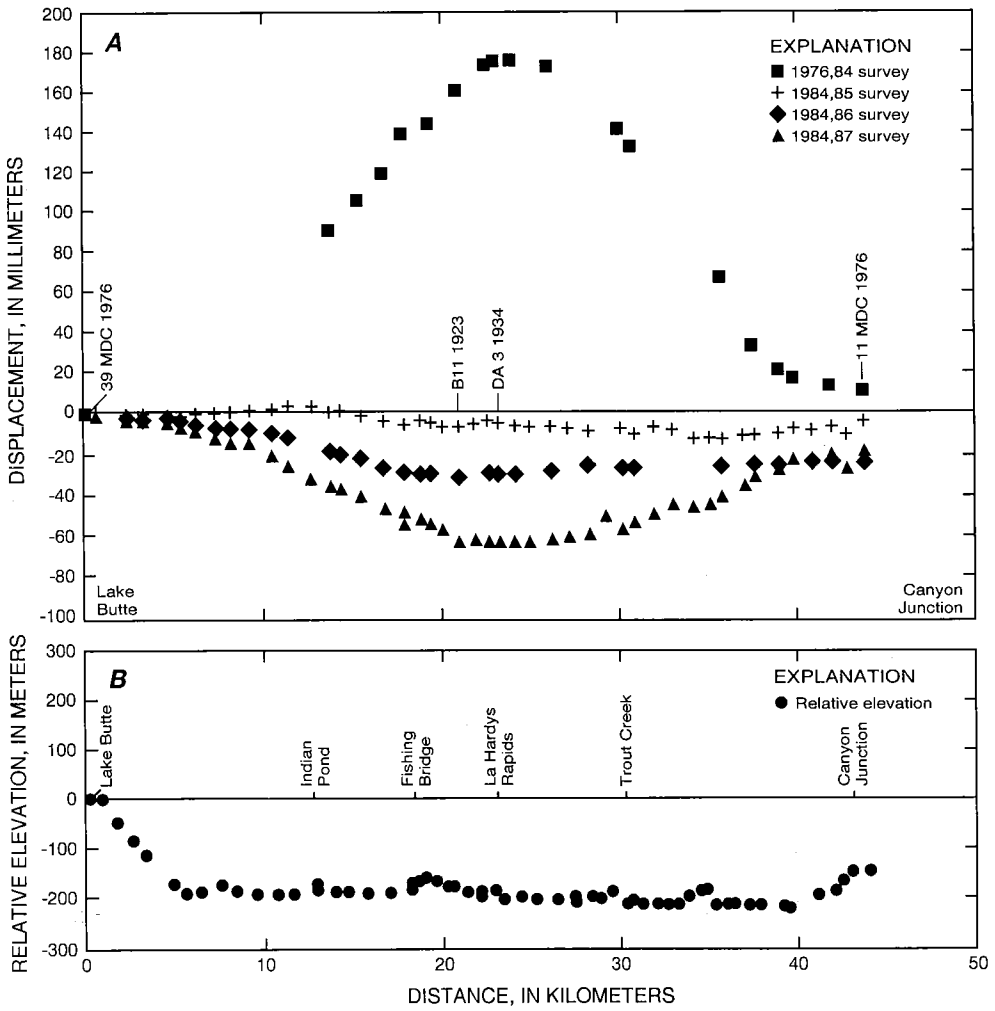

Figure 44. *A*, Vertical displacement and *B*, topographic profiles along eastern leveling line from Lake Butte to Canyon Junction. Displacement profiles are based on successive surveys from 1976 to 1987. Also shown, locations of selected benchmarks and place names. Elephant Back Fault Zone intersects leveling line at Le Hardys Rapids (benchmark DA 3 1934). (From Dzurisin and others, 1990).

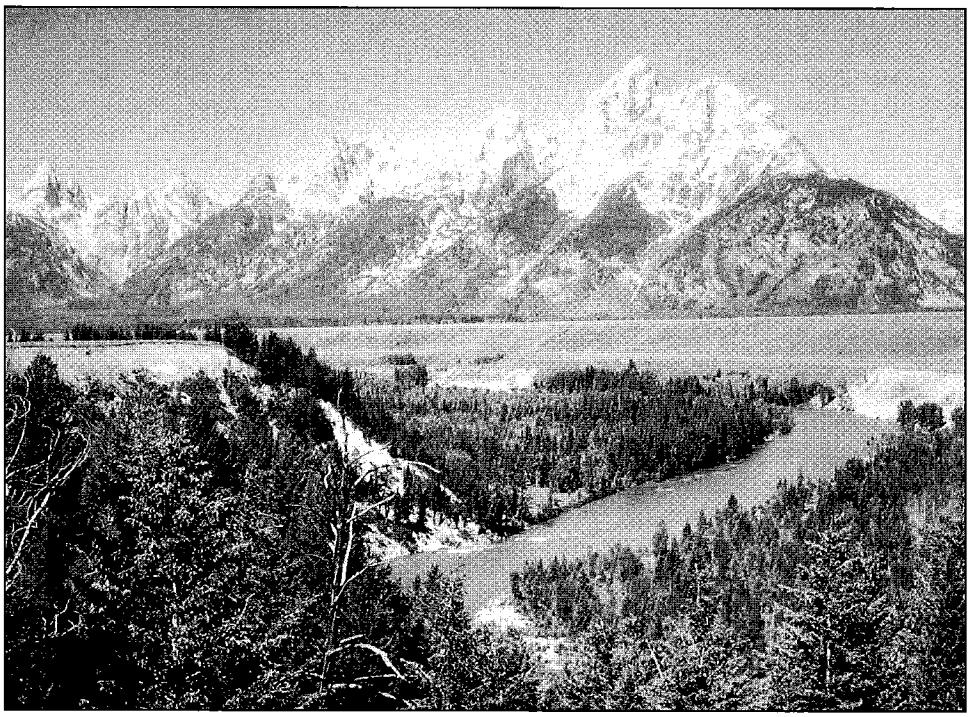

Figure 45. View of Cathedral Group of peaks from Snake River overlook, Stop 28.

glomerate with lesser amounts of Precambrian crystalline rocks, Paleozoic limestone, Pennsylvanian sandstone, and Eocene andesite rocks, all of which are indicative of a Yellowstone-Absaroka glacial source area. The dropoff to the north is a depositional ice-contact slope formed at an ice front. The outwash was largely carried by Spread Creek, which flowed westward along the south of the glacier toward this stop. Looking across the river to the right of the Burned Ridge moraine, the lower terrace level can be seen to extend northward to its source at the Jackson Lake moraines. This terrace is pitted with numerous potholes. Looking down the Snake River, the prominent lowermost terrace marks the lowest level eroded by multiple floods during the Jackson Lake phase.

SELECTED REFERENCES

Allen, E.T., and Day, A.L., 1935, Hot springs of the Yellowstone National Park: Carnegie Institution of Washington Publication 466, 525 p.

Bargar, K.E., 1978, Geology and thermal history of Mammoth Hot Springs, Yellowstone National Park, Wyoming: U.S. Geological Survey Bulletin 1444, 55 p.

Bargar, K.E., and Beeson, M.H., 1985, Hydrothermal alteration in research drill hole Y–3, Lower Geyser Basin, Yellowstone National Park, Wyoming: U.S. Geological Survey Professional Paper 1054–C, 23 p.

Bargar, K.E., and Fournier, R.O., 1988, Effects of glacial ice on subsurface temperatures of hydrothermal systems in Yellowstone National Park, Wyoming—fluid-inclusion evidence: Geology, v. 16, p. 1077–1080.

Bargar, K.E., Fournier, R.O., Theodore, T.G., 1985, Particles in fluid inclusions from Yellowstone National Park—bacteria?: Geology, v. 13, p. 483–486.

Benz, H.M., and Smith, R.B., 1984, Simultaneous inversion for lateral velocity variations and hypocenters in the Yellowstone region using earthquake and controlled source data: Journal of Geophysical Research, v. 89, p. 1208–1220.

Bhattacharyya, B.K., and Leu, L.K., 1975, Analysis of magnetic anomalies over Yellowstone National Park—mapping of Curie point isothermal surface for geothermal reconnaissance: Journal of Geophysical Research, v. 80, p. 4461–4465.

Blank, H.R., Jr., and Gettings, M.E., 1974, Complete Bouguer gravity map—Yellowstone Island Park region: U.S. Geological Survey Open-File Map 74-22, scale 1:125,000.

Boyd, F.R., 1961, Welded tuffs and flows in the rhyolite plateau of Yellowstone National Park, Wyoming: Geological Society of America Bulletin, v. 72, p. 387–426.

Brock, T.D., 1978, Thermophilic microorganisms and life at high temperatures: New York, Springer–Verlag, 465 p.

Brokaw, M.A., 1985, Upper crustal interpretation of Yellowstone determined from ray trace modeling of seismic refraction data: M.S. thesis, University of Utah, Salt Lake City, 180 p.

Christiansen, R.L., 1984, Yellowstone magmatic evolution—its bearing on understanding large-volume explosive volcanism, *in* Explosive volcanism—inception, evolution and hazards: Washington, D.C., National Academy of Sciences, p. 84–95.

———1989, Days 1, 2 and 3—The Yellowstone Plateau volcanic field, *in* Bonnichsen, B., Christiansen, R.L., Morgan, L.A., Moye, F.J., Hackett, W.R., Leeman, W.P., Honjo, N., Jenks, M.D., and Godchaux, M.M., Excursion 4A—silicic

volcanic rocks in the Snake River Plain–Yellowstone Plateau province, *in* Chapin, C.E., and Zidek, J., eds., Field excursions to volcanic terranes in the western United States, volume II—Cascades and Intermountain West: New Mexico Bureau of Mines and Mineral Resources Memoir 47, p. 137–153.

Christiansen, R.L., and Blank, H.R., Jr., 1972, Volcanic stratigraphy of the Quaternary rhyolite plateau in Yellowstone National Park: U.S. Geological Survey Professional Paper 729–B, 18 p.

———Geologic map of the Old Faithful quadrangle, Yellowstone National Park, Wyoming: U.S. Geological Survey Geologic Quadrangle Map GQ-1189, scale 1:62,500.

Christiansen, R.L., and Hutchinson, R.A., 1987, Rhyolite-basalt volcanism of the Yellowstone Plateau and hydrothermal activity of Yellowstone National Park, Wyoming: Geological Society of America Centennial Field Guide, p. 103–107.

Clifton, C.G., Walters, C.C., and Simoneit, B.R.T., 1990, Hydrothermal petroleums from Yellowstone National Park, Wyoming: Applied Geochemistry, v. 5, p. 169–191.

Craig, Harmon, Lupton, J.E., Welhan, J.A., and Poreda, R., 1978, Helium isotope ratios in Yellowstone and Lassen Park volcanic gases: Geophysical Research Letters, v. 5, p. 897–900.

Daniel, R.G., and Boore, D.M., 1982, Anomalous shear wave delays and surface wave velocities at Yellowstone caldera, Wyoming: Journal of Geophysical Research, v. 87, p. 2731–2744.

Dzurisin, C.D., Savage, J.C., and Fournier, R.O., 1990, Recent crustal subsidence at Yellowstone caldera, Wyoming: Bulletin of Volcanology, v. 52, p. 247–270.

Dzurisin, C.D., and Yamashita, K.M., 1987, Vertical surface displacements at Yellowstone caldera, Wyoming, 1976–1985: Journal of Geophysical Research, v. 92, p. 13753–13766.

Dzurisin, C.D., Yamashita, K.M., and Johnson, D.J., 1986, Preliminary results of precise leveling and trialteration surveys in Yellowstone National Park, Wyoming, 1985: U.S. Geological Survey Open-File Report 86–265–B, 28 p.

Eaton, G.P., Christiansen, R.L., Iyer, H.M., Pitt, A.M., Mabey, D.R., Blank, Jr., H.R., Zietz, Isidore, and Gettings, M.E., 1975, Magma beneath Yellowstone National Park: Science, v. 188, p. 787–796.

Fournier, R.O., 1983, Active hydrothermal systems as analogues of fossil systems, *in* The role of heat in the development of energy and mineral resources in the Northern Basin and Range Province: Geothermal Resources Council Special Report 13, p. 263–284.

———1987, Conceptual models of brine evolution in magmatic-hydrothermal systems, *in* Decker, R.W., Wright, T.L., and Stauffer, P.H., eds., Hawaiian volcanism: U.S. Geological Survey Professional Paper 1350, p. 1487–1506.

———1989, Geochemistry and dynamics of the Yellowstone National Park hydrothermal system, Wyoming: Annual Review of Earth and Planetary Sciences, v. 17, p. 13–53.

———1991, The transition from hydrostatic to greater than hydrostatic fluid pressure in presently active continental hydrothermal systems in crystalline rock: Geophysical Research Letters, v. 18, no. 5, p. 955–958.

Fournier, R.O., Kennedy, B.M., and Truesdell, A.H., 1989, A hydrologic model to account for variations in $^{3}He/^{4}He$ in thermal waters throughout Yellowstone National Park [abs.]: Abstracts, 28th International Geologic Congress, Washington, D.C., v. 1, p. 506.

Fournier, R.O., and Pitt, A.M., 1985, The Yellowstone magmatic-hydrothermal system, *in* Stone, Claudia, ed., International Symposium on Geothermal Energy, international volume: Geothermal Resources Council Transactions, p. 319–327.

Fournier, R.O., Thompson, J.M., Cunningham, C.G., and Hutchinson, R.A., 1991, Conditions leading to a recent small hydrothermal explosion at Yellowstone National Park: Geological Society of America Bulletin, v. 103, p. 1114–1120.

Fournier, R.O., Thompson, J.M., and Hutchinson, R.A., 1986, Fluctuations in composition of Cistern Spring, Norris Geyser Basin, Yellowstone National Park, Wyoming—variable boiling and mixing 1962–1985 [abs.]: Fifth International Symposium Water–Rock Interaction, Reykjavík, Iceland, p. 206–209.

Fournier, R.O., White, D.E., and Truesdell, A.H., 1976, Convective heat flow in Yellowstone National Park, *in* Proceedings, Second United Nations Symposium on the Development and Use of Geothermal Resources: Washington, D.C., U.S. Government Printing Office, v. I, p. 731–739.

Friedman, Irving, Pierce, K.L., Obradovich, J.D., and Long, W.D., 1973, Obsidian hydration dates glacial loading(?): Science, v. 180, p. 733–734.

Gooch, F.A., and Whitfield, J.E., 1888, Analyses of waters of the Yellowstone National Park, with an account of the methods of analysis employed: U.S. Geological Survey Bulletin 47, 84 p.

Hamilton, W.L., 1985, Deformation models for interpreting warped Holocene terraces of Yellowstone Lake and the Yellowstone River at the Yellowstone caldera, Wyoming [abs.]: Eos, Transactions of the American Geophysical Union, v. 66, no. 46, p. 853.

Hayden, F.V., 1883, Twelfth annual report of the U.S. Geological and Geographical Survey of the territories—A report of progress of the exploration in Wyoming and Idaho for the year 1878, in two parts, part II: Washington, D.C., U.S. Government Printing Office, 490 p.

Iyer, H.M., Evans, J.R., Zandt, G., Stewart, R.M., Cookley, J.M., and Roloff, J.N., 1981, A deep low-velocity body under the Yellowstone caldera, Wyoming—delineation using teleseismic *P*-wave residuals and tectonic interpretations: Geological Society of America Bulletin, v. 92, p. 792–798.

Jackson, S.M., Smith, R.B., and Olson, T.L., 1984, Recent uplift of the Yellowstone caldera from precision gravity measurements [abs.]: Eos, Transactions of the American Geophysical Union, v. 65, no. 45, p. 1118.

Keith, T.E.C., White, D.E., and Beeson, M.H., 1978, Hydrothermal alteration and self sealing in Y–7 and Y–8 drill holes in the northern part of Upper Geyser Basin, Yellowstone National Park, Wyoming: U.S. Geological Survey Professional Paper 1054–A, 26 p.

Kennedy, B.M., Lynch, M.A., Reynolds, J.H., and Smith, S.P., 1985, Intensive sampling of noble gases in fluids at Yellowstone—I., Early overview of the data; regional patterns: Geochimica et Cosmochimica et Acta, v. 49, p. 1251–1261.

Kennedy, B.M., Reynolds, J.H., Smith, S.P., and Truesdell, A.H., 1987, Helium isotopes—Lower Geyser Basin, Yellowstone National Park: Journal of Geophysical Research, v. 92, p. 12477–12489.

Kharaka, Y.K., Mariner, R.H., Ambats, Gil, Evans, W.C., White, L.D., Bullen, T.D., and Kennedy, B.M., 1990, Origins of water and solutes in and north of the Norris–Mammoth cor-

ridor, Yellowstone National Park: Geothermal Resources Council Transactions, pt. I, v. 14, p. 705–714.

Kharaka, Y.K., Mariner, R.H., Bullen, T.D., Kennedy, B.M., and Sturchio, N.C., 1991, Geochemical investigations of hydraulic connections between Corwin Springs known geothermal resources area and adjacent parts of Yellowstone National Park, chap. F *in* Sorey, M.L., ed., Effects of potential geothermal development in the Corwin Springs known geothermal resources area, Montana, on the thermal features of Yellowstone National Park: U.S. Geological Survey Water-Resources Investigations Report 91–4052, p. F1–F38.

Lehman, J.A., Smith, R.B., Schilly, M.M., Braile, L.W., 1982, Upper crustal structure of the Yellowstone caldera from delay time analyses and gravity correlations: Journal of Geophysical Research, v. 87, p. 2713–2730.

Love, J.D., and Good, J.M., 1970, Hydrocarbons in thermal areas, northwestern Wyoming: U.S. Geological Survey Professional Paper 644–B, 23 p.

Meyer, G.A., and Lock, W.K., 1986, Origin and deformation of Holocene shoreline terraces, Yellowstone Lake, Wyoming: Geology, v. 14, p. 699–702.

Morgan, Paul, Blackwell, D.D., and Spafford, R.E., 1977, Heat flow measurements in Yellowstone Lake and the thermal structure of the Yellowstone caldera: Journal of Geophysical Research, v. 82, p. 3719–3732.

Muffler, L.J.P., White, D.E., Beeson, M.H., and Truesdell, A.H., 1982, Geologic map of Upper Geyser Basin, Yellowstone National Park, Wyoming: U.S. Geological Survey Miscellaneous Investigations Map I–1371, scale 1:4800, 1 sheet.

Muffler, L.J.P., White, D.E., and Truesdell, A.H., 1971, Hydrothermal explosion craters in Yellowstone National Park: Geological Society of America Bulletin, v. 82, p. 723–740.

Muffler, L.J.P., White, D.E., Truesdell, A.H., and Fournier, R.O., 1982, Geologic map of Lower Geyser Basin, Yellowstone National Park, Wyoming: U.S. Geological Survey Miscellaneous Investigations Map I–1373, scale 1:24,000, 1 sheet.

Obradovich, J.D., 1992, Geochronology of the Late Cenozoic volcanism of Yellowstone National Park and adjoining areas, Wyoming and Idaho: U.S. Geological Survey Open-File Report 92–408, 45 p.

Obradovich, J.D., and Izett, G.A., 1991, $^{40}Ar/^{39}Ar$ ages of upper Cenozoic Yellowstone Group tuffs [abs.]: Geological Society of America Abstracts with Programs, v. 23, no. 2, p. 84.

Pearson, F.J., Jr., and Truesdell, A.H., 1978, Tritium in the waters of Yellowstone National Park: U.S. Geological Survey Open-File Report 78-701, p. 327–329.

Pelton, J.R., and Smith, R.B., 1979, Recent crustal uplift in Yellowstone National Park: Science, v. 206, p. 1179–1182.

———1982, Contemporary vertical surface displacements in Yellowstone National Park: Journal of Geophysical Research, v. 87, p. 2745–2751.

Pierce, K.L., 1979, History and dynamics of glaciation in the northern Yellowstone National Park area: U.S. Geological Survey Professional Paper 729–F, 90 p.

———1982, History and dynamics of glaciation in the northern Yellowstone National Park area: Wyoming Geological Association Thirty-Third Annual Field Conference Guidebook, p. 27–29.

Pierce, K.L., Adams, K.D., and Sturchio, N.C., 1991, Geologic setting of the Corwin Springs known geothermal resources area—Mammoth Hot Springs area in and adjacent to Yellowstone National Park, chap. C *in* Sorey, M.L., ed., Effects of potential geothermal development in the Corwin Springs known geothermal resources area, Montana, on the thermal features of Yellowstone National Park: U.S. Geological Survey Water-Resources Investigations Report 91–4052, p. C1–C37.

Pierce, K.L., and Good, J.M., 1982, Emphasizing glacial geology, northern Yellowstone National Park, *in* Goolsby, J.E., ed., Geology of Yellowstone Park area: Wyoming Geological Association Field Trip Road Logs, Field Trip No. 2.

———1990, Quaternary geology of Jackson Hole, Wyoming, *in* Roberts, S., ed., Geologic field tours of western Wyoming: Geological Survey of Wyoming Public Information Circular 29, Field Trip No. 4, p. 78–87.

Pierce, K.L., and Morgan, L.A., 1992, The track of the Yellowstone hot spot: volcanism, faulting, and uplift, Chap. 1, *in* Link, P.K., Kuntz, M.A., and Platt, L.B., eds., Regional geology of eastern Idaho and western Wyoming: Geological Society of America Memoir 179, p. 1–53.

Pierce, K.L., Obradovich, J.D., and Friedman, Irving, 1976, Obsidian hydration dating and correlation of Bull Lake and Pinedale glaciations near West Yellowstone, Montana: Geological Society of America Bulletin, v. 87, p. 703–710.

Rowe, J.J., Fournier, R.O., and Morey, G.W., 1973, Chemical analyses of thermal waters in Yellowstone National Park, Wyoming, 1960–1965: U.S. Geological Survey Bulletin 1303, 31 p.

Schoen, Robert, 1969, Rate of sulfuric acid formation in Yellowstone National Park: Geological Society of America Bulletin, v. 80, p. 643.

Schoen, Robert, and Rye, R.O., 1970, Sulfur isotope distribution in solfataras, Yellowstone National Park: Science, v. 170, p. 1082–1084.

Smedes, H.W., and Prostka, H., 1972, Stratigraphic framework of the Absaroka Volcanic Supergroup in the Yellowstone National Park region: U.S. Geological Survey Professional Paper 729–C, 33 p.

Smith, R.B., and Braile, L.W., 1984, Crustal structure and evolution of an explosive silicic volcanic system at Yellowstone National Park, *in* Explosive volcanism—inception, evolution and hazards: Washington, D.C., National Academy of Sciences, p. 111–144.

Smith, R.B., and Christiansen, R.L., 1980, Yellowstone Park as a window on the Earth's interior: Scientific American, v. 242, p. 104–117.

Smith, R.B., Shuey, R.T., Freidline, R.O., Otis, R., and Alley, L.B., 1974, Yellowstone hot spot—new magnetic and seismic evidence: Geology, v. 2, p. 451–455.

Sorey, M.L., ed., 1991, Effects of potential geothermal development in the Corwin Springs known geothermal resources area, Montana, on the thermal features of Yellowstone National Park: U.S. Geological Survey Water-Resources Investigations Report 91–4052.

Stanley, W.D., Boehl, J.E., Bostick, F.X., and Smith, H.W., 1977, Geothermal significance of magnetotelluric sounding in the eastern Snake River Plain—Yellowstone region: Journal of Geophysical Research, v. 82, p. 2501–2514.

Sturchio, N.C., Binz, C.M., and Lewis, C.H., III, 1987, Thorium–uranium disequilibrium in a geothermal discharge zone at Yellowstone: Geochimica et Cosmochimica Acta, v. 51, p. 2025–2034.

Sturchio, N.C., Bohlke, J.K., and Binz, C.M., 1989, Radium–thorium disequilibrium and zeolite-water ion exchange in a Yellowstone hydrothermal environment: Geochimica et Cosmochimica Acta, v. 53, p. 1025–1034.

Thompson, J.M., and Hutchinson, R.A., 1980, Boundary Creek thermal area of Yellowstone National Park—II. Thermal water analyses: Geothermal Resources Council Transactions, v. 4, p. 189–192.

Thompson, J.M., Presser, T.S., Barnes, R.B., and Bird, D.B., 1975, Chemical analyses of the waters of Yellowstone National Park, Wyoming, from 1965–1973: U.S. Geological Survey Open-File Report 75–25, 59 p.

Thompson, J.M., and Yadav, Sandhya, 1979, Chemical analyses of waters from geysers, hot springs, and pools in Yellowstone National Park, Wyoming, from 1974–1978: U.S. Geological Survey Open-File Report 79–704, 49 p.

Truesdell, A.H., and Fournier, R.O., 1976, Conditions in the deeper parts of the hot-spring systems of Yellowstone National Park, Wyoming: U.S. Geological Survey Open-File Report 76–428, 29 p.

Truesdell, A.H., Nathenson, Manuel, and Rye, R.O., 1977, The effects of subsurface boiling and dilution on the isotopic compositions of Yellowstone thermal waters: Journal of Geophysical Research, v. 82, p. 3694–3704.

Truesdell, A.H., Rye, R.O., Whelan, J.F., and Thompson, J.M., 1978, Sulfate chemical and isotopic patterns in thermal waters of Yellowstone National Park, Wyoming: U.S. Geological Survey Open-File Report 78–701, p. 435–436.

U.S. Geological Survey, 1972a, Surficial geologic map of Yellowstone National Park: U.S. Geological Survey Miscellaneous Geologic Investigations Map I–710, scale 1:125,000, 1 sheet.

———1972b, Geologic map of Yellowstone National Park: U.S. Geological Survey Miscellaneous Geologic Investigations Map I–711, scale 1:125,000, 1 sheet.

White, D.E., 1967, Some principles of geyser activity, mainly from Steamboat Springs, Nevada: American Journal of Science, v. 265, p. 641–684.

———1978, Conductive heat flows in research drill holes in thermal areas of Yellowstone National Park, Wyoming: U.S. Geological Survey Journal of Research, v. 6, p. 765–774.

White, D.E., Fournier, R.O., Muffler, L.J.P., and Truesdell, A.H., 1975, Physical results of research drilling in thermal areas of Yellowstone National Park, Wyoming: U.S. Geological Survey Professional Paper 892, 70 p.

White, D.E., Hutchinson, R.A., and Keith, T.E.C., 1988, The geology and remarkable thermal activity of Norris Geyser Basin, Yellowstone National Park, Wyoming: U.S. Geological Survey Professional Paper 1456, 84 p.

White, D.E., Muffler, L.J.P., and Truesdell, A.H., 1971, Vapor-dominated hydrothermal systems compared with hot-water systems: Economic Geology, v. 66, p. 75–97.

APPENDIX A. SUPPLEMENTAL INFORMATION SUPPLIED TO FIELD-TRIP PARTICIPANTS IN ADDITION TO THIS FIELD GUIDE.

The maps and articles listed below were distributed to the WRI-7 field trip participants. They provide additional information about many of the subjects discussed in this guide. The trail guides are available at a nominal charge from the U.S. National Park Service, and many of the geologic maps are for sale in Yellowstone National Park at Visitor Centers.

Maps:

Grand Teton National Park Official Map and Guide (U.S. National Park Service).

Yellowstone National Park Official Map and Guide (U.S. National Park Service).

Trail Guide to the Upper Geyser Basin.

Trail Guide to Fountain Paint Pot and Firehole Lake Drive.

Trail Guide to Norris Geyser Basin.

Trail Guide to Mammoth Hot Springs Area.

Trail Guide to Mud Volcano.

Surficial Geologic Map of Yellowstone National Park (U.S. Geological Survey Map I–710).

Geologic Map of Yellowstone National Park (U.S. Geological Survey Map I–711).

Geologic Map of Upper Geyser Basin (U.S. Geological Survey Map I–1371 by Muffler and others, 1982).

Geologic Map of Lower Geyser Basin (U.S. Geological Survey Map I–1373 by Muffler and others, 1982).

Articles:

Effects of Potential Geothermal Development in the Corwin Springs Known Geothermal Resources Area, Montana, on the Thermal Features of Yellowstone National Park (Sorey, ed., 1991, U.S. Geological Survey Water-Resources Investigations Report 91-4052).

Effects of Glacial Ice on Subsurface Temperatures of Hydrothermal Systems in Yellowstone National Park, Wyoming—Fluid-Inclusion Evidence (Bargar and Fournier, 1988).

Geochemistry and Dynamics of the Yellowstone National Park Hydrothermal System (R.O. Fournier, 1989).

Geology and Thermal History of Mammoth Hot Springs, Yellowstone National Park, Wyoming (Bargar, 1978, U.S. Geological Survey Bulletin 1444; contains a 1:4,800 map of Mammoth Hot Springs).

History and Dynamics of Glaciation in the Northern Yellowstone National Park Area (Pierce, 1982; abstract with two figures).

Hydrothermal Alteration in Research Drill Hole Y–3, Lower Geyser Basin, Yellowstone National Park, Wyoming (Bargar and Beeson, 1985, U.S. Geological Professional Paper 1054–C).

Hydrothermal Explosion Craters in Yellowstone National Park (Muffler and others, 1971).

Obsidian Hydration Dating and Correlation of Bull Lake and Pinedale Glaciations Near West Yellowstone, Montana (Pierce and others, 1976).

Quaternary Geology of Jackson Hole, Wyoming (Pierce and Good, 1990).

The Track of the Yellowstone Hot Spot—Volcanism, Faulting and Uplift (Pierce and Morgan, 1992).

Yellowstone Magmatic Evolution—Its Bearing on Understanding Large-Volume Explosive Volcanism (R.L. Christiansen, 1984).

APPENDIX B. ACTIVITY OF SELECTED GEYSERS IN YELLOWSTONE NATIONAL PARK, SPRING 1992.

[Data of R.A. Hutchinson, U.S. National Park Service, Yellowstone National Park. Special thanks are extended to the Yellowstone National Park naturalist staff, especially Tom Houghan and Ann Deutch, and all the Thermal Volunteers who have contributed extensive amounts of personal time in monitoring and determining current geyser activity of the park. Supers, super long eruptions that are interspersed with more numerous regular eruptions]

Geyser	Interval	Duration	Height (m)
	Upper Geyser Basin		
Old Faithful	74.46 minutes	1.5–5.5 minutes	32–56
Anemone	7–13 minutes (avg. 7 min.)	20–45 seconds	1–2
Artemisia	11 hours, 36 minutes (1990)	5.5–25 minutes	2–9
Aurum	4 hours, 2 minutes	0.9–1.2 minutes	4–6
Beehive	18 hours, 49 minutes	4.5–5.25 minutes	40–55
Castle	10 hours, 54 minutes	15–20 minutes	20–25
Daisy	100 minutes	3.5–4.5 minutes	20–30
Depression	6 hours, 18 minutes	2.5–3.5 minutes	1–2
Fan and Mortar	Rare; 2–4 days	60–90 minutes	15–35
Fantail	Dormant	1–5 minutes	2–9
Giant	Irregular, rare; most recent: 10/20/91	90–115 minutes	45–60
Giantess	Irregular, rare; most recent: 3/25/92	12–43 hours	20–55
Grand	7 hours, 23 minutes (longer if rift active)	9–16 minutes	40–60
Grotto	~6 hours, longer for marathons	Hours	4–6
Lion	65 minutes within a series 11 hours, 13 minutes for a series of one or more eruptions.	2–6 minutes	15–20
Little Cub	76 minutes	1–15 minutes	1–2.5
Oblong	Undetermined (7 hours, 17 min. in 1989)	6–8 minutes	3–8
Penta	<1 day to >5 days, irregular	2–3 minutes	1–2
Plate	103 minutes	2.5–4 minutes	1–2
Plume	42 minutes; varies diurnally	1–1.5 minutes	6–8
Rift	Hours to days	Hours	1–2
Riverside	7 hours, 8 minutes	20 minutes	20–25
Splendid	Dormant	4–10 minutes	25–45
Sunset Lake	Dormant	Seconds	0.5–5
Vault	Rare; 57 minutes in an eruptive series	3–20 minutes	1–4
	Midway Geyser Basin		
Excelsior	Dormant since 9/16/85	1.5–2 minutes	8–25
Flood	10–42 minutes; bimodal pattern	8–8.5 minutes	2–4
Opal Pool	Dormant, rare	20 minutes	6–20
Till	Active, undetermined, est. 8–9 hours	30 minutes	4–7
West Flood	42 minutes	0.5–2 minutes	0.5–1.5
	Lower Geyser Basin		
Great Fountain	11–15 hours	45–60 minutes	25–45
White Dome	Irregular; 19–271 minutes	2 minutes	7–9
Pink Cone	15 hours, 14 minutes (1989 avg.)	1 hour	4–6
Morning	Dormant since 8/29/91	10–25 minutes	15–45
Fountain	~6–9 hours	Irregular	9–25
Clepsydra	Almost continuous	Hours–Days	6–10
Deep Blue	20–30 minutes	2.5–3.5 minutes	1–13
Deep Blue's Satellite vent	Dormant	Continuous	10–15
Kaleidoscope	Irregular	0.5–2 minutes	1–10
Unnamed 1964 blowout	Irregular, now rare	Not applicable	10–14
Imperial	Dormant (continuous minor boil)	Months	0.5–1
	Norris Geyser Basin		
Steamboat	4 days–50 years; latest 10/2/91	3–40 minutes	70–120
Echinus	50–60 minutes	7–13+ minutes	10–30
	Supers: 2–3 hours	Supers: 30–60+ minutes	10–30
Ledge	Dormant	5–90+ minutes	20–35
Porkchop	Destroyed 9/5/89 by hydrothermal explosion	47+ months	3–11
Vixen	Very rare	Seconds	1–3